USAID
FROM THE AMERICAN PEOPLE

FULL REPORT

MAPPING THE EXPOSURE OF SOCIOECONOMIC AND NATURAL SYSTEMS OF WEST AFRICA TO COASTAL CLIMATE STRESSORS

OCTOBER 2014

This report is made possible by the support of the American people through the U.S. Agency for International Development (USAID). The contents are the sole responsibility of Tetra Tech ARD and do not necessarily reflect the views of USAID or the U.S. Government.

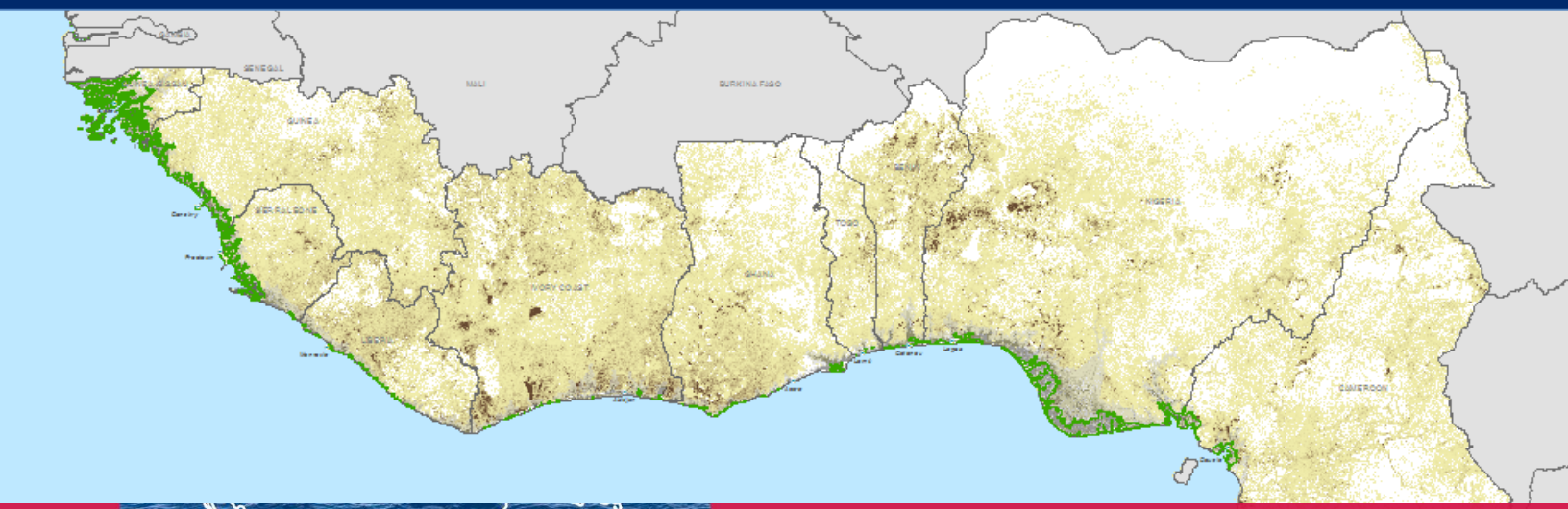

ARCC

African and Latin American Resilience to Climate Change Project

This report was prepared by a team from the Center for International Earth Science Information Network (CIESIN) at the Earth Institute of Columbia University through a subcontract to Tetra Tech ARD. Alex de Sherbinin led the team, which included Tricia Chai-Onn, Malanding Jaiteh, Linda Pistolesi, and Emilie Schnarr (geographic information system [GIS] analysts), as well as Valentina Mara (statistician).

Acknowledgements

CIESIN would like to thank Bryan Jones of Baruch College of the City University of New York (CUNY) for producing population projections for the 10 countries of West Africa included in this report. Sylwia Trzaska of CIESIN provided valuable suggestions at the early stages of the study's development.

Cover image: West Africa mangroves, sea-level rise, and deforestation

All maps, spatial data inputs, and reports/documentation associated with this vulnerability mapping study can be found at http://ciesin.columbia.edu/data/wa-coastal.

This publication was produced for the United States Agency for International Development by Tetra Tech ARD, through a Task Order under the Prosperity, Livelihoods, and Conserving Ecosystems (PLACE) Indefinite Quantity Contract Core Task Order (USAID Contract No. AID-EPP-I-00-06-00008, Order Number AID-OAA-TO-11-00064).

Tetra Tech ARD Contacts:

Patricia Caffrey
Chief of Party
African and Latin American Resilience to Climate Change (ARCC)
Burlington, Vermont
Tel.: 802.658.3890
Patricia.Caffrey@tetratech.com

Anna Farmer
Project Manager
Burlington, Vermont
Tel.: 802.658.3890
Anna.Farmer@tetratech.com

FULL REPORT

MAPPING THE EXPOSURE OF SOCIOECONOMIC AND NATURAL SYSTEMS OF WEST AFRICA TO COASTAL CLIMATE STRESSORS

AFRICAN AND LATIN AMERICAN RESILIENCE TO CLIMATE CHANGE (ARCC)

OCTOBER 2014

TABLE OF CONTENTS

ACRONYMS AND ABBREVIATIONS

ACE2	Altimeter Corrected Elevations 2
ACLED	Armed Conflict Location and Event Dataset
ARCC	African and Latin American Resilience to Climate Change
ASTER	Advanced Spaceborne Thermal Emission and Reflection Radiometer
BMZ	German Federal Ministry for Economic Cooperation and Development
CESR	Center for Environmental Systems Research, University of Kassel
CIESIN	Center for International Earth Science Information Network
CONF	Conflict Data for Political Violence (indicator code)
CROPS	Cocoa, Coconut, Palm Oil, Rubber, and Banana Production (metric tons) (indicator code)
CVI	Coastal Vulnerability Index
DECRG	World Bank Development Economics Research Group
DEM	Digital Elevation Model
DEM	Digital Elevation Model
DESYCO	Decision Support System for Coastal Climate Change Impact Assessment
DFO	Dartmouth Flood Observatory
DHS	Demographic and Health Survey
DIVA	Dynamic Interactive Vulnerability Assessment
DMSP	Defense Meteorological Satellite Program
DMSP-OLS	Defense Meteorological Satellite Program-Optical Line Scanner
DN	Digital Number
DST	Decision Support Tool
ERS1	Economic and Social Research Institute
ESI	Economic Systems Index
ETM+	Enhanced Thematic Mapper Plus
FAO	Food and Agriculture Organization of the United Nations
GAR	Global Assessment Report on Risk Reduction
GCLME	Guinea Current Large Marine Ecosystem Project

GDEM	Global Digital Elevation Model
GDP	Gross Domestic Product
GEF	Global Environment Facility
GegIS	Regional Impact Simulator
GIS	Geographic Information System
GLOBE	Global Observations to Benefit the Environment
GLWD	Global Lakes and Wetlands Database
GPW	Gridded Population of the World
GRP	Gross Regional Product
IMR	Infant Mortality Rate
IPCC	Intergovernmental Panel on Climate Change
IUCN	International Union for Conservation of Nature
LECZ	Low-Elevation Coastal Zone
MARK	Market Accessibility (Travel Time to Markets) (indicator code)
MEDUC	Maternal Education Levels (indicator code)
MODIS	Moderate Resolution Imaging Spectrometer
NASA	National Aeronautics and Space Administration
NEMA	National Emergency Management Agency
NGDC	NOAA National Geophysical Data Center
NOAA	National Oceanic and Atmospheric Administration
OECD	Organization for Economic Cooperation and Development
OLS	Operational Linescan System
OSM	OpenStreetMap
PA	Protected Areas
PACI	Poverty and Adaptive Capacity Index
PEI	Population Exposure Index
POP	Population Density (indicator code)
POPG	Population Growth (indicator code)
POV	Subnational Poverty and Extreme Poverty (indicator code)
SEDAC	NASA Socioeconomic Data and Applications Center
SimCLIM	Simulator of Climate Change Risks and Adaptation Initiatives

SLR	Sea-Level Rise
SRTM	Shuttle Radar Topography Mission
SSP4	Shared Socioeconomic Pathway 4
SVI	Social Vulnerability Index
TM	Thematic Mapper
UNEP	United Nations Environment Programme
UNEP/GRID	United Nations Environment Programme Global Resource Information Database
UNEP-WCMC	United Nations Environment Programme World Conservation Monitoring Centre
UNICEF	United Nations Children's Fund
UNISDR	United Nations International Strategy for Disaster Reduction
URBN	Urban, Built-Up Areas (indicator code)
USAID	United States Agency for International Development
USD	United States Dollar
VA	Vulnerability Assessment
WDPA	World Database on Protected Areas
WWF	World Wildlife Fund

ABOUT THIS SERIES

ABOUT THE STUDIES ON CLIMATE CHANGE VULNERABILITY AND ADAPTATION IN WEST AFRICA

This document is part of a series of studies produced by the African and Latin American Resilience to Climate Change (ARCC) project that addresses adaptation to climate change in West Africa. Within the ARCC West Africa studies, this document is part of the subseries Climate Change and Water Resources in West Africa. ARCC has also developed a subseries on Agricultural Adaptation to Climate Change in the Sahel, Climate Change and Conflict in West Africa, and Climate Change in Mali.

THE SUBSERIES ON CLIMATE CHANGE AND WATER

Upon the request of the United States Agency for International Development (USAID), ARCC undertook the West Africa water studies to increase understanding of the potential impacts of climate change on water resources in West Africa and to identify means to support adaptation to these changes. Other documents in the Climate Change and Water Resources in West Africa series include Transboundary River Basins, Coastal Biophysical and Institutional Analysis, and An Assessment of Groundwater Management.

1.0 INTRODUCTION

Spatial vulnerability assessments are useful tools for understanding patterns of vulnerability and risk to climate change at multiple scales (de Sherbinin, 2014). The demand for vulnerability maps among development agencies and governments is increasing as greater emphasis is placed on scientifically sound methods for targeting adaptation assistance. Such mapping is useful because climate variability and extremes, the sensitivity of populations and systems to climatic stressors, and adaptive/coping capacities are all spatially differentiated. The interplay of these factors produces different patterns of vulnerability.

This climate vulnerability mapping study seeks to illuminate some of the economic, social, and natural systems in West Africa that will be exposed to future sea-level rise, storm surge, and riparian floods. It covers the Guinea Current countries, extending from Guinea-Bissau in the northwest to Cameroon in the southeast. The combined population of all 10 countries is 265 million people. Seven percent of that population, or 19 million people, lives in the low-elevation coastal zone (LECZ) of less than 10 meters above mean sea level (Center for International Earth Science Information Network [CIESIN], 2013), and that number is growing rapidly owing to in-migration and high fertility. Although there have been Africa-wide assessments of the likely impacts of sea-level rise and storm surge on coastal areas (Hinkel et al., 2012; Brown et al., 2011), and broader vulnerability mapping has been conducted for the continent (López-Carr et al., 2014; Busby et al., 2013; Thornton et al., 2008), to date there has been no focused assessment on the likely exposure of different systems to seaward stressors among the Guinea Current countries. This report seeks to bridge that gap. Although all 10 countries are exposed to seaward impacts, the coastal fringe from Côte d'Ivoire to Nigeria is a relatively low-lying region of rapid population growth and intense economic development and, as such, is particularly vulnerable to future surge and sea-level-rise impacts. This mapping study is intended to support the programming and priority-setting of the United States Agency for International Development (USAID) as well as other stakeholders, such as the Interim Guinea Current Commission.

In this study, the coastal zone is defined as a 200 kilometer strip from the coastline inland. The areas covered are somewhat larger than what might normally be construed as "coastal," but we have included a larger area in recognition of the fact that the economic impacts of climate change in the coastal zone will not be confined to the coastline itself, but will extend further inland. This is especially the case if one considers not only direct impacts but also secondary impacts on livelihoods and economies tied to coastal cities. Almost half of the region's population—124 million people—live in this 200 kilometer strip (CIESIN, 2012). We used best available data on coastal elevation—the Altimeter Corrected Elevations 2 (ACE2) data set described below—and flood risk to identify areas at potential risk of inundation from sea-level rise, surge, or river-bank flooding. In the absence of more detailed modeling studies of surge risk and likely future relative changes in sea level for coastal West Africa, we define the areas at risk of sea-level rise and storm surge as being in LECZ bands of 0–5, 5–10, and 10–20 meters above mean sea level.[1] Although global mean sea-level rise by the end of this century is predicted to range from 0.3–1.2 meters depending on the rate of warming and the response of ice sheets (Kopp et al., 2014), storm surge can greatly expand the area affected by seaward impacts. The region already faces

[1] For the large-format poster maps that are associated with this report, we expanded the number of LECZ bands to 0–2, 2–4, 4–6, 6–10, and 10–20 meters above mean sea level. For the smaller map scales used in this report, a high number of narrow bands could not be depicted in such a way as to be interpretable without magnification.

storm surges with high winds and intense wave action resulting in coastal erosion (Niang, 2012; Appeaning Addo, 2013), and this pattern is likely to increase and perhaps intensify as a result of higher sea surface temperatures (Emanuel, 2005). For this reason, and because a 1 meter sea-level rise band would be difficult to represent cartographically in a regional map, we consider elevation bands up to 20 meters above mean sea level.

We created two composite indices (one representing social vulnerability and another representing economic systems), projected the population of the region to 2050, and examined the natural systems that will be exposed. This report includes a brief review of coastal-climate exposure and the data available to measure it (Section 2.0), and then proceeds to a broader description of data and methods for the exposed systems (Section 3.0) followed by results (Section 4.0). Section 5.0 provides overall conclusions. Data descriptions (map metadata) for each of the data sets used in this study are provided in Annex 1. A glossary of technical terminology is included before the reference section, and terms that are included are in bold text.

2.0 COASTAL EXPOSURE REVIEW

In this section, we describe commonly used methods for assessing coastal vulnerability and available data, providing a rationale for our approach to measuring seaward stressors on land-based coastal populations and systems.

A high percentage of West Africa's population is concentrated in coastal cities vulnerable to sea-level rise, and the Intergovernmental Panel on Climate Change (IPCC) estimates that by 2020, more than 50 million people will inhabit the coast from the Niger Delta in Nigeria to Ghana's capital city, Accra (Joiner et al., 2012). Table 2.1 from the IPCC Fourth Assessment Report chapter on coastal systems and low-lying areas (Nicholls et al., 2007) summarizes the primary coastal stressors that operate globally. Most of these stressors operate to some degree in the West Africa context, although the region is not affected by the kind of cyclonic activity that generates the highest wind speeds and storm surges. Though included in Table 2.1, we do not address the impacts of ocean temperature and acidification on fisheries in this study.

TABLE 2.1: MAIN CLIMATE DRIVERS FOR COASTAL SYSTEMS

Includes trends due to climate change, and their main physical and ecosystem effects
(Trend: ↑ = increase; ? = uncertain; R = regional variability)

Climate driver (trend)	Main physical and ecosystem effects on coastal systems (discussed in Section 6.4.1)
CO_2 concentration (↑)	Increased CO_2 fertilisation; decreased seawater pH (or 'ocean acidification') negatively impacting coral reefs and other pH sensitive organisms.
Sea surface temperature (↑, R)	Increased stratification/changed circulation; reduced incidence of sea ice at higher latitudes; increased coral bleaching and mortality (see Box 6.1); poleward species migration; increased algal blooms
Sea level (↑, R)	Inundation, flood and storm damage (see Box 6.2); erosion; saltwater intrusion; rising water tables/impeded drainage; wetland loss (and change).
Storm intensity (↑, R)	Increased extreme water levels and wave heights; increased episodic erosion, storm damage, risk of flooding and defence failure (see Box 6.2).
Storm frequency (?, R) Storm track (?, R)	Altered surges and storm waves and hence risk of storm damage and flooding (see Box 6.2).
Wave climate (?, R)	Altered wave conditions, including swell; altered patterns of erosion and accretion; re-orientation of beach plan form.
Run-off (R)	Altered flood risk in coastal lowlands; altered water quality/salinity; altered fluvial sediment supply; altered circulation and nutrient supply.

Source: Nicholls et al., 2007

One of the consequences of temperature increases associated with climate change is sea-level rise (SLR). Relative SLR will vary globally based on a number of factors. The factors most directly associated with climate change are the melting of ice caps and glaciers (or "eustatic" sea-level rise) and **thermal expansion** of the oceans (or "steric" sea-level rise). Tectonic and crustal activity can lead to **subsidence** (or "isostatic" sea-level rise) and lifting of land masses in the coastal zone.[2] Subsidence can

[2] Uplift occurs in areas where land masses are colliding (e.g., the eastern Pacific Rim) or in high-latitude areas affected by glaciation, where land masses are still rebounding after the retreat of the ice sheets. West Africa is not a region with high levels of uplift.

also be affected by processes such as the extraction of water and resources such as gas and oil, soil compaction, and the deprivation in delta areas of sediment that is trapped by upstream dams (Vorosmarty et al., 2009). The Niger Delta, for example, is affected by all of these factors, and studies at one site found rates of subsidence of 2.5cm per year (Ibe, 1996).

Global mean sea level has already risen from 1901 to 2010 by 0.19 meters (IPCC, 2013). Table 2.2 shows the projected sea-level rise for the mid- and late-21st century according to the IPCC Fifth Assessment Report. These are in the range of 0.4 to 0.63 meters by the end of the century, depending on the emissions scenario. Note that more extreme scenarios of up to 2 meters of SLR by the end of this century are conceivable should there be an abrupt increase in the rate of ice-sheet loss in the West Antarctic and Greenland (Pfeffer et al., 2008), and should all ice sheets eventually melt, the total SLR would be approximately 68 meters (National Geographic, 2013). More recent estimates by Kopp et al. (2014) suggest a range of global mean sea-level rise of 0.3–1.2 meters, depending on the rate of warming and the response of ice sheets.

TABLE 2.2: PROJECTED CHANGE IN GLOBAL MEAN TEMPERATURE AND SLR

		2046–2065		2081–2100	
	Scenario	**Mean**	***Likely* range[c]**	**Mean**	***Likely* range[c]**
Global Mean Surface Temperature Change (°C)[a]	RCP2.6	1.0	0.4 to 1.6	1.0	0.3 to 1.7
	RCP4.5	1.4	0.9 to 2.0	1.8	1.1 to 2.6
	RCP6.0	1.3	0.8 to 1.8	2.2	1.4 to 3.1
	RCP8.5	2.0	1.4 to 2.6	3.7	2.6 to 4.8
	Scenario	**Mean**	***Likely* range[d]**	**Mean**	***Likely* range[d]**
Global Mean Sea Level Rise (m)[b]	RCP2.6	0.24	0.17 to 0.32	0.40	0.26 to 0.55
	RCP4.5	0.26	0.19 to 0.33	0.47	0.32 to 0.63
	RCP6.0	0.25	0.18 to 0.32	0.48	0.33 to 0.63
	RCP8.5	0.30	0.22 to 0.38	0.63	0.45 to 0.82

Source: IPCC, 2013–Table SPM.2

Accelerated SLR represents a significant planning and management challenge to coastal nations, especially in developing countries where vulnerability is high, adaptation options are limited, and spatial data and information are limited for planning purposes (Brown et al., 2014). SLR has resulted in increased erosion and inundation of vulnerable areas, which threaten coastal life and property. Sea levels are expected to rise around Africa, and impacts include flooding, saltwater intrusion, loss of beaches and recreational activities including tourism, loss of infrastructure, and changes to river flows and outputs on the coast. In Africa, data are generally missing on the present rates of sea-level change, coastal geomorphology, and socioeconomic trends (Hinkel et al., 2012). Basic data on coastal topography are available through publicly accessible global data sets such as the National Aeronautics and Space Administration (NASA) Shuttle Radar Topography Mission (SRTM) global **digital elevation model** (DEM) (90 meter resolution); the European Space Agency ACE2 data set (which merges SRTM with Satellite Radar Altimetry) (90 meter resolution) (Berry et al., 2008); and the Advanced Spaceborne Thermal Emission and Reflection Radiometer (ASTER) Global Digital Elevation Model (GDEM) (15 meter resolution). It should be emphasized that all global DEMs are of limited accuracy. LIDAR data are most accurate but are not available over large areas of the world, and especially in West Africa. In our assessment, ACE2 has the advantage over SRTM and ASTER GDEM of accurately returning ground values in areas of dense forest cover such as mangroves; for this reason and based on comparisons with SRTM that showed that ACE2 consistently returned slightly lower elevations, we chose to use this data set for this study.

In addition to sea-level rise, storm surge is another important factor in coastal vulnerability. The measurement and recording of the spatial extent and height reached by coastal storm surges is required for better prediction and assessment of coastal risk. To date, there has been little mapping of storm surge in West Africa, but a method developed by Brakenridege et al. (2013) using NASA Moderate Resolution Imaging Spectrometer (MODIS) sensors to measure the areal extent of land inundation caused by storms surges could be useful for future monitoring. However, while MODIS operates in "always-on" mode and provides 250 meter resolution over much of the Earth's surface, monitoring is much more difficult in regions such as coastal West Africa with high cloud cover. We examined the Dartmouth Flood Observatory (DFO) data for West Africa, but could not find data that would provide evidence of storm-surge risk, since the imagery would also need to be collected coincident with known surge events.

Several tools and approaches address SLR and storm surge in the coastal zone. Here we focus on two commonly used ones that also have been applied in Africa: the Coastal Vulnerability Index (CVI) and the Dynamic Interactive Vulnerability Assessment (DIVA) model. The CVI is a simple method to assess coastal vulnerability to SLR and surge (Gornitz et al., 1994), providing a numerical basis for ranking sections of coastline based on potential change as a result of several factors, including SLR, geology, wave action, and geomorphology (Gornitz et al., 1991). A vulnerable coastline is characterized by low coastal relief, subsidence, extensive shoreline retreat, and high wave/tide energies. In a study assessing Accra's coastal vulnerability to climate change, local data sets were used to generate a CVI, and it was found that the risk level for the entire coast can be categorized as moderate (Appeaning Addo, 2013).

Ramieri et al. (2011) assess a number of coastal impact assessment models, including DIVA, Simulator of Climate Change Risks and Adaptation Initiatives (SimCLIM), Regional Impact Simulator (GegIS), and Delft3D. To our knowledge, DIVA is the only model that has been applied in West Africa to date. Using DIVA, Hinkel et al. (2012) conducted a quantitative assessment of the potential SLR impacts at continental and national scales with the goal of determining the biophysical and socioeconomic consequences of SLR and socioeconomic development. DIVA is based on a data model that divides the world's coast into 12,148 variable-length coastal segments and associates up to 100 data values with each segment. It combines global SLR due to warming with estimates of local vertical land movement to determine relative SLR. Based on the relative SLR, DIVA assesses three types of biophysical impacts: 1) dry land loss due to coastal erosion, 2) coastal flooding, and 3) salinity intrusion in deltas and estuaries. Given certain flood extents, land elevations, population densities, the existence of dikes, and relative sea level, the expected number of people flooded annually is estimated over time. In a similar way, the expected monetary value of damage caused by sea and river floods is estimated based on a damage function. DIVA can be run with or without applying adaptation options. In the results, Nigeria, Guinea-Bissau, Guinea, Benin, Ghana, Sierra Leone, Gambia, Liberia, Cameroon, and Côte d'Ivoire are ranked among the top 15 most-vulnerable countries in Africa (Hinkel et al., 2012).

Although the DIVA model is a useful tool for coastal vulnerability impact assessments at the global, regional, and national levels, since the average coastal segment is approximately 70 kilometers in length, it cannot accurately capture more localized dynamics (Ramieri et al., 2011). Furthermore, the DIVA model is no longer publicly accessible, and inquiries with the model developer were not answered. However, we did obtain DIVA storm-surge and SLR outputs from Dasgupta et al. (2009) and we compared the outputs with ACE2. We opted to use ACE2 data because DIVA results were based on the older SRTM data that show higher elevations than ACE2 in many forested coastal areas.

Although we focus mainly on seaward (coastal) hazards, we also address flood risk, since it can often occur in areas that are simultaneously affected by storm surge associated with tropical storms and it is relevant to social and economic impacts within a 200-kilometer buffer inland from the coastline. Floods may result when extreme precipitation events cause rivers and water bodies to overflow their banks, or

when low-lying areas with poor drainage are inundated. River-bank flooding in the immediate coastal zone may be accompanied by storm surge, which backs up river flow and can be exacerbated by SLR.

Flood risk is an issue in many coastal areas of West Africa and particularly affects urban areas (Dickson et al., 2012; Guinea Current Large Marine Ecosystem Project [GCLME], 2010; Douglas et al., 2008; ActionAid, 2006). In 2009, many West African cities experienced torrential rains that caused loss of life and the destruction of important socioeconomic infrastructure (GCLME, 2010). In Nigeria, floods represent a major issue for urban areas due to the low-lying topography, limited capacity of drainage systems, and blockage of waterways and drainage channels (Adeoye et al., 2009). The frequency and magnitude of urban flooding and its impacts have more than doubled in recent time, owing to population growth and settlement in flood-prone areas (e.g., Agbola and Agunbiade, 2009) and the more intense and frequent rainstorms potentially associated with climate change. For example, in a flood impact assessment in Nigeria, Adeoye et al. (2009) determined that the impacts of floods have increased from significant to threatening during the past three decades, based on flood records from the National Emergency Management Agency (NEMA) and records of flood events recorded in Nigerian newspapers.

The DFO has compiled and continuously updates a global archive of large flood events collected from news, governmental, instrumental, and remote-sensing sources. The archive includes: 1) an online table of recent events only; 2) Excel files for all events from 1985 to present; and 3) **Geographic Information System (GIS)** file sets that provide flood catalog numbers and area-affected map outlines. It includes the archive data and images for each flood event from the NASA MODIS sensor. The DFO's World Atlas of Flood Hazard, which is presently viewable online by selecting a 10°x10° tile, provides a visual representation of present and past flood events around the globe. However, cloud cover and other imaging constraints sometimes restrict the ability to capture peak inundation (Brakenridge et al., n.d.), a problem particularly significant along the West African coast. Another data source for assessing global flood hazard, the Global Estimated Risk Index for Flood Hazard developed by the United Nations Environment Programme (UNEP)/Global Resource Information Database/Europe for the Global Assessment Report (GAR), is built upon satellite data from DFO as well as hydrological models and records of extreme rainfall events (UNEP/United Nations International Strategy for Disaster Reduction [UNISDR], 2013). This data set is modeled and only available at a relatively coarse spatial resolution, and hence only approximates the degree of risk in any given location. It is the only available data set, thus we chose to use it to represent the relative risk of riparian areas to flood hazards.

Map metadata for each of the data layers included in the exposure component is found in Annex 1, Section A-1.1. For those interested in further exploration of data and methods in coastal vulnerability assessment, Ramieri et al. (2011) provide a useful review of a range of models and methods, and Newton and Weichselgarnter (2014) and Maloney and Preston (2014) provide recent assessments that showcase evolving methods.

3.0 DATA AND METHODS

In the previous section, we described the data sets and modeling methods that have been commonly used to assess exposure to seaward hazards, providing the rationale for the exposure data sets we chose to use for this study. In this section, we cover the data and methods used to create two spatial indices, the social vulnerability index and economic system index, as well as the data layers used in the assessment of natural systems. The spatial indices converted indicators from raw values to indices on a 0–100 scale, where 100 equals higher levels of social vulnerability and economic exposure, respectively. Our approach is framed by the IPCC Special Report on Extreme Events (SREX) conceptual framework, which construes risk as emanating from the spatial intersection of exposure to extreme events and vulnerable systems (IPCC 2012).

3.1 SOCIAL VULNERABILITY

Social vulnerability is variously defined in the literature (Parry et al., 2007; O'Brien et al. 2007), and a range of spatial indices have been created to represent differential patterns of vulnerability (de Sherbinin, 2014; Fekete, 2012; Cutter et al., 2003). Each definition and approach has different purposes. Our primary purpose was to create a Social Vulnerability Index (SVI) that would begin to represent the population exposure to coastal impacts as well as the poverty, education, and conflict levels that might indicate higher levels of "defenselessness." A list of indicators included in this index is found in Table 3.1. (Many other indicators could have been used, but we chose only those indicators for which we had data.) Full metadata are found in Annex 1 (Section A1.2). High values on the raw scale for each of the indicators (except for maternal education, which was inverted) result in higher vulnerability scores on the 0–100 scale. Histograms of the data distributions and the indicator values are available in Section A1.2. For selected indicators, such as population density, we trimmed the tails (winsorized) at the high end of the scale. Where data are skewed, winsorization ensures a greater spread in the distribution of the transformed indicator, which is important for index construction (Organization for Economic Cooperation and Development [OECD], 2008). The indicators were combined in a weighted average to produce the overall SVI; all indicators were assigned a weight of 1, except maternal education levels (MEDUC), which was assigned a weight of 2. The reasons for this were 1) conceptually, maternal education is an important factor in adaptive capacity (Muttarak and Lutz, 2014); and 2) the indicator was derived from a spatial interpolation of *Demographic and Health Survey* (DHS) cluster-level values, and thus has a higher spatial resolution than the poverty indicator (POV). POV is reported at a mix of country-level and subnational units, whereas MEDUC is based on a spatially interpolated mesh of survey cluster points, better pinpointing areas of highest social vulnerability.

TABLE 3.1: SOCIAL VULNERABILITY INDICATORS

Indicator Code	Indicator	Date or Date Range
POP	Population density	2010
POPG	Population growth	2000–2010
POV	Subnational poverty and extreme poverty	2005
MEDUC	Maternal education levels	circa 2008
MARK	Market accessibility (travel time to markets)	circa 2000
CONF	Conflict data for political violence	1997–2013

Because areas of high population density and growth (high exposure, leading to higher vulnerability) are generally associated with urban areas that have lower levels of poverty and higher degrees of adaptive capacity (low vulnerability), to some degree the population factors cancel out the poverty and adaptive capacity indicators. This is the issue of "compensability" — i.e., the way in which a high score on one indicator offsets a low score on another (German Federal Ministry for Economic Cooperation and Development [BMZ], 2014; OECD, 2008). To account for this, we created two sub-indices, a Population Exposure Index (PEI), which only includes population density (POP) and population growth (POPG); and a Poverty and Adaptive Capacity Index (PACI), which will be composed of subnational poverty (POV), maternal education levels (MEDUC), market accessibility (MARK), and conflict (CONF). These sub-indices allow us to isolate the population indicators from the poverty and conflict metrics.

3.2 ECONOMIC SYSTEMS

For the Economic Systems Index (ESI), our primary purpose was to create an index that would begin to show relative levels of economic activity that could be exposed to seaward hazards. The indicators included in this index are found in Table 3.2. (In this case too, many other indicators could have been used, but we chose only those indicators for which we had data.) Map metadata for each of the data layers included in this component is found in Annex 1, Section A-1.3. For crops, we focused primarily on higher-value export crops rather than on grains. For each of the indicators, high values on the raw scale result in higher ESI scores on the 0–100 scale. Histograms of the data distributions and the indicator values are available in Annex 1, Section A-1.3. For most of the indicators, we trimmed the tails (winsorized) at the high end of the scale. The indicators were combined in an unweighted average to produce the overall ESI.

TABLE 3.2: ECONOMIC SYSTEM INDICATORS

Indicator Code	Indicator	Date or Date Range
GDP	Gross Domestic Product (gridded)	2010
URBN	Urban, built-up areas	2010
CROPS	Cocoa, coconut, palm oil, rubber, and banana production (metric tons)	2000

In addition to the ESI, we overlaid urban, built-up areas and the West Africa road network with the LECZ and flood-risk layers to assess urban areas and road networks at potential risk of flooding (see Section 4.0 for results).

3.3 NATURAL SYSTEMS

For natural systems, we were interested in:

- The intersection of seaward hazards with mangrove forests (Giri et al., 2010);
- Forest-cover loss from 2000 to 2012 (Hansen et al., 2013);
- Wetlands from the Global Lakes and Wetlands Database (GLWD): Lakes and Wetlands Grid (World Wide Fund for Nature [WWF] and the Center for Environmental Systems Research, University of Kassel [CESR], 2004); and
- Threatened mammals, amphibians, and birds based on the International Union for Conservation of Nature (IUCN) Red List database.

For this mapping exercise, we included all IUCN Red List threat categories: critically endangered, endangered, and vulnerable. The wetlands map also includes protected areas information from the

World Database of Protected Areas (WDPA) (World Conservation Monitoring Center of the United Nations Environment Programme [UNEP-WCMC], 2013).

We did not create an index for natural systems since there was no logical way to do so. Map metadata for each of the data layers included in this component is found in Annex 1, Section A-1.4.

4.0 RESULTS

4.1 SOCIAL VULNERABILITY

There are a number of areas that appear to experience high social vulnerability. Figure 4.1 shows results for the SVI overlaid with the 0–20 m LECZ. A combination of high population density, high population growth, and conflict make the Niger Delta and Lagos a "hotspot" of vulnerability in the LECZ. Abidjan also appears as a hotspot, though the political violence there has largely subsided since 2011. Other high vulnerability areas on the coast include Conakry (Guinea), Freetown (Sierra Leone), Accra and Cape Coast (Ghana), Cotonou (Benin), and Douala (Cameroon). Figure 4.2 shows the map of the PEI, which combines population density and growth rates from 2000–2010 in an overall index. This map highlights the coastal cities that have a high population density and are growing at a rapid pace owing to a combination of in-migration and high fertility. For the countries from Guinea-Bissau to Côte d'Ivoire (and also Togo), the only areas with high scores are coastal cities. Ghana, Benin, Cameroon, and especially Nigeria have some urbanized areas away from the coast that have high PEI scores. Finally, Figure 4.3 presents the PACI, which is the SVI without the population indicators. Broadly, the region from Guinea-Bissau to western Côte d'Ivoire has higher levels of poverty and lower adaptive capacity. Benin is also marked by relatively high PACI scores. In the Niger Delta, high poverty rates, conflict, and spatial isolation (market accessibility) combine to create a hotspot.

All else being equal, more densely populated areas that are highly exposed to climate-related hazards will put more people at risk. The West African coastal zone is not only densely populated but it is also attracting new migrants. CIESIN (2011) estimates that between 1970 and 2010 the coastal ecosystems of West Africa received some 14 million migrants. Between migration and high fertility rates, the populations of West Africa's coastal cities are rapidly growing and by 2020 the coastline between Accra and the Niger delta is expected to become a continuous urban megalopolis of more than 50 million inhabitants (Boko et al., 2007). For this study we examined the population in the coastal zone using ACE2 elevation data together with an alpha version of the Gridded Population of the World v.4 (GPWv4), which is based on spatially high resolution input data and circa 2010 population counts for most countries in West Africa. Table 4.1 provides results. Nigeria has the largest population in the 0–5m zone, with 9.5m people, which is more than the combined total for all other countries combined (5.9m). The highest percentage of national populations in the 0–5m zone are in Guinea-Bissau (17.9 percent), followed by Liberia (16.0 percent) and Benin (13.4 percent).

FIGURE 4.1: SOCIAL VULNERABILITY INDEX (SVI) AND 20M LECZ

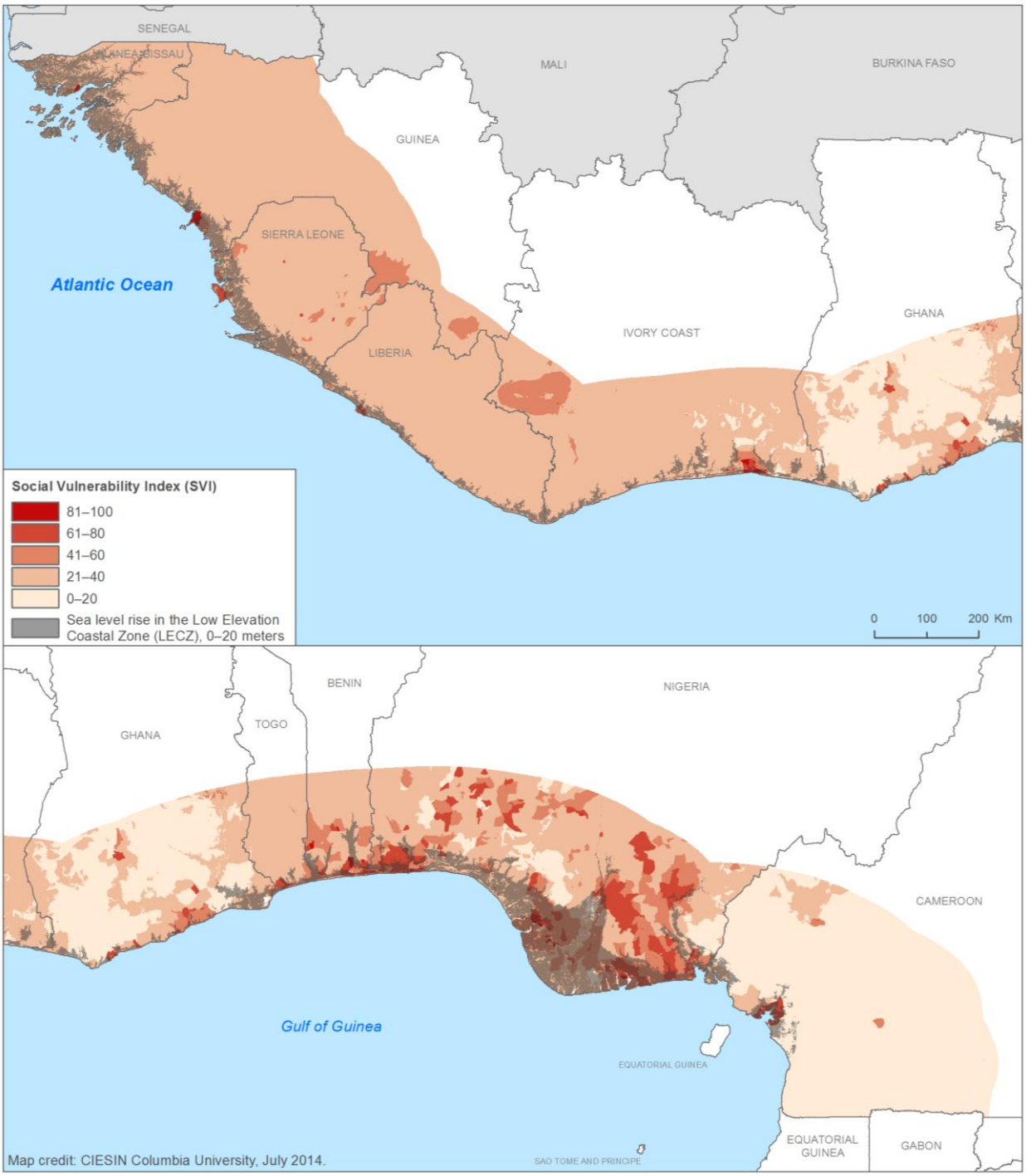

FIGURE 4.2: POPULATION EXPOSURE INDEX (PEI) AND 20M LECZ

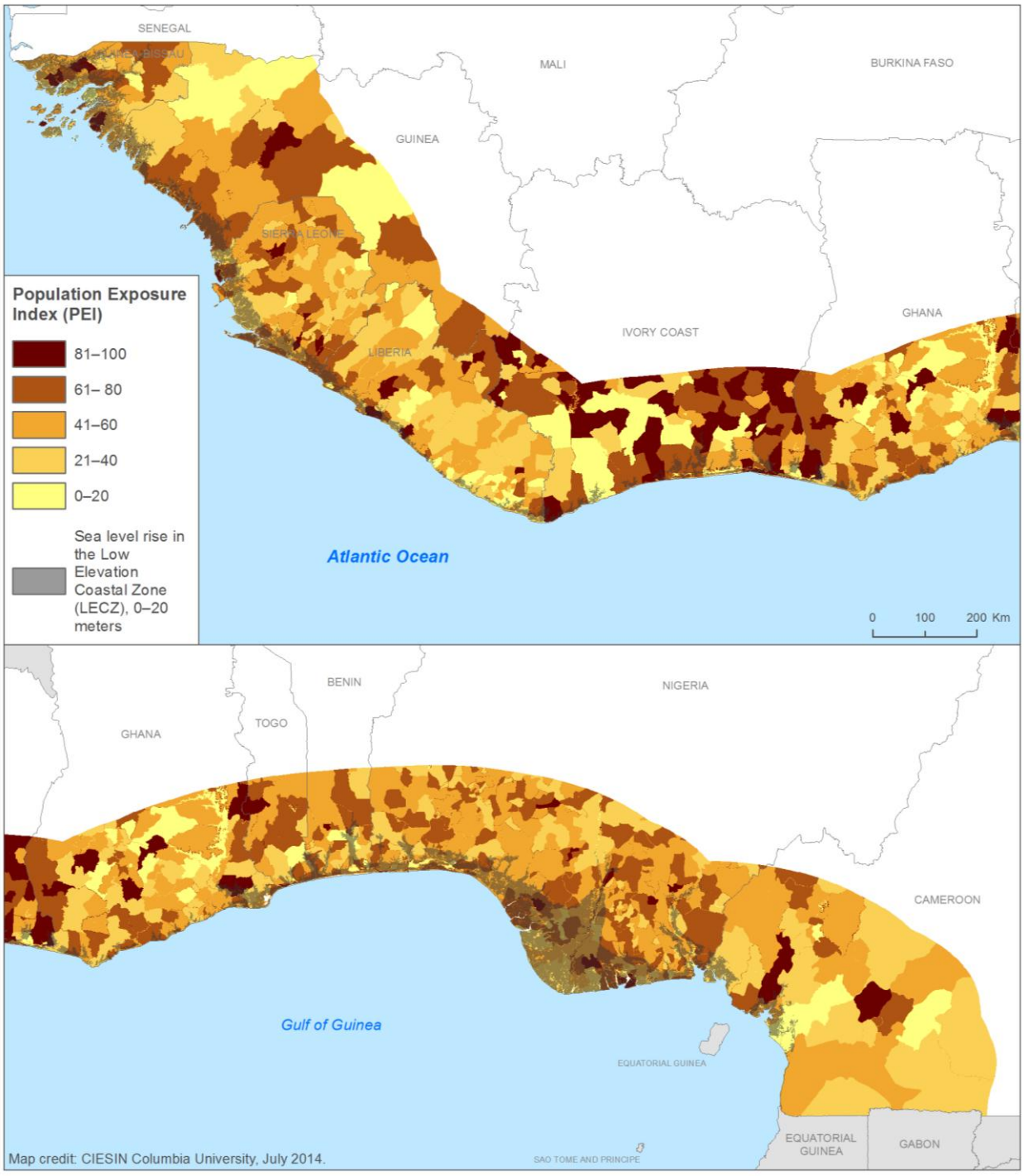

FIGURE 4.3: POVERTY AND ADAPTIVE CAPACITY INDEX (PACI) AND 20M LECZ

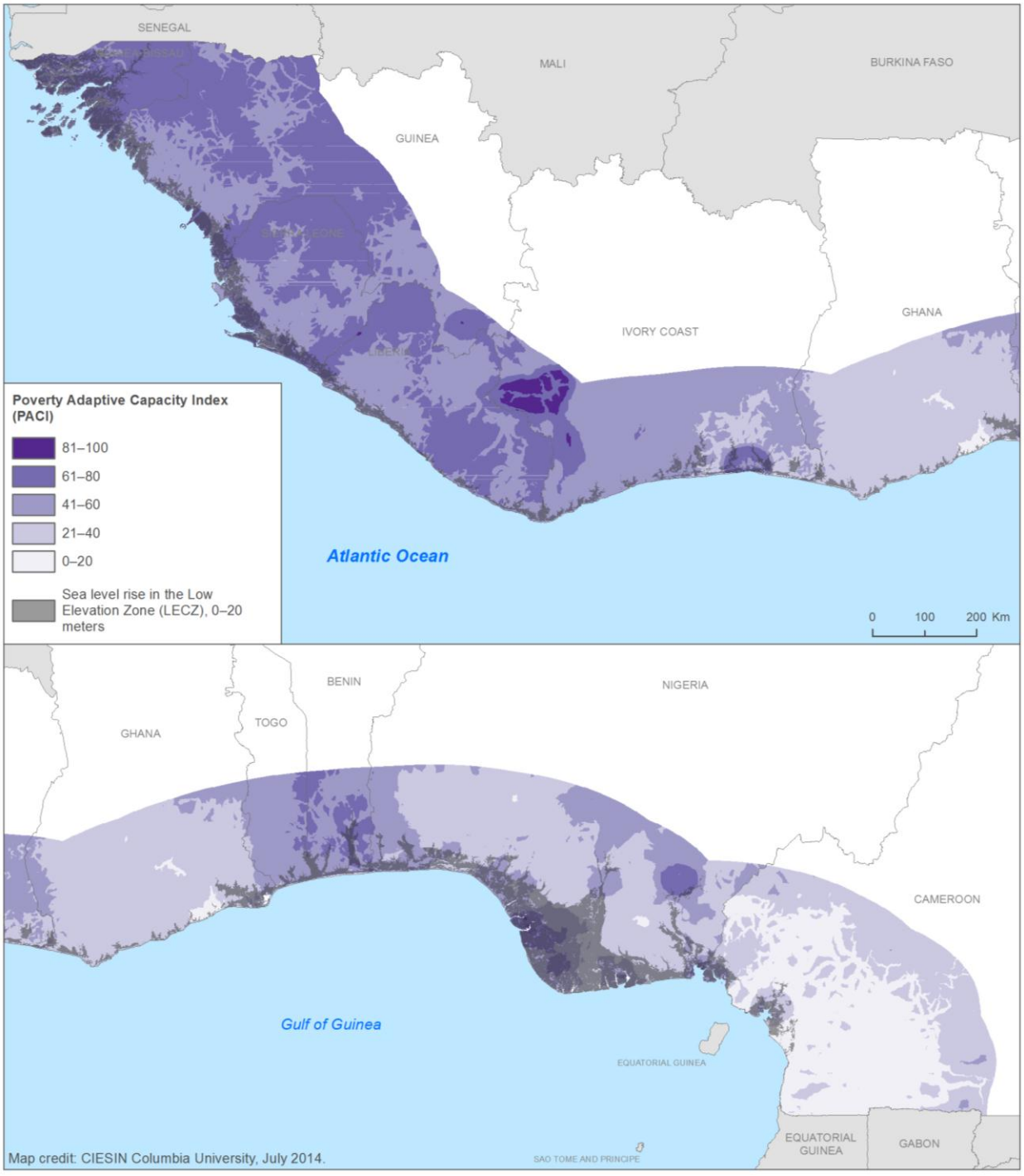

TABLE 4.1: POPULATION IN LECZ (2010)

	Low-Elevation Coastal Zone			
Country	**0–5m**	**5–10m**	**10–20m**	**Total**
Benin	1,290,406	375,489	366,009	2,031,904
Cameroon	822,134	562,668	555,440	1,940,242
Ghana	536,922	352,704	952,086	1,841,712
Guinea	1,033,318	121,910	242,315	1,397,544
Guinea-Bissau	303,377	135,371	297,016	735,764
Côte d'Ivoire	663,636	320,279	361,078	1,344,993
Liberia	704,139	203,434	173,243	1,080,815
Nigeria	9,463,101	4,983,488	6,467,375	20,913,965
Sierra Leone	307,686	161,808	261,849	731,343
Togo	277,135	364,857	302,785	944,777

Projections of CIESIN's GPWv4 to 2030 and 2050 based on the Shared Socioeconomic Pathway 4 (SSP4) were produced by Bryan Jones of Baruch College. SSP4 reflects a divided world in which the cities, which have relatively high standards of living, are attractive to internal and international migrants. In low income countries, rapidly growing rural populations live on shrinking areas of arable land due to both high population pressure and expansion of large-scale mechanized farming by international agricultural firms (O'Neill et al., 2014). This pressure induces large migration flows to the cities, contributing to fast urbanization, although urban areas do not provide many opportunities for the poor and there is a massive expansion of slums and squatter settlements. While it is impossible to predict exactly how populations will grow, this approach is at least internally coherent and plausible. Figure 4.4 presents the results, which, consistent with the SSP4 scenario, shows significant urbanization, particularly in the LECZ from Abidjan to Douala. Côte d'Ivoire, Togo, and particularly Cameroon show higher rates of rural depopulation than the other countries.

Table 4.2 provides the projected population to 2050 in the three LECZ bands, 0–5, 5–10, and 10–20. Based on these projections, the increase in the exposed population is dramatic: there is a more than three-fold increase in population in the 0–5m LECZ band from 2010 to 2050, from 15.4 to 56.6 million people, with 73 percent of the total (41.5 million) in Nigeria. For the broader LECZ, some 115 million people in the region will live between 0–20m elevation, compared to 33 million today. Even those living outside the directly exposed areas will be affected if city infrastructure and services are disrupted owing to storm surge and related coastal flooding.

FIGURE 4.4: CHANGE IN POPULATION FROM 2010 TO 2030 AND 2050

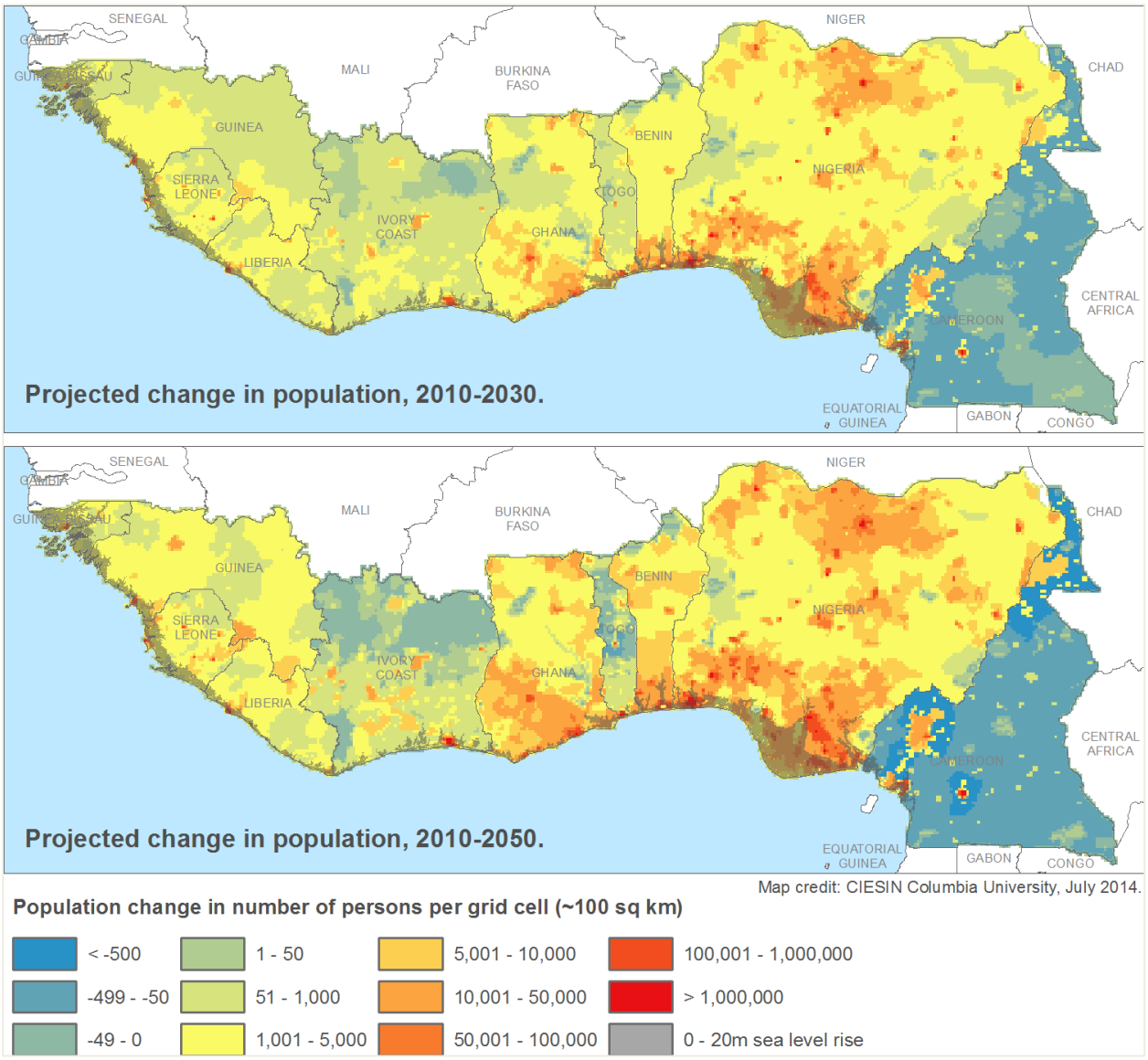

TABLE 4.2: POPULATION IN LECZ (2050)

	Low-Elevation Coastal Zone			
Country	**0–5m**	**5–10m**	**10–20m**	**Total**
Benin	2,302,618	532,252	755,612	3,590,482
Cameroon	1,692,305	1,174,391	1,178,763	4,045,458
Ghana	864,562	527,778	1,613,495	3,005,835
Guinea	1,731,232	204,946	342,059	2,278,237
Guinea-Bissau	510,810	227,061	460,644	1,198,515
Côte d'Ivoire	1,690,100	583,759	856,590	3,130,450
Liberia	4,797,432	1,013,893	608,597	6,419,923
Nigeria	41,577,719	18,459,392	28,316,341	88,353,452
Sierra Leone	499,025	225,713	371,710	1,096,447
Togo	988,469	581,211	852,616	2,422,296

4.2 ECONOMIC SYSTEMS

Figure 4.5 depicts the results for the ESI for West Africa overlaid with 0–20m elevation zone. As can be seen from the map, much of each country's economic activity is found in the coastal zone, and especially in the capital cities. There are very high levels of economic exposure in the Niger Delta, Lagos, and Cotonou, and slightly lower levels in Lomé, Accra, Abidjan, Monrovia, Freetown, and Conakry. Figures 4.6–4.14 show the exposure of West Africa's coastal cities to coastal stressors, moving from Douala, Cameroon in the east to Bissau, the capital of Guinea-Bissau, in the west. The urban "footprints" are based on 2010 night-time lights data with thresholds applied to identify high, medium, and low density urban development.[3] The most exposed cities are the same as the ones listed above.

Table 4.3 represents an estimate of the total GDP that is exposed by country based on data from United Nations Environment Programme Global Resource Information Database (UNEP/GRID) Geneva (see Annex A1.3). As with population, Nigeria's total is the largest by far; it is three times that of the combined total of the other countries ($5.5 billion to $1.7 billion). The economic activity of Lagos and oil extraction facilities in the delta, all of which fall below 5m elevation, contribute to this total.

[3] The intensity of lighting is highly correlated with population density (Doll, 2008), so while we cannot assign specific density classes to each category, the lights do a better job than the gridded population data from GPWv4 (CIESIN, 2014) or Afripop (Linard, C., Gilbert, M., et al., 2012, Population Distribution, Settlement Patterns and Accessibility Across Africa in 2010, *PLoS One, 7(2),* e31743) in describing the morphology and relative degrees of development within urban areas.

FIGURE 4.5: ECONOMIC SYSTEM INDEX (ESI) AND THE 20M LECZ

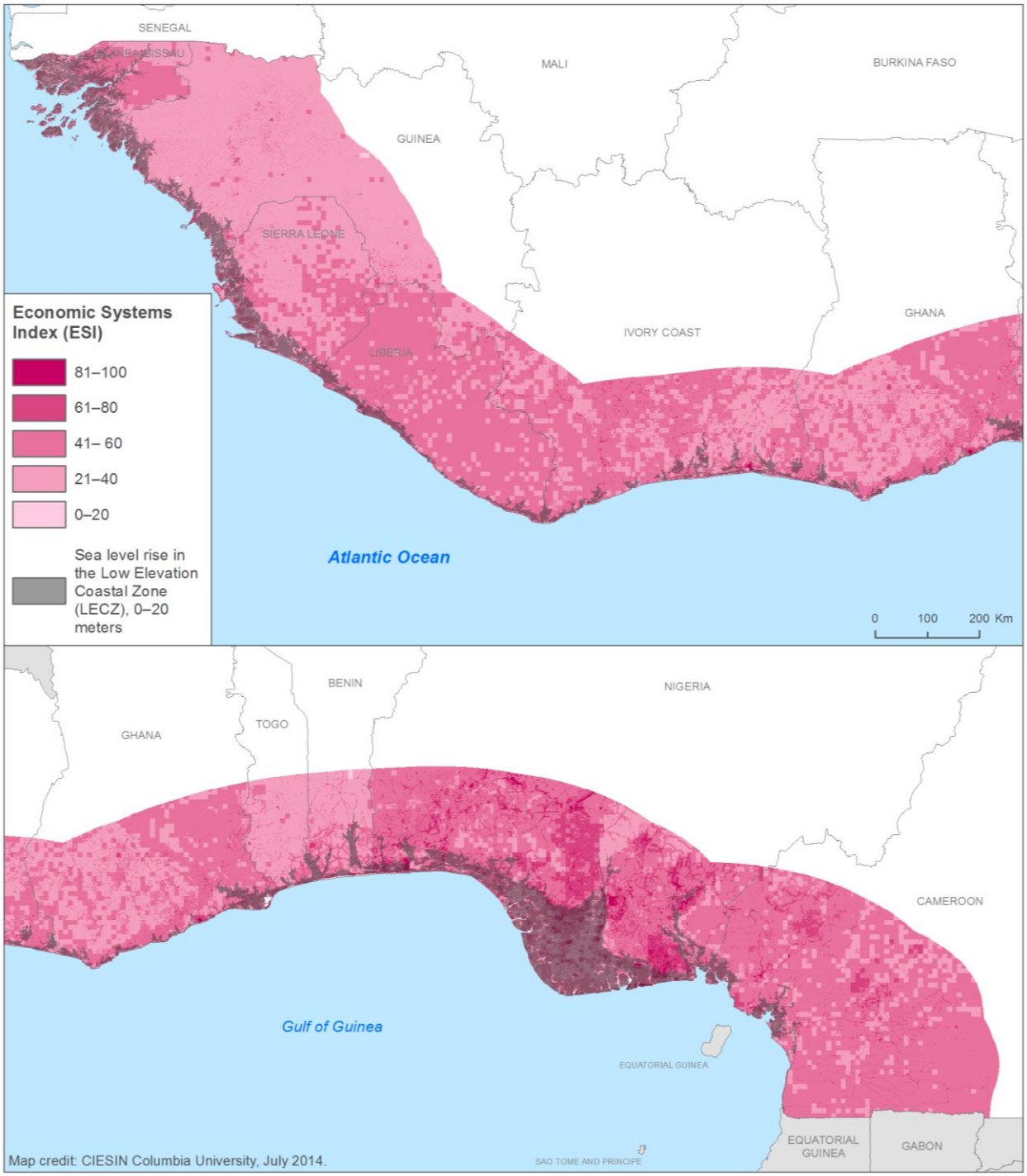

TABLE 4.3: GROSS DOMESTIC PRODUCT IN LECZ (IN U.S. DOLLARS)

	Low-Elevation Coastal Zone			
Country	**0–5m**	**5–10m**	**10–20m**	**Total**
Benin	532,081	319,155	302,589	1,153,825
Cameroon	215,782	612,780	829,633	1,658,195
Ghana	181,864	229,302	570,726	981,892
Guinea	59,062	197,834	448,209	705,105
Guinea-Bissau	20,800	21,303	75,663	117,766
Côte d'Ivoire	447,176	324,693	387,781	1,159,650
Liberia	160,504	47,769	25,523	233,796
Nigeria	5,472,782	2,922,801	3,168,258	11,563,841
Sierra Leone	47,531	31,477	47,254	126,262
Togo	73,402	350,550	83,241	507,193

FIGURE 4.6: URBAN AREAS AND LECZ FOR DOUALA, CAMEROON

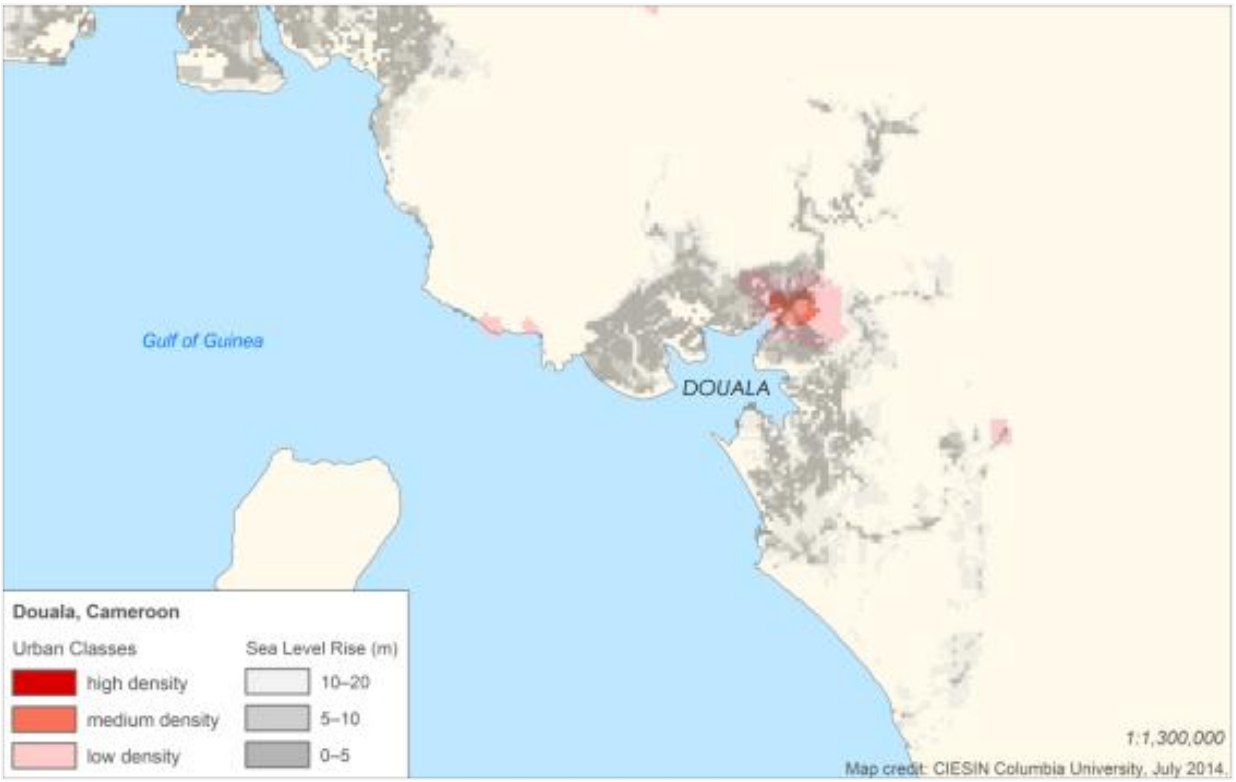

FIGURE 4.7: URBAN AREAS AND LECZ IN THE NIGER DELTA, NIGERIA

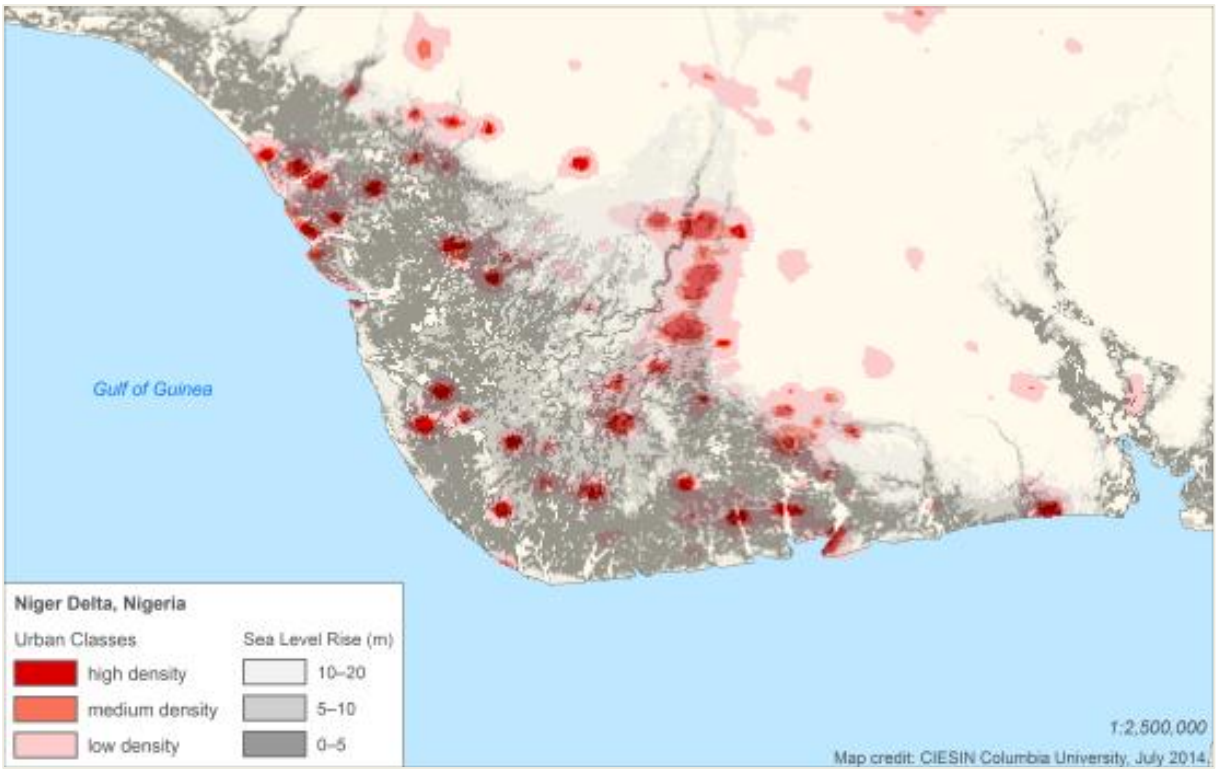

FIGURE 4.8: URBAN AREAS AND LECZ FOR LAGOS AND COTONOU

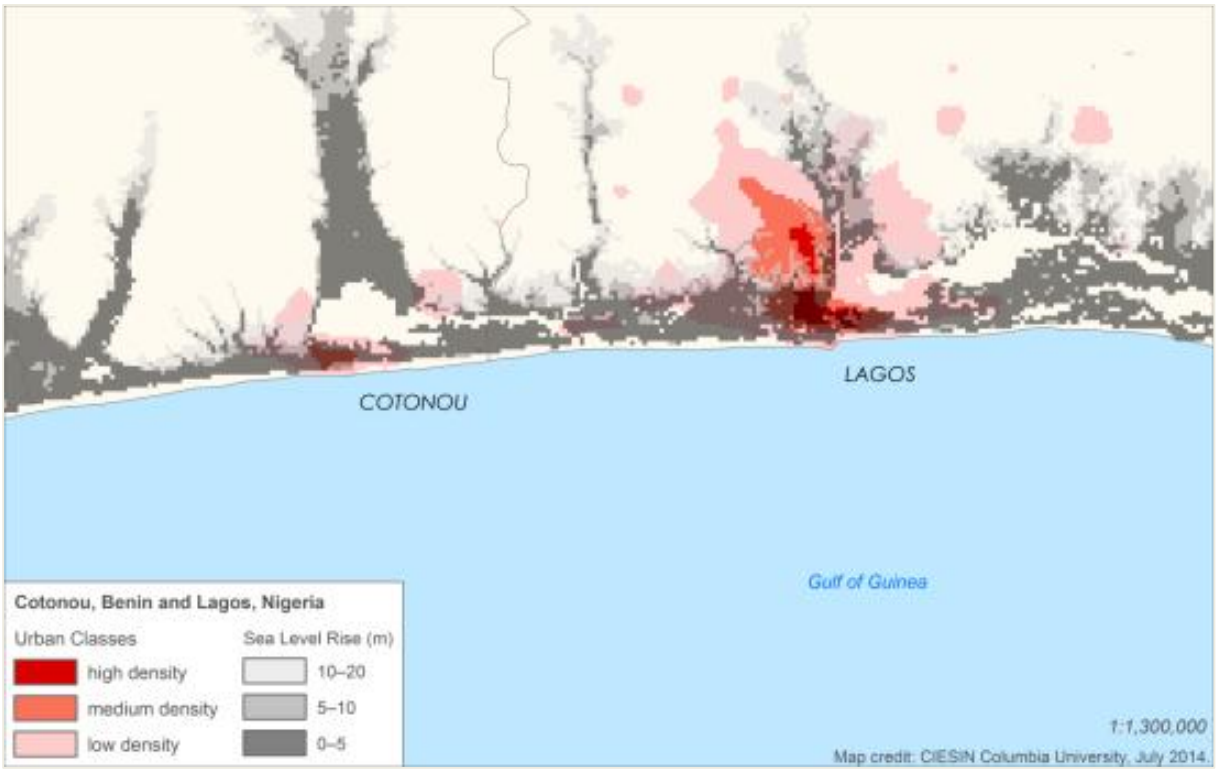

FIGURE 4.9: URBAN AREAS AND LECZ FOR ACCRA AND LOME

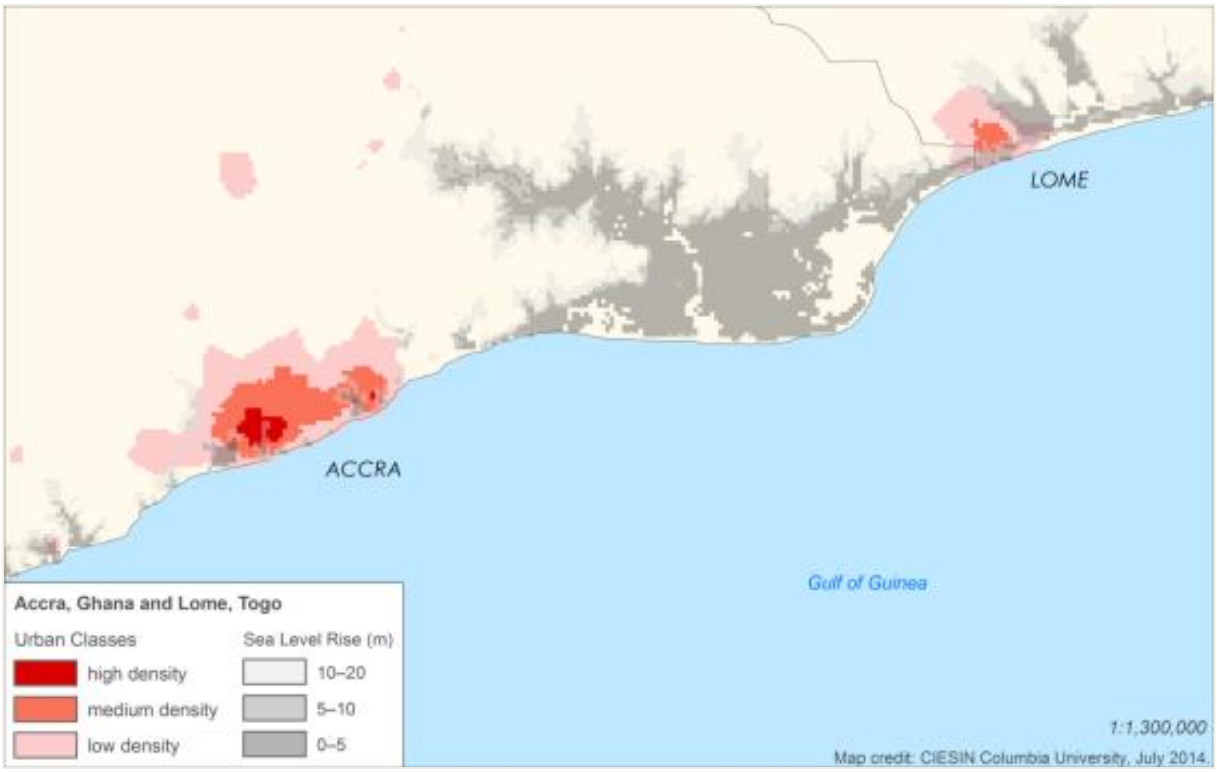

FIGURE 4.10: URBAN AREAS AND LECZ FOR ABIDJAN

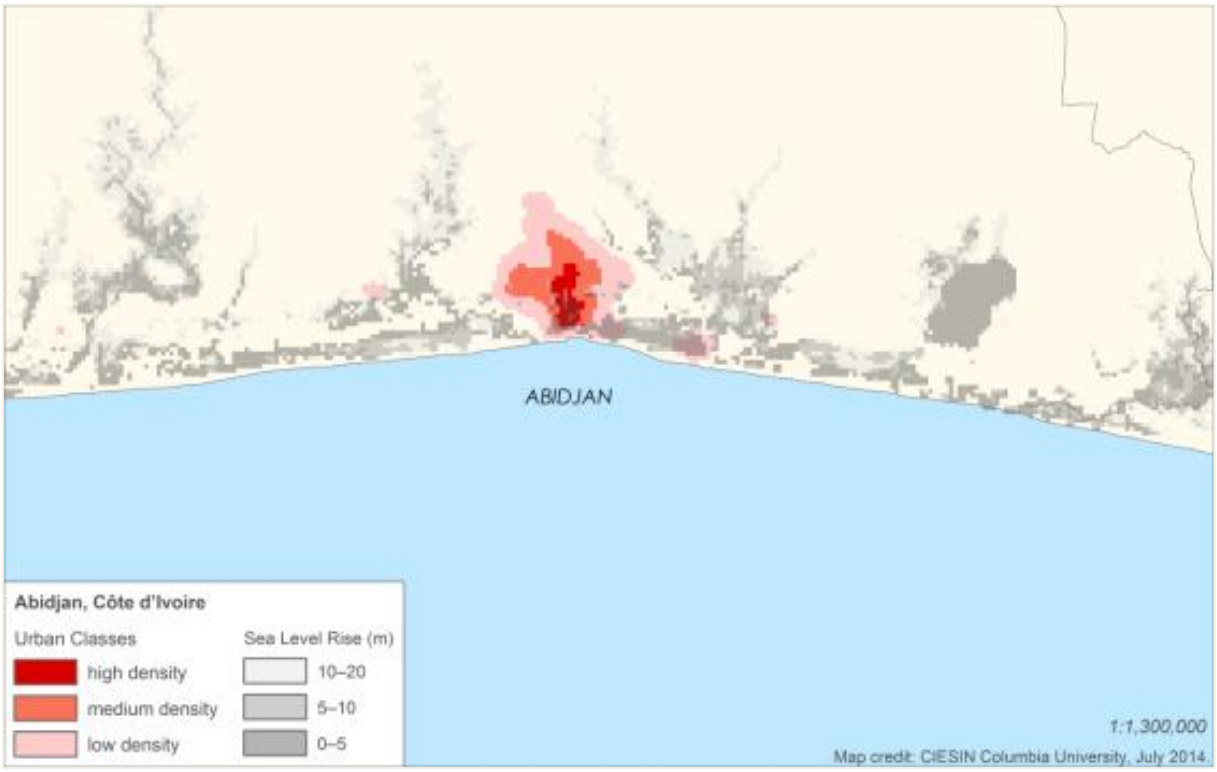

FIGURE 4.11: URBAN AREAS AND LECZ FOR MONROVIA, LIBERIA

FIGURE 4.12: URBAN AREAS AND LECZ FOR FREETOWN, SIERRA LEONE

FIGURE 4.13: URBAN AREAS AND LECZ FOR CONAKRY, GUINEA

FIGURE 4.14: URBAN AREAS AND LECZ FOR BISSAU

Figure 4.15 provides a map of the road networks that are exposed to flood risk and sea-level rise/storm surge. Road networks along the coast from Côte d'Ivoire to Lagos are particularly at risk of coastal inundation. Although the resolution of these data are relatively coarse, flood risk is highest in Sierra Leone, western Ghana, and coastal Togo, Benin and near Lagos, Nigeria, suggesting that roads may be regularly inundated or washed out.

FIGURE 4.15: ROAD NETWORKS, FLOOD RISK, AND THE LECZ

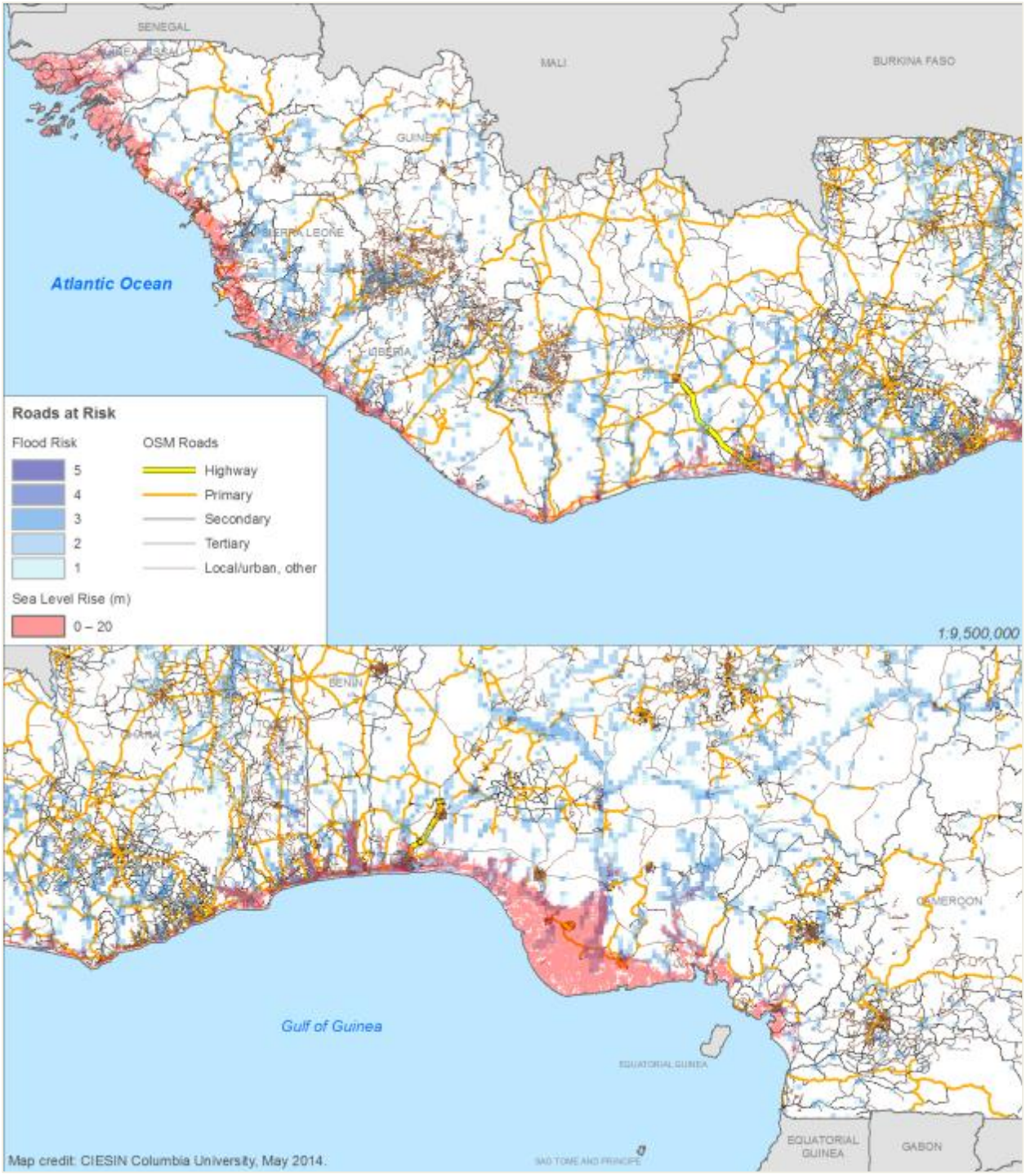

4.3 NATURAL SYSTEMS

In this section, we review coastal stressors on a number of sensitive natural systems. We focus on mangrove areas, forest cover loss, the number of endangered species, and wetland ecosystems. Figure 4.16 provides a map of the LECZ in relation to mangrove distribution. Once again the Niger Delta comes out as being particularly exposed, along with a stretch of mangroves from Guinea-Bissau to Sierra Leone. Box 4.1 provides a more detailed study of mangrove loss in the Niger Delta.

Figure 4.17 provides a map of deforestation from 2000 to 2012 based on data from Hansen et al. (2013) aggregated to one sq. km pixels in relation to the LECZ. Twusami and Merem (2006) (Box 4.1) find that mangrove forests are declining in areas of oil development in the Niger Delta; visual inspection by the authors of the high resolution deforestation data together with the mangrove extents layer found that in some areas mangroves are expanding. Thus, the areal change in mangrove forests in the Delta requires further study. However, Figure 4.17 depicts clear areas of intense deforestation in the coastal zone of Côte d'Ivoire and western Ghana; in Ghana this is linked to gold mining activities.

BOX 4.1: CASE STUDY: NIGER DELTA REGION OF SOUTHERN NIGERIA

The Niger Delta Region of Southern Nigeria is a particularly vulnerable area along the coast due to oil infrastructure development and consequent environmental degradation. This unique region possesses the world's third-largest wetland with significant biological diversity. Petroleum exploration has triggered adverse environmental impacts and threated biodiversity. To assess how much change has occurred in the area, Twusami and Merem (2006) obtained socioeconomic and environmental data from federal archives, Landsat, and other organizations in Nigeria for two time periods (1985 and 2000). They concluded that water-body, mangrove, and closed-forest areas have decreased, while settlement areas, croplands, and mixed forests have increased. Two Landsat Thematic Mapper (TM) and Enhanced Thematic Mapper Plus (ETM+) satellite images from May 1985 and June 2000 were obtained and the data were processed. Outputs for the region were mapped in order to show the spatial evolution of coastal environmental changes in the delta (see Box Figure below).

BOX FIGURE: CLASSIFIED IMAGE OF LANDSAT TM, MAY 1985 (LEFT) AND JUNE 2000 (RIGHT)

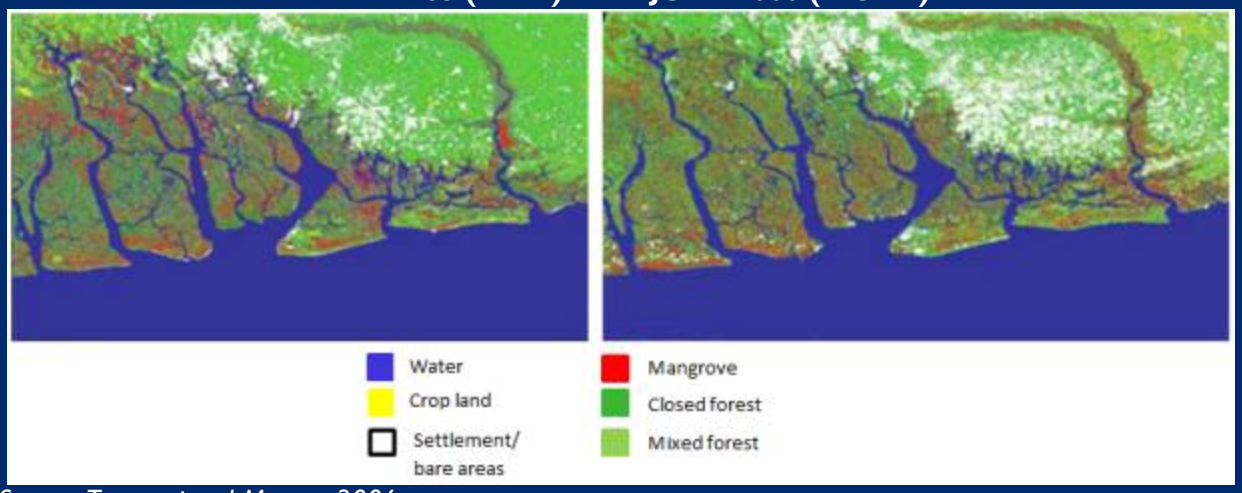

Source: Twusami and Merem, 2006

FIGURE 4.16: MANGROVES AND THE LECZ

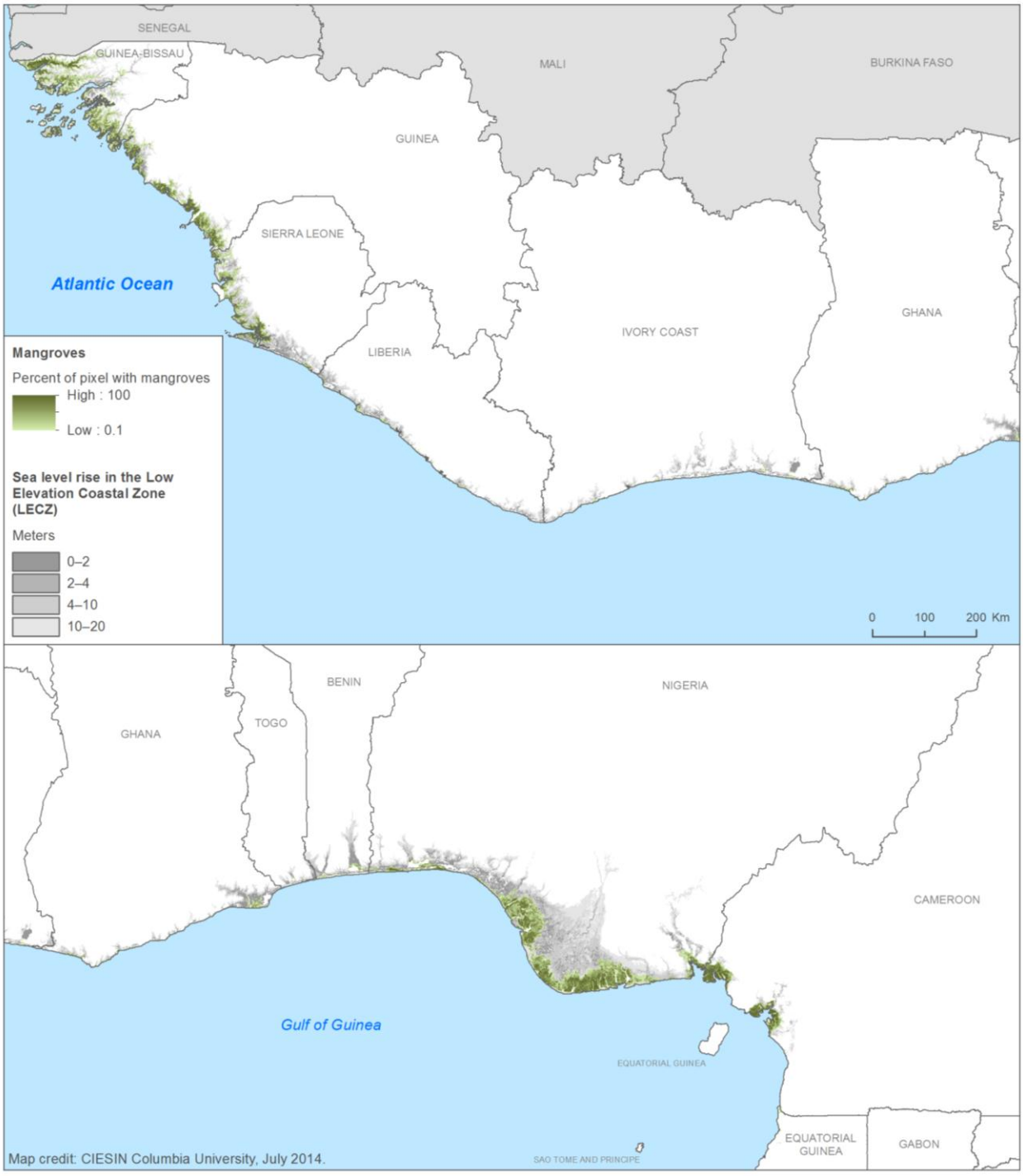

Coastal wetlands provide a large number of goods and services that contribute to the economic welfare of the local and global communities, including the protection of shorelines from erosion, storm buffering, climate regulation, carbon sequestration, and preservation of biodiversity. Sea-level rise is a major threat that results in inundation, erosion, and saltwater intrusion. In some areas, coastal wetlands will migrate inland as a result (de Sherbinin et al., 2012). According to Parry et al. (2007, section 9.4.6), "In the Gulf of Guinea, sea-level rise could induce overtopping and even destruction of the low-barrier beaches that

limit the coastal lagoons, while changes in precipitation could affect the discharges of rivers feeding them. These changes could also affect lagoonal fisheries and aquaculture." Blankespoor et al. (2012) estimated the capacity of the coastline to retreat and for coastal wetland ecosystems to migrate inland as the coastline recedes in 76 developing countries under a one-meter SLR scenario. Data on wetlands were extracted from all GLWD, Version 3, at a resolution of 1km x 1km. In order to assess the impact of SLR on wetlands and the potential for adaptation, the wetlands migratory potential characteristic in the DIVA database was used. Benin was identified as one of the top 10 countries with the greatest expected loss of wetlands in square kilometers based on current extent, though it is acknowledged that some of those wetlands may migrate inland.

FIGURE 4.17: DEFORESTATION AND THE LECZ

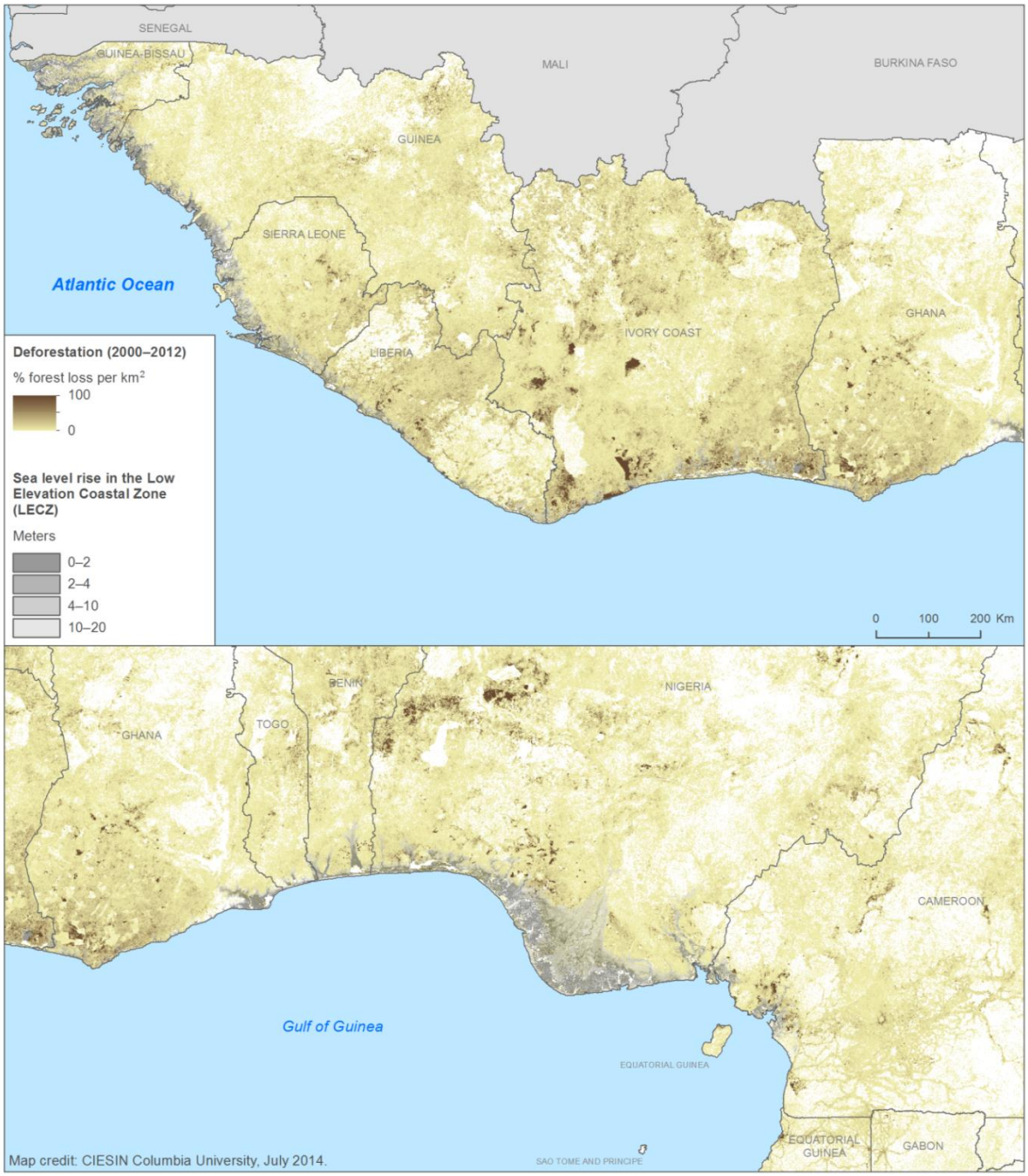

Figure 4.18 depicts wetlands (coastal wetlands, brackish and saline wetlands, salt pans, and swamp and flooded forests), protected areas, and the LECZ. In general, mangroves will be highly susceptible to SLR impacts because they thrive in brackish waters that are at or just above sea level. The degree to which mangroves, sea grasses, marshlands, and estuaries can migrate inland as sea level rises will in part be determined by the degree of protection around the larger wetland area and the buffer between the natural system and the built environment (de Sherbinin et al., 2012; Blankespoor et al., 2012). The Bijagos islands of Guinea-Bissau have the greatest protection (although the management capacity may be limited); apart from this large park, in the rest of West Africa there are only four small marine protected areas in Côte d'Ivoire and one in the Niger Delta.

FIGURE 4.18: WETLANDS, PROTECTED AREAS, AND THE LECZ

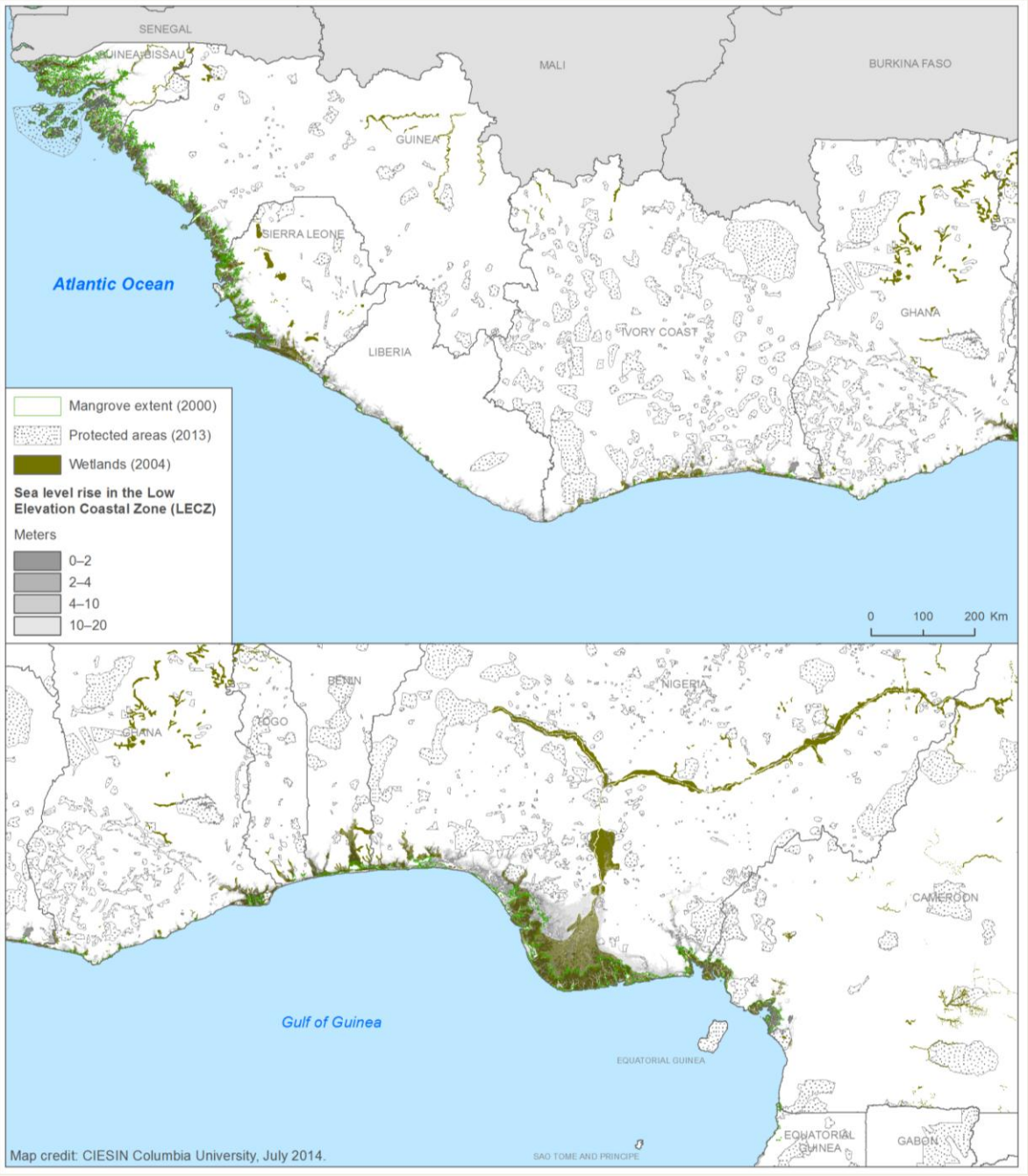

While wetlands can provide important natural protection against storm surge, a major issue for the littoral region of West Africa is coastal erosion, particularly in areas without wetland protection. According to a report on the Guinea Current Large Marine Ecosystem (GCLME Coordinating Unit, 2006, p. 9):

> "The rate of the coastal retreat can average several meters per year (for example, erosion rates caused by port structures in Liberia, Togo, Benin, and Nigeria sometimes reach a staggering 15–25 m per year). Although the coastline is highly subject to natural erosion and sedimentation processes due to high wave energy, strong littoral transport amongst others, erosion has been intensified mainly by human activities, notably through sand mining and exploitation, disturbance of the hydrographical cycles, river damming, port construction, dredging, and mangrove deforestation."

In addition, according to Aliou (2012), this type of erosion is having a major impact on the coastal wetlands of Benin. Erosion is exacerbated by sand mining for construction purposes (ActionAid, 2006). The problem is generalized throughout much of West Africa (Niang, 2012), and Ibe (1996) estimates that some areas of the Niger Delta have rates of coastal retreat of up to 10 meters per year. It is likely that more intense wave action and higher mean sea level and surge will result in high levels of coastal erosion.

Finally, we examine the number of threatened species in the region to determine if there are higher numbers in areas with greater exposure to coastal stressors. Figure 4.19 provides maps of the number of threatened species in all threat categories by class (amphibians, birds, and mammals). Figure 4.20 provides maps of the number of threatened species for all classes by threat category. There are high numbers of threatened species, rising to 27 threatened species per kilometer, in the tropical forest region from Sierra Leone to southern Côte d'Ivoire and in the highlands of Cameroon. In general, it does not appear that coastal areas have much higher numbers of threatened species, though there is one critically endangered species (the pygmy hippopotamus, *C. liberiensis heslopi*) in the Niger Delta that would be vulnerable to SLR, though it is not known at present if it is already extinct. The highest density of threatened species appears to be associated with inland forest areas that are probably being affected by habitat loss from agricultural expansion.

FIGURE 4.19: THREATENED SPECIES BY CLASS AND THE LECZ

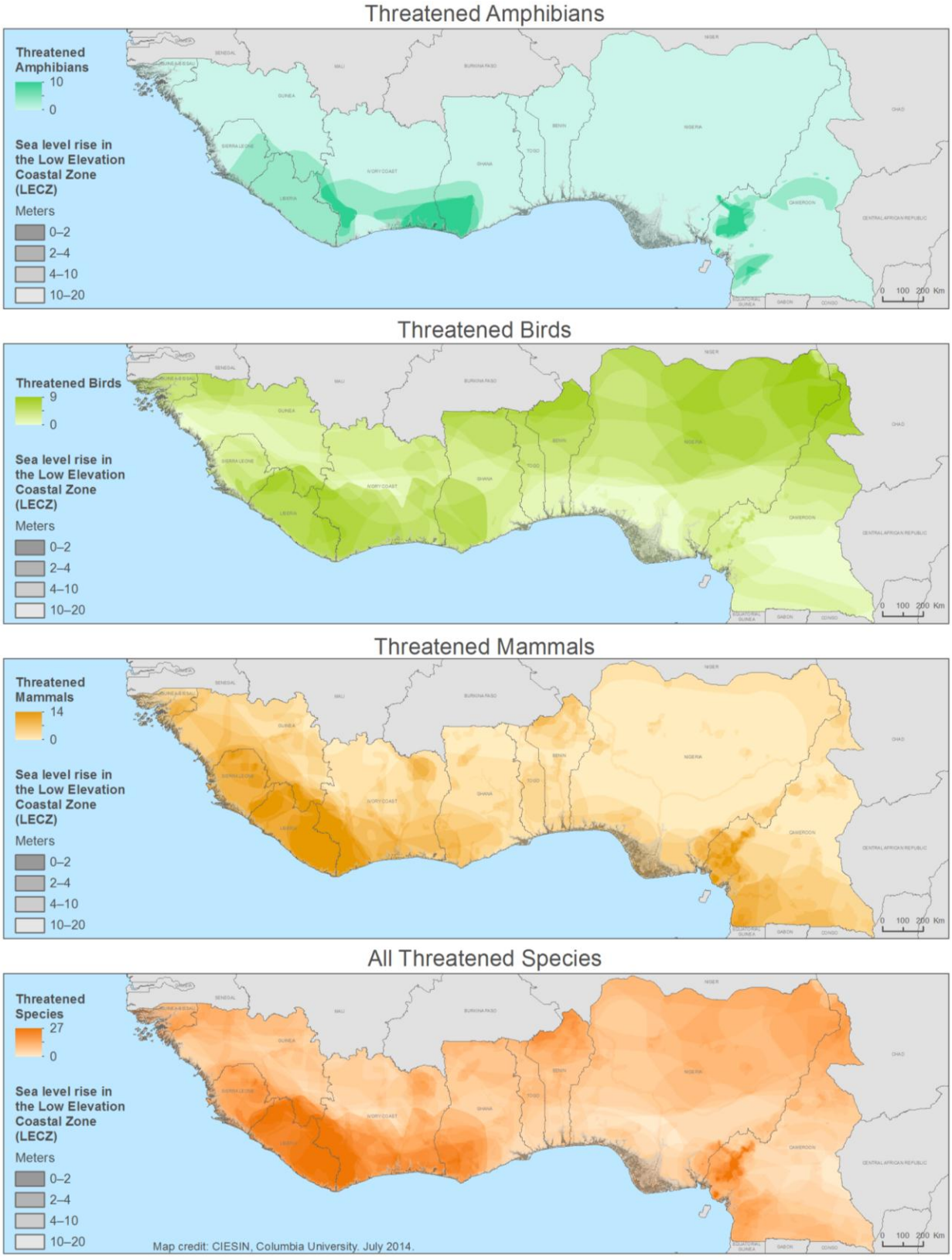

FIGURE 4.20: THREAT LEVELS AND THE LECZ

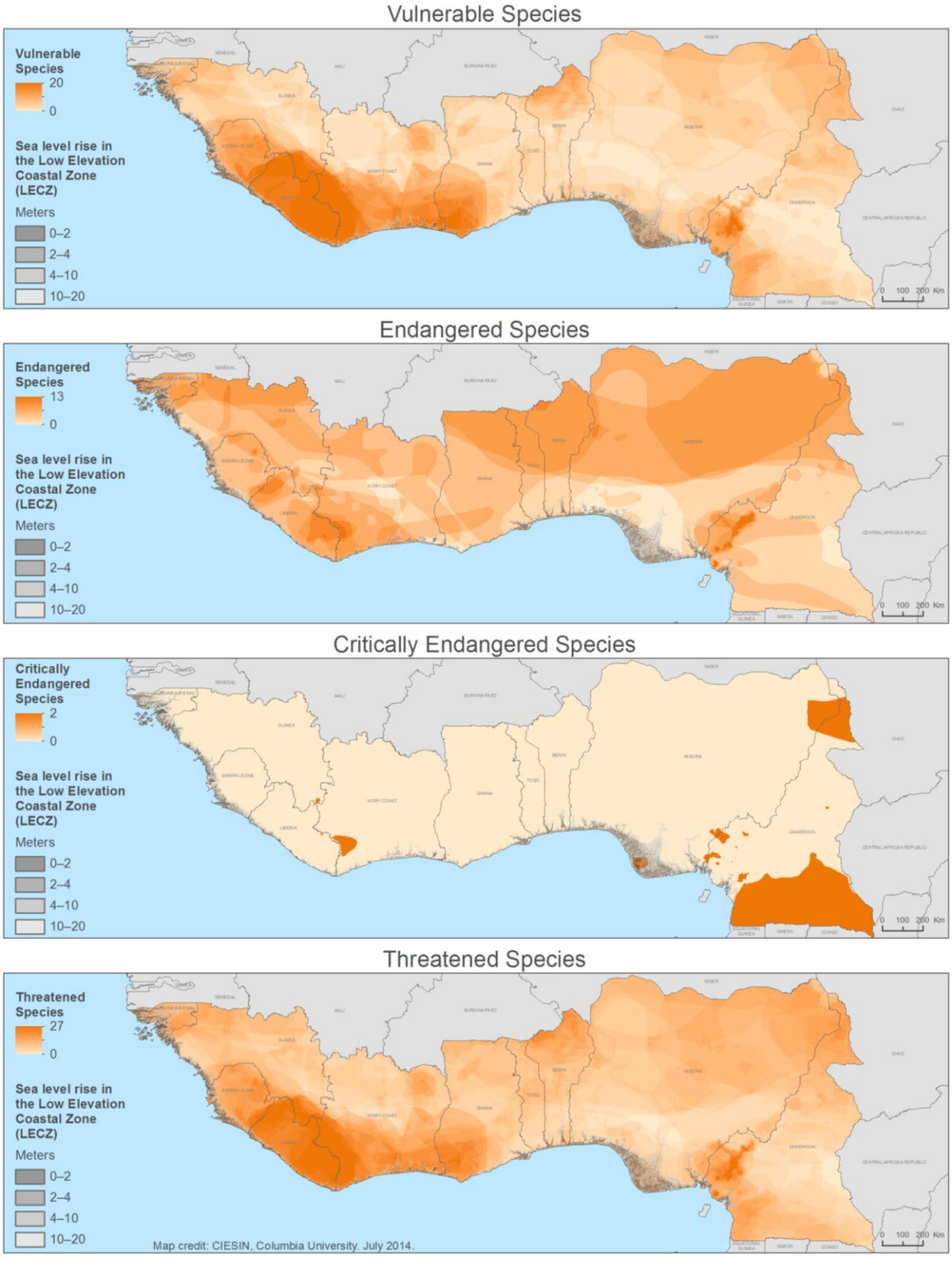

5.0 CONCLUSIONS

This preliminary study of coastal vulnerability in West Africa highlights both a number of areas that appear to experience high vulnerability and risk, but also has some limitations owing to a combination of mapping scale, data gaps, and uncertainties. Taking these in turn, areas of high population and social and economic exposure in the LECZ include the Niger Delta, Lagos, and Cotonou. This has to do with the intense urban and economic development in these areas. Projections suggest that population numbers for Nigeria and Benin in the 0–20m band could rise from 22 million today to 92 million in 2050. In the Delta these patterns are associated with oil and gas exploitation and high levels of poverty and conflict.

Coast lines tend to rise more steeply in the western portions of the region, from Guinea to Liberia, resulting in lower levels of overall exposure. Côte d'Ivoire, Ghana, and Togo lie somewhere between these two extremes. Accra, for example, has the advantage of being largely outside the 20m elevation LECZ. Guinea-Bissau is low-lying but is thinly populated with very little in the way of economic assets exposed. Overall, the combination of armed conflict, economic assets, and population density (in Lagos, Benin City, Delta, and Port Harcourt), and projected population growth puts Nigeria at the top of the list of high exposure countries in West Africa. In terms of natural systems, the coastal mangroves, salt marshes, estuaries, and lagoons of West Africa are all highly vulnerable to seaward stressors while simultaneously providing a buffering capacity against storm surge. These systems are currently under-protected.

Turning to the limitations, the scale and spatial resolution of the vulnerability maps represents a relatively coarse level of analysis that masks substantial sub-regional and local detail. While most data were available at 30 arc-second resolution (~1 sq. km at the equator), processes of coastal inundation obviously operate at much finer resolutions. Urban-scale assessments to identify variations of vulnerability within specific coastal cities would require higher resolution spatial data, such as ACE2's 3 arc-second elevation grids (or better yet, LIDAR elevation data) and detailed street, infrastructure, and building data sets. Poster-size maps are available for a number of maps in this report, but the small maps of roughly 1:1,000,000 scale found in this report render difficult the identification of areas at high risk from coastal stressors.

Data gaps are a perennial problem in any vulnerability mapping exercise, and this problem is exacerbated when there is a need for consistent cross-country data sets covering large regions. The following data would have been useful to the present analysis but could not be located:

- Exposure data:
  - Spatially explicit rates of relative sea level rise since 1950;
  - Spatially explicit projections of sea level rise to 2050 and 2100; and
  - Detailed bathymetric, coastal topography, and wind field data to estimate storm surge.
- Social vulnerability data:
  - Higher resolution poverty and adaptive capacity data.
- Infrastructure data:
  - Power plants;

- Industrial facilities; and
- Complete and spatially accurate roads data.

- Natural systems data:
  - Bird nesting areas;
  - Areas of high endemism;
  - Areas of habitat loss (partially fulfilled by the deforestation data); and
  - Coastal erosion rates.

There are a number of uncertainties inherent in any assessment of this kind. Some of the uncertainties relate to the spatial and measurement accuracy, validity, and reliability of the data included. While we sought to retain a relatively select sub-set of data with higher accuracy (e.g., by comparing multiple data sets where available), some of the data have unknown uncertainty levels (e.g., maps of species distributions, poverty head counts, and GDP). There are also uncertainties inherent in the index creation for the SVI and ESI, such as uncertainties in thresholds for certain values on the raw scale and functional relationships among indicators that make up these indices. We do not have empirical evidence that would allow us to benchmark any indicators to any "absolute" vulnerability level. Vulnerability is a construct, the outcome of complex interactions in the coupled human-environment system. It is easier to observe in the aftermath of a major shock than to measure beforehand.[4] The research community also does not fully understand the functional form of the relationship among indicators or among the components that contribute to vulnerability (Hinkel, 2011). Following standard practice, we assume a linear relationship between the input layers and the conceptual category being measured. Yet the functional relationship might be very different. It might be a step function, or sigmoid, or asymptotic if there are critical thresholds involved; or it might be exponential if high values trigger cascading problems that do not show up at lower levels (Baptista, 2014; de Sherbinin et al., 2014).

As next steps, it is worth considering the development of higher spatial resolution impact assessments for selected areas of particular concern because of their importance for biodiversity conservation or exposure of populations and economic assets. Impact assessments vary in their sophistication, from simple overlay analyses identifying the population or land area exposed to hazards of different magnitudes (with area but not magnitude explicitly mapped) to modeling approaches based on probability distribution functions for different magnitude events that include damage functions and cost curves. One approach would be to use DIVA, but with a narrower focus on specific segments of the coast containing settlements with populations greater than 0.5 million or 1 million, analyzing results with an eye towards illuminating urban adaptation responses. A number of frameworks and risk assessment tools at the urban scale are available and could be applied and tailored to the regional context (e.g., Moench et al., 2011; Dickson et al., 2012). In lieu of DIVA, one could consider the Decision Support System for Coastal Climate Change Impact Assessment (DESYCO) decision support system (Torresan et al., 2012) with a primary focus on infrastructure and ecosystem impacts. Another option might be to take a sectoral approach, focusing on a particularly important element of the economic infrastructure for urban populations (e.g., electricity generation, water supply, or road infrastructure) and assessing likely impacts on these sectors from climate extremes (e.g., flood, surge, or drought) or longer-term projected trends. This approach would require higher quality data inputs than were available for this study.

---

[4] The literature speaks of vulnerability being an emergent phenomena (Birkmann and Fernando, 2008). It is revealed when the system is stressed by climatic, economic, or other shocks and perturbations.

A spatial decision support tool (i.e., a "DST" or mapping system) for West African coastal climate adaptation planning could be of use to a range of decision makers in the region. A major purpose of such a system would be to nurture a shared understanding of climate risks in the region, across multiple stakeholders, and grounded in the best science and data in order to support robust climate adaptation decision making. Although climate adaptation planning is already taking place in the region, at least to some degree, these planning processes are not always guided by a strong evidence base, and may not be grounded in a realistic view of future projections of population and economic activity. The DST would not be a "final product" as much as a process of building a system while working with stakeholders in an iterative manner. The system would foster a policy environment of continuous learning as ongoing observations are incorporated within a platform that supports both exploratory investigation of patterns and trends as well as formal statistical tests. It should support transparent examination of how risks, responses, and results would be linked up across multiple sectors, multiple jurisdictions, and multiple stakeholder groups.

6.0 GLOSSARY

Closed forest: A forest with tree canopy coverage of 60 to 100 percent.

Digital elevation model: A digital model or three-dimensional representation of a terrain's surface created from terrain elevation data.

Geographic information system (GIS): A computer application used to store, view, and analyze geographical information, especially maps.

Subsidence: Areas where the land is sinking owing to tectonics, isostasy (where weight is added), global SLR, natural substrate compaction, and water extraction.

Thermal expansion: The tendency of matter to change in volume in response to a change in temperature. When a substance is heated, its particles begin moving more and thus usually maintain a greater average separation.

7.0 SOURCES

ActionAid. (2006). Climate change, urban flooding, and the rights of the urban poor in Africa: Key findings from six African cities. ActionAid.

Adeoye, N. O., Ayanlade, A., & Babatimehin, O. (2009). Climate change and menace of floods in Nigerian cities: Socioeconomic implications. *Advances in Natural and Applied Sciences, 3*(3), 369-377.

Agbola, T., & Agunbiade, E. M. (2009). Urbanization, slum development and security of tenure: The challenges of meeting Millenium Development Goal 7 in metropolitan Lagos, Nigeria. de Sherbinin, A., Rahman, A., Barbieri, A., Fotso, J. C. & Zhu Y. (Eds.), *Urban Population-Environment Dynamics in the Developing World: Case Studies and Lessons Learned*. Paris: Committee for International Cooperation in National Research in Demography (CICRED).

Aliou, D. M. (2012). Personal Communication.

Appeaning Addo, K. (2013). Assessing coastal vulnerability index to climate change: The case of Accra–Ghana. *Proceedings of the 12th International Coastal Symposium (Plymouth, England), Journal of Coastal Research,* (65), 1892-1897. Retrieved from 10.2112/si65-320.1

Baptista, S. (2014). *Design and use of composite indices in assessments of climate change vulnerability and resilience.* Technical Paper for the USAID African and Latin American Resilience to Climate Change (ARCC) project. Washington, D.C.: USAID.

Berry, P.A.M., Smith, R., & Benveniste, J. (2008). ACE2: The new global digital elevation model. IAG International Symposium on Gravity, Geoid & Earth Observation 2008, Chania, Crete, 23-27 June 2008.

Birkmann J., & Fernando N. (2008). Measuring revealed and emergent vulnerabilities of coastal communities to tsunami in Sri Lanka. *Disasters, 32*(1), 82-105. Retrieved from 10.1111/j.1467-7717.2007.01028.x.

Blankespoor, B., Dasgupta, S., & Laplante, B. (2012). Sea-level rise and coastal wetlands: Impacts and costs. *Policy research working paper*: The World Bank, Development Research Group, Computational Tools & Environment and Energy Teams.

BMZ (German Federal Ministry for Economic Cooperation and Development). (2014). The vulnerability sourcebook: Concept and guidelines for standardised vulnerability assessments. Berlin, Germany: GIZ (Deutsche Gesellschaft fur Internationale Zusammenarbeit).

Boko, M., Niang, I., Nyong, A., Vogel, C., Githeko, A., Medany, M., . . . Yanda, P. (2007). Climate change 2007: Impacts, adaptation and vulnerability. Contribution of Working Group II to the Fourth Assessment Report of the Intergovernmental Panel on Climate Change. In O. F. C. M.L. Parry, J.P. Palutikof, P.J. van der Linden, and C.E. Hanson (Ed.). Cambridge, UK: IPCC.

Brakenridge, G.R. Global Active Archive of Large Flood Events: Dartmouth Flood Observatory, University of Colorado.

Brakenridge, G.R., Syvitski, J.P.M., Overeem, I., Higgins, S.A., Kettner, A.J., Stewart-Moore, J.A., & Westerhoff, R. (2013). Global mapping of storm surges and the assessment of coastal vulnerability. *Natural Hazards, 66*(3), 1295-1312. Retrieved from 10.1007/s11069-012-0317-z

Brown, S., Kebede, A. S., & Nicholls, R. J. (2011). Sea-level rise and impacts in Africa, 2000 to 2100. White paper by the School of Civil Engineering and the Environment, University of Southampton. Southampton, UK: University of Southampton.

Brown, S., Nicholls, R. J., Hanson, S., Brundrit, G., Dearing, J. A., Dichson, M. E., . . . Woodroffe, C. D. (2014). Shifting perspectives on coastal impacts and adaptation. *Nature Climate Change*, 4, 752-755.

Busby, J.W., Smith, T.G., White, K.L., & Strange, S.M. (2013). Climate change and insecurity: Mapping vulnerability in Africa. *International Security, 37*(4), 132-172. Retrieved from 10.1162/ISEC_a_00116

Center for International Earth Science Information Network (CIESIN) Columbia University. (2014). Gridded Population of the World, version 4 (alpha). Palisades, NY: NASA Socioeconomic Data and Applications Center (SEDAC).

Center for International Earth Science Information Network (CIESIN) Columbia University. (2013). Low elevation coastal zone (LECZ) urban-rural population and land area estimates, version 2. Palisades, NY: NASA Socioeconomic Data and Applications Center (SEDAC).

Center for International Earth Science Information Network (CIESIN), Columbia University, (2012). National aggregates of geospatial data: Population, landscape and climate estimates, v3 (PLACE III), Palisades, NY: NASA Socioeconomic Data and Applications Center (SEDAC).

Center for International Earth Science Information Network (CIESIN), Columbia University. (2011). *MR4: estimating net migration by ecosystem and by decade: 1970–2010 Migration and global environmental change*. London: Foresight.

Cutter, S.L., B.J. Boruff, & W.L. Shirley. (2003). Social vulnerability to environmental hazards. *Social Science Quarterly, 84*(2), 242-261. Retrieved from 10.1111/1540-6237.8402002

Dasgupta, S., Laplante, B., Murray, S., & Wheeler, D. (2009). *Sea-level rise and storm surges: A comparative analysis of impacts in developing countries*. World Bank policy research working paper 4901.

de Sherbinin, A. (2014). *Spatial climate change vulnerability assessments: A review of data, methods and issues*. Technical paper for the USAID African and Latin American Resilience to Climate Change (ARCC) project. Washington, D.C.: USAID.

de Sherbinin, A., Chai-Onn, T., Giannini, A., Jaiteh, M., Levy, M., Mara, V., & Pistolesi, L. (2014). *Mali climate vulnerability mapping*. Technical report for the USAID African and Latin American Resilience to Climate Change (ARCC) project. Washington, D.C.: USAID. Retrieved from http://community.eldis.org/.5bf8c6aa

de Sherbinin, A., Lacko, A., & Jaiteh, M. (2012). Evaluating the risk to Ramsar Sites from climate change induced sea-level rise. *Ramsar Convention on Wetlands of International Importance Scientific and Technical Review Panel (STRP) briefing note no. 5*. Gland, Switzerland: Ramsar Secretariat.

Dickson, E., Baker, J. L., Hoornweg, D., & Tiwari, A. (2012). Urban risk assessments: Understanding disaster and climate risk in cities. Washington, D.C.: World Bank.

Doll, C.N.H. (2008). CIESIN Thematic Guide to Night-time Light Remote Sensing and its Applications, Palisades, NY: Center for International Earth Science Information Network of Columbia University. Retrieved from http://sedac.ciesin.columbia.edu/tg/.

Douglas, I., Alam, K., Maghenda, M., Mcdonnell, Y., Mclean, L., & Campbell, J. (2008). Unjust waters: Climate change, flooding and the urban poor in Africa. *Environment and Urbanization*, 20, 187-205.

Ellison, J., & Zouh, I. (2012). Vulnerability to climate change of mangroves: assessment from Cameroon, Central Africa. *Biology, 1*(3), 617-638. Retrieved from 10.3390/biology1030617

Emanuel, K. (2005). Increasing destructiveness of tropical cyclones over the past 30 years. *Nature,* 436, 686-688. Retrieved from 10.1038/nature03906

Fekete, A. (2012). Spatial disaster vulnerability and risk assessments: challenges in their quality and acceptance. *Natural Hazards*, 61, 1161-1178. http://dx.doi.org/10.1007/s11069-011-9973-7

GCLME Coordinating Unit. (2006). Guinea Current Large Marine Ecosystem (GCLME) transboundary diagnostic analysis: GCLME Coordinating Unit with support from the GEF, UNIDO, UNDP, UNEP, US-NOAA, NEPAD, FAO, and IMO.

GCLME. (2010). State of the coastal and marine ecosystems in the guinea current large marine ecosystem region: Interim Guinea Current Commission with the assistance of GEF/UNIDO/UNDP/UNEP/US-NOAA/NEPAD/FAO and IMO.

Giri, C., Ochieng, E., Tieszen, L. L., Zhu, Z., Singh, A., Loveland, T., . . . Duke, N. (2010). Status and distribution of mangrove forests of the world using earth observation satellite data. *Global Ecology and Biogeography, 20*(1), 154-159. Retrieved from 10.1111/j.1466-8238.2010.00584.x

Gornitz, V., White, T.W., & Cushman, R.M. (1991). Vulnerability of the U.S. to future sea-level rise. Coastal Zone '91. In *Proceedings of Seventh Symposium on Coastal and Ocean Management* (pp. 2354-2368): ASCE.

Gornitz, V.M., Daniels, R.C., White, T.W., & Birdwell, K.R. (1994). The development of a coastal risk assessment database: Vulnerability to sea-level rise in the U.S. Southeast. *Journal of Coastal Research* (ArticleType: research-article/Issue Title: Special Issue No. 12. Coastal Hazards: Perception, Susceptibility and Mitigation / Full publication date: 1994/Copyright © 1994 Coastal Education & Research Foundation, Inc.), 327-338. Retrieved from 10.2307/25735608

Hansen, M.C., Potapov, P.V., Moore, R., Hancher, M., Turubanova, S.A., Tyukavina, A., . . . Townshend, J. R. (2013). High-resolution global maps of 21st-century forest cover change. [Research Support, Non-U.S. Gov't, Research Support, U.S. Gov't, Non-P.H.S.]. *Science, 342*(6160), 850-853. Retrieved from 10.1126/science.1244693

Hinkel, J. (2011). Indicators of vulnerability and adaptive capacity: Towards a clarification of the science–policy interface. *Global Environmental Change*, 21(1), 198-208. Retrieved from http://dx.doi.org/10.1016/j.gloenvcha.2010.08.002

Hinkel, J., Brown, S., Exner, L., Nicholls, R.J., Vafeidis, A.T., & Kebede, A.S. (2012). Sea-level rise impacts on Africa and the effects of mitigation and adaptation: an application of DIVA. *Regional Environmental Change, 12*(1), 207-224. Retrieved from 10.1007/s10113-011-0249-2

Ibe, A.C. 1996. "The Niger Delta and Sea-Level Rise." In: *Sea-level rise and coastal subsidence: Causes, consequences, and strategies*, J. Milliman and B.U. Haq (Eds.). Dordrecht, NL: Kluwer Academic Publishers.

IPCC. (2013). Summary for Policymakers. *Climate change 2013: The physical science basis*. Contribution of Working Group I to the Fifth Assessment Report of the Intergovernmental Panel on Climate Change [Stocker, T.F., Qin, D., Plattner, G.-K., Tignor, M., Allen, S.K., Boschung, J., Nauels, A., Xia, Y., Bex, V., and Midgley, P.M. (eds.)]. Cambridge University Press, Cambridge, United Kingdom and New York, NY, USA.

IPCC. (2012). Managing the risks of extreme events and disasters to advance climate change adaptation. In C. B. Field, et al. (Eds.), *A Special Report of Working Groups I and II.* Cambridge: Intergovernmental Panel on Climate Change.

Joiner, E., Kennedo, D., & Sampson, J. (2012). Vulnerability to climate change in West Africa: Adaptive capacity in the regional context. In J. W. Busby, K. L. White & T. G. Smith (Eds.), *Student working paper no. 4*: CCAPS: Climate Change and African Political Stability.

Kopp, R.E., Horton, R.M., Little, C.M., Mitrovica, J.X., Oppenheimer, M., Rasmussen, D.J., Strauss, B.H., & Tebaldi, C. (2014). Probabilistic 21st and 22nd century sea-level projections at a global network of tide-gauge sites. *Earth's Future*, 2, 383–406.

Gilbert, M., Snow, R.W., Noor, A.M., & Tatem, A.J. (2012) Population Distribution, Settlement Patterns and Accessibility across Africa in 2010. *PLOS One*. Retrieved from 10.1371/journal.pone.0031743

Linard, C., Gilbert, M., et al. (2012). Population Distribution, Settlement Patterns and Accessibility Across Africa in 2010. *PLoS One, 7(2),* e31743.

López-Carr, D., Pricope, N.G., Aukema, J.E., Jankowska, M.M., Funk, C., Husak, G., and Michaelsen, J. (2014). A spatial analysis of population dynamics and climate change in Africa: Potential vulnerability hot spots emerge where precipitation declines and demographic pressures coincide. *Population & Environment,* 35, 323–339.

Maloney, M.C., & Preston, B.L. (2014). A geospatial dataset for U.S. hurricane storm surge and sea-level rise vulnerability: Development and case study applications. *Climate Risk Management*, 2, 26–41.

Moench, M., Tyler, S., et al. (2011), Catalyzing urban climate resilience: applying resilience concepts to planning practice in the Asian Cities Climate Change Research Network (ACCCRN Program) (2009–2011), 306 pp, ISET-Boulder: Bangkok.

Muttarak, R., & Lutz, W. (2014). Is education a key to reducing vulnerability to natural disasters and hence unavoidable climate change? *Ecology and Society,* 19(1), 42.

National Geographic. (2013). If all the ice melted. September 2013. Retrieved from http://ngm.nationalgeographic.com/2013/09/rising-seas/if-ice-melted-map.

Newton, A., and Weichelsgartner, J. (2014). Hotspots of coastal vulnerability: A DPSIR analysis to find societal pathways and responses. *Estuarine, Coastal and Shelf Science,* 140, 123-133.

Niang, I. (2012). Coastal erosion and the adaptation to climate change in coastal West Africa. *Adaptation and Mitigation Strategies*, 249-250.

Nicholls, R. J., Wong, P. P., Burkett, V. R., Codignotto, J. O., Hay, J. E., McLean, R. F., . . . Woodroffe, C. D. (2007). Coastal systems and low-lying areas. Climate change 2007: Impacts, adaptation and vulnerability. Contribution of Working Group II to the Fourth Assessment Report of the Intergovernmental Panel on Climate Change. In O. F. C. M.L. Parry, J.P. Palutikof, P.J. van der Linden, and C.E. Hanson (Ed.), (pp. 315-356). Cambridge, UK: Cambridge University Press.

O'Brien, K.L., Eriksen, S., Nygaard, L., and Schjolden, A. (2007). Why different interpretations of vulnerability matter in climate change discourses. *Climate Policy,* 7, 73-88.

O'Neill, B. C., Kriegler, E., Riahi, K., Ebi, K. L., Hallegatte, S., et al. (2014). A new scenario framework for climate change research: the concept of shared socioeconomic pathways. *Climatic Change*, *122*(3), 387-400.

OECD (Organization for Economic Cooperation and Development). (2008). *Handbook on constructing composite indicators: Methodology and user guide*. Paris: OECD.

Parry, M. L., Canziani, O. F., Palutikof, J. P. et al. (2007). *Technical Summary. Climate change 2007: Impacts, adaptation and vulnerability*. Contribution of Working Group II to the Fourth Assessment Report of the Intergovernmental Panel on Climate Change. M.L. Parry, O.F. Canziani, J.P. Palutikof, P.J. van der Linden and C.E. Hanson (Eds.). Cambridge, UK: Cambridge University Press, pp. 23-78.

Pfeffer, W., Harper, J., O'Neel, S. (2008). Kinematic constraints on glacier contributions to 21st-century sea-level rise. *Science,* 321(5994), 1340-1343.

Ramieri, E., Hartley, A., Barbanti, A., Duarte Santos, F., Gomes, A., Hilden, M., . . . Santini, M. (2011). Methods for assessing coastal vulnerability to climate change. *ETC CCA technical paper*: European Environment Agency: European Topic Centre on Climate Change Impacts, Vulnerability and Adaptation.

Thornton, P.K., Jones, P.G., Owiyo, T., Kruska, R.L., Herrero, M., Orindi, V., Bhadwal, S., Kristjanson, P., Notenbaert, A., Bekele, N. and Omolo, A. (2008). Climate change and poverty in Africa: Mapping hotspots of vulnerability. *AfJARE*, 2(1) March 2008.

Torresan, S., Gallina, V., Giannini, V., Rizzi, J., Zabeo, A., Critto, A., Marcomini, A. (2012). DESYCO: a Decision Support System to provide climate services for coastal stakeholders dealing with climate change impacts. Proceedings of the EGU General Assembly 2012, held 22-27 April 2012 in Vienna, Austria.

Twusami, Y. A., & Merem, E. C. (2006). GIS and remote sensing applications in the assessment of change within a coastal environment in the Niger Delta region of Nigeria. *International Journal of Environmental Research and Public Health, 3*(1), 98-106.

UNEP/UNISDR (United Nations Environment Programme/UN International Strategy for Disaster Reduction). (2013). Global estimated risk index for flood hazard. Châtelaine, Genève UNEP/DEWA/GRID-Europe.

UNEP-WCMC (World Conservation Monitoring Center of the United Nations Environment Programme). (2013). World Database on Protected Areas (WDPA), July 2013 Release [Downloaded: July 2013]. The WDPA is a joint product of UNEP and IUCN, prepared by UNEP-WCMC, supported by IUCN WCPA and working with Governments, the Secretariats of MEAs and collaborating NGOs. For further information: protectedareas@unep-wcmc.org or http://www.wdpa.org.

Vörösmarty, C. J., Syvitski, J., Day, J., de Sherbinin, A., Giosan, L., and Paola, C. (2009). Battling to save the world's river deltas. *Bulletin of the Atomic Scientists*. March/April 2009. Retrieved from http://dx.doi.org/10.2968/065002005.

WWF and CESR (World Wide Fund for Nature and the Center for Environmental Systems Research, University of Kassel). (2004). The Global Lakes and Wetlands Database (Level 3). Retrieved from http://worldwildlife.org/publications/global-lakes-and-wetlands-database-lakes-and-wetlands-grid-level-3.

ANNEX 1: DATA DESCRIPTIONS

The map metadata are divided into the following sections: Climate exposure layers (Section A-1.1), social vulnerability data layers (Section A-1.2), economic system data layers (Section A-1.3), and natural system data layers (Section A-1.4). Where raw data layers have been converted to indicators, we also provide histograms of the data distribution in native units (raw scale) and in transformed scores on the 0–100 scale.

A-1.1 CLIMATE EXPOSURE LAYERS

FIGURE A-1.1.1: ELEVATION (ACE2)

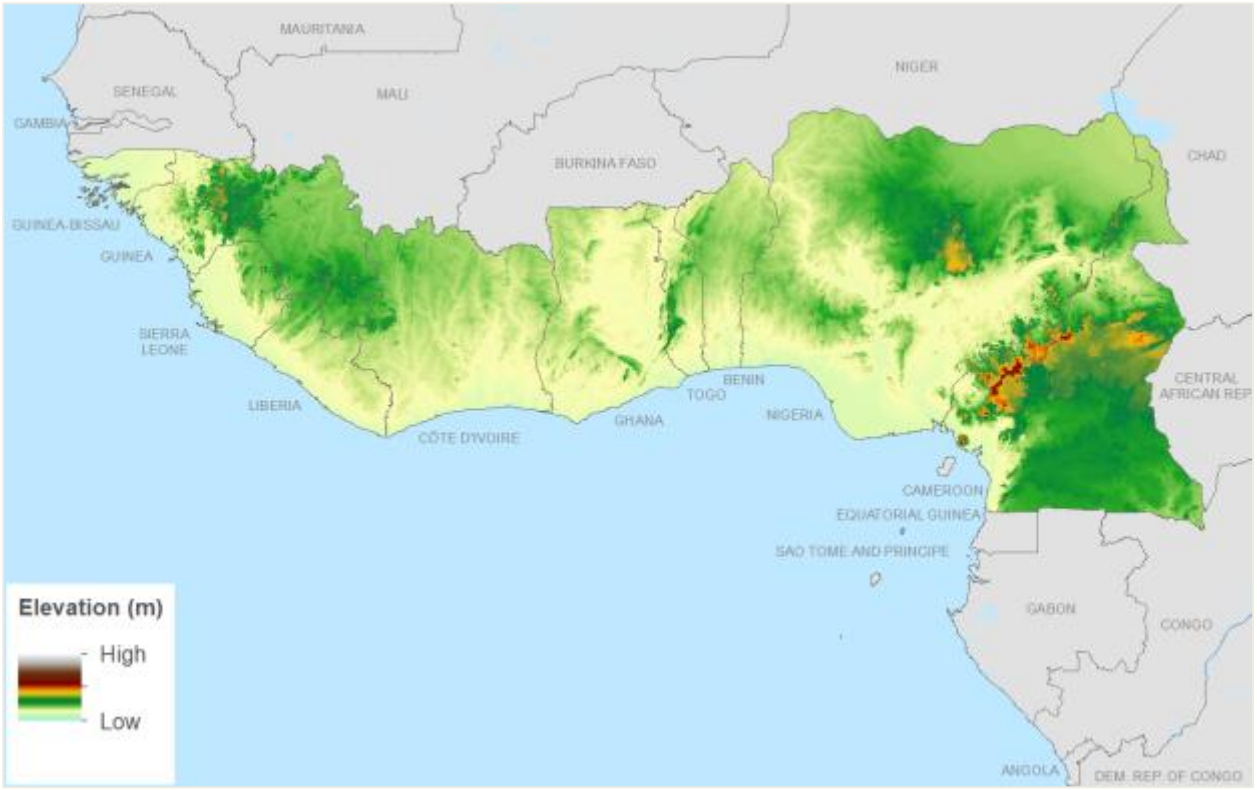

TABLE A-1.1.1: ACE2

Title:	ACE2, Altimeter Corrected Elevations 2
Indicator Code:	ACE2
Component:	Exposure
Rationale:	ACE2 provides a best available measure of coastal elevation in forested ecosystems.
URL:	http://tethys.eaprs.cse.dmu.ac.uk/ACE2/shared/overview
Data Set:	The new ACE2 data set has been created by synergistically merging the SRTM dataset with Satellite Radar Altimetry within the region bounded by 60°N and 60°S. Over the areas lying outside the SRTM latitude limits, other sources have been used including Global Observations to Benefit the Environment (GLOBE) and the original Altimeter Corrected Elevations (ACE) digital elevation model (DEM), together with new matrices derived from reprocessing the Economic and Social Research Institute (ERS1) Geodetic Mission data set with an enhanced retracking system, and the inclusion of data from other satellites. The scientific reference for this data set is: Berry, P.A.M., Smith, R., and Benveniste, J. (2008). ACE2: the new Global Digital Elevation Model. IAG International Symposium on Gravity, Geoid & Earth Observation 2008, Chania, Crete, 23–27 June 2008.
Units:	Meters
Limitations:	All global DEMs have limitations in accuracy since they are based on satellite data. Lidar data would be more accurate but are not available over large areas of the world, and especially in West Africa.
Spatial Extent:	Global
Spatial Resolution:	30 arc-second (1km)
Year of Publication:	2009
Time Period:	
Additional Notes:	
Date:	5/7/2014
Format:	Raster
File Name:	00N000E_LAND_30S.raw, 00N015E_LAND_30S.raw, 00N015W_LAND_30S.raw, 00N030E_LAND_30S.raw, 00N030W_LAND_30S.raw, 15N000E_LAND_30S.raw, 15N015E_LAND_30S.raw, 15N015W_LAND_30S.raw, 15N030E_LAND_30S.raw, 15N030W_LAND_30S.raw, 30N000E_LAND_30S.raw, 30N015E_LAND_30S.raw, 30N015W_LAND_30S.raw, 30N030E_LAND_30S.raw, 30N030W_LAND_30S.raw
Contact person:	N/A
Contact details:	N/A

FIGURE A-1.1.2: FLOOD RISK

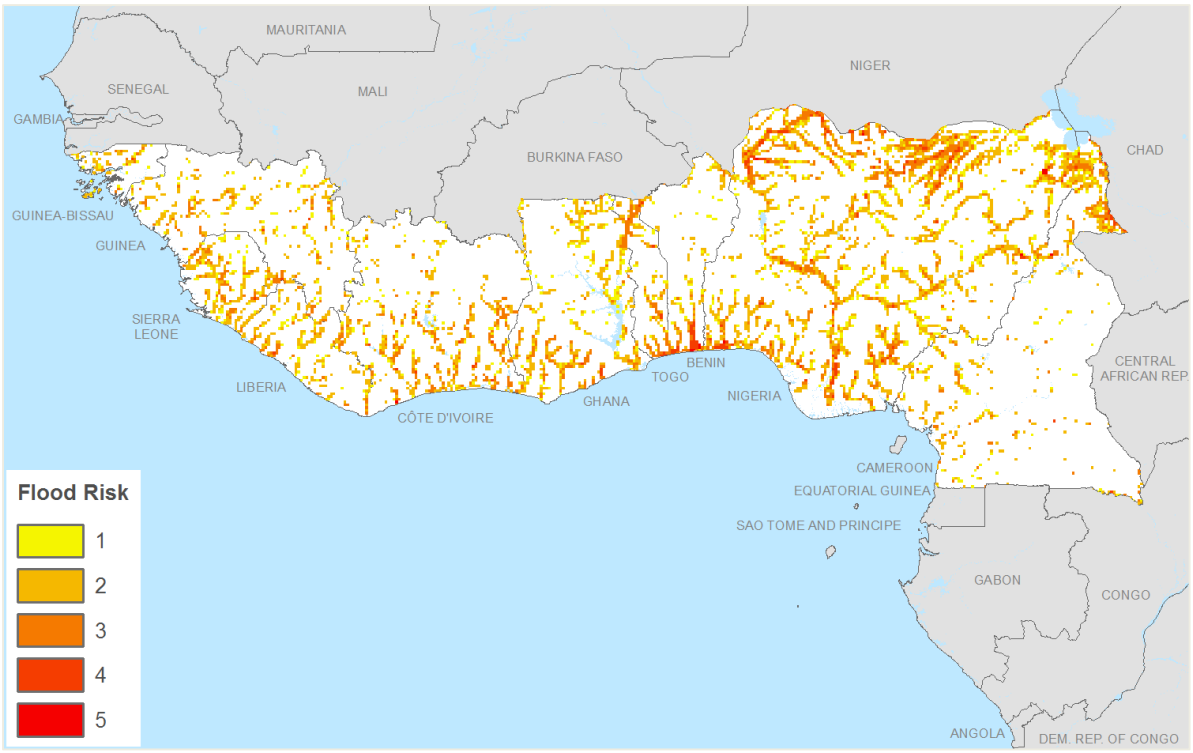

TABLE A-1.1.2: FLOOD RISK

Title:	**Global estimated risk index for flood hazard**
Indicator Code:	FLRSK
Component:	Exposure
Rationale:	Floods are important causes of economic loss as well as morbidity (owing to the contribution of standing water to disease spread) and mortality.
URL:	http://preview.grid.unep.ch/index.php?preview=data&events=floods&evcat=5&lang=eng
Data Set:	This data set includes an estimate of the global risk induced by flood hazard. Unit is estimated risk index from 1 (low) to 5 (extreme). This product was designed by UNEP/GRID-Europe for the Global Assessment Report on Risk Reduction (GAR). It was modeled using global data. Credit: UNEP/GRID-Europe.
Units:	Flood risk zones from 1 to 5
Limitations:	This data set is modeled and at a coarse spatial resolution, and hence only approximates the degree of risk in any given location.
Spatial Extent:	Global
Spatial Resolution:	8 arc-minutes (approximately 14km at the equator)
Year of Publication:	2011
Time Period:	
Additional Notes:	
Date:	5/7/2014
Format:	Raster
File Name:	floodrisk.tif
Contact person:	N/A
Contact details:	N/A

A-1.2 SOCIAL VULNERABILITY DATA LAYERS

FIGURE A-1.2.1: POPULATION DENSITY, 2010

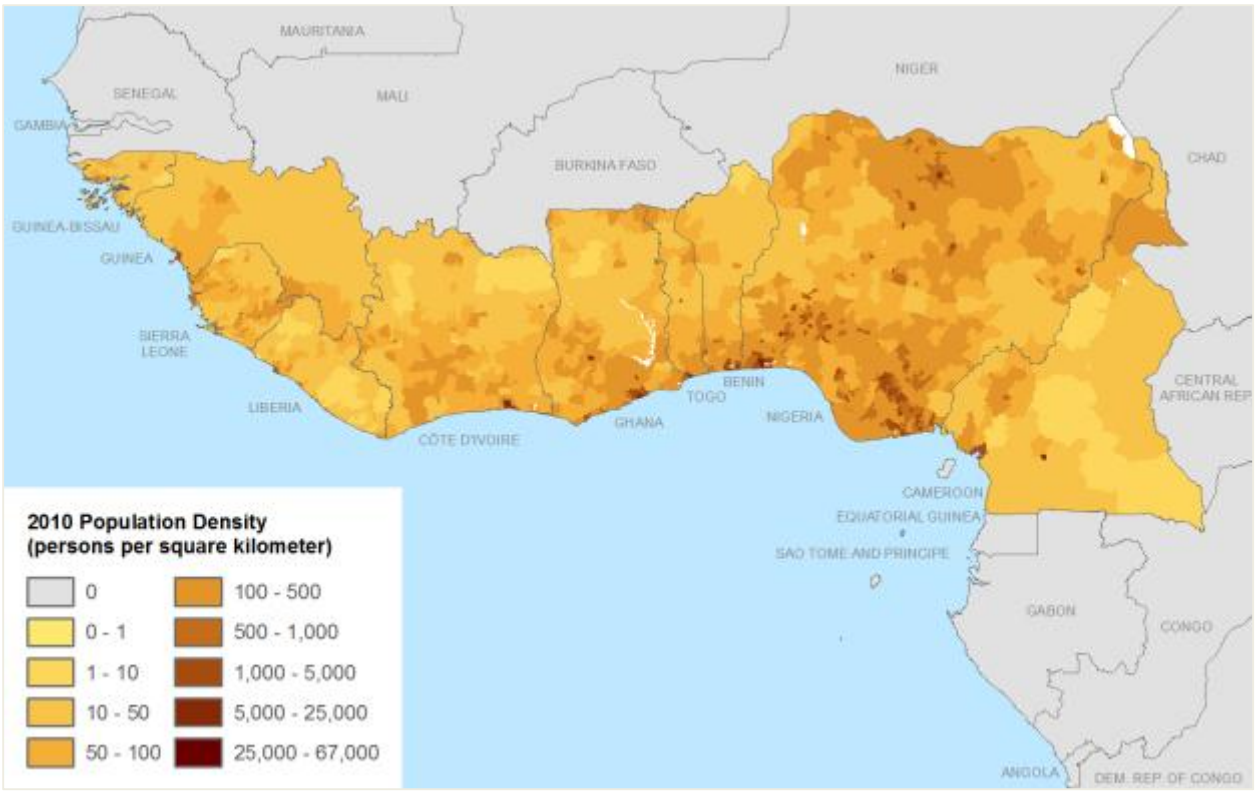

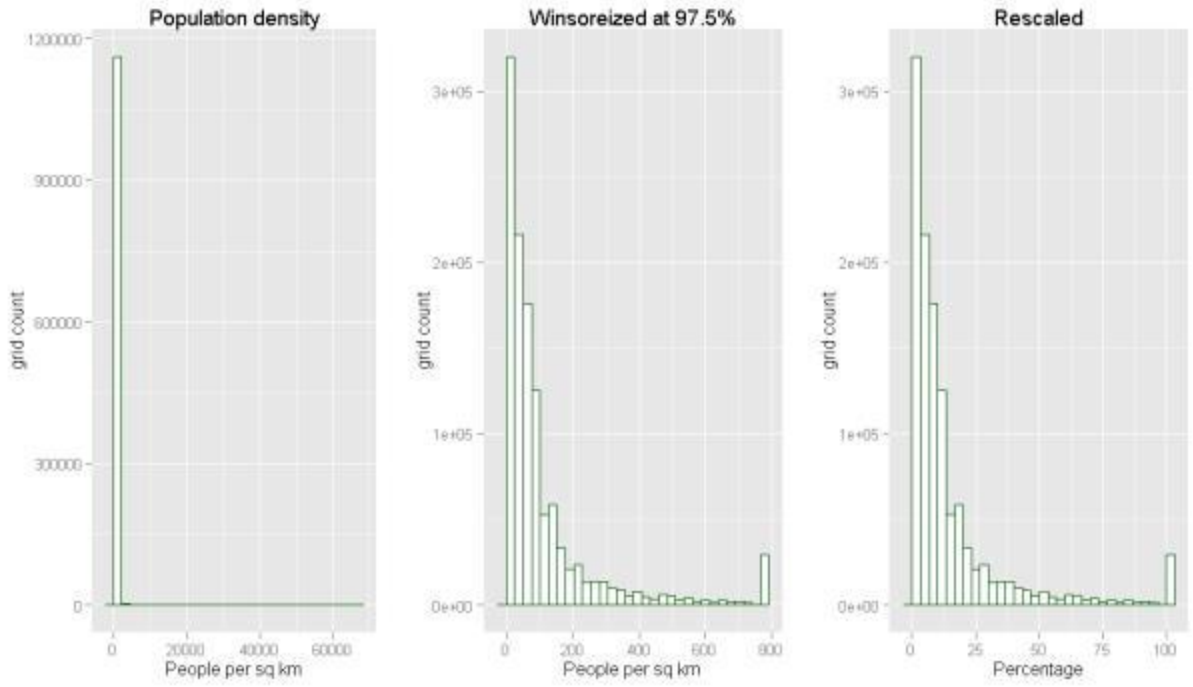

TABLE A-1.2.1: POPULATION DENSITY, 2010

Title:	**Population Density, 2010**
Indicator Code:	POPD
Component:	Adaptive Capacity
Rationale:	Areas with higher population density have more valued attributes exposed to climate stressors.
URL:	The 2010 Gridded Population of the World, Version 4, is in the process of being developed. Version 3 is available at: http://sedac.ciesin.columbia.edu/data/set/gpw-v3-population-count-future-estimates
Data Set:	Gridded Population of the World (GPW), Version 4 (in production). GPW depicts the distribution of human population across the globe. It provides globally consistent and spatially explicit human population information and data for use in research, policy making, and communications. This is a gridded, or raster, data product that renders global population data at the scale and extent required to demonstrate the spatial relationship of human populations and the environment across the globe. The purpose of GPW is to provide a spatially disaggregated population layer that is compatible with data sets from social, economic, and Earth science fields. The gridded data set is constructed from national or subnational input units (usually administrative units) of varying resolutions. The native grid cell resolution of GPWv4 is 30 arc-seconds, or ~1km at the equator. Suggested citation: Center for International Earth Science Information Network (CIESIN), Columbia University. 2005. Gridded Population of the World, Version 4 (GPWv4): Population Count Grid. Alpha version. Palisades, NY: NASA Socioeconomic Data and Applications Center (SEDAC).
Units:	Persons per square kilometer
Limitations:	
Spatial Extent:	Global
Spatial Resolution:	30 arc seconds (~1km)
Year of Publication:	2014
Time Period:	2010
Additional Notes:	The population density raster is derived by dividing GPWv4 2010 population count raster by a land area raster.
Date:	January 2014
Format:	Raster
File Name:	coastal_wa_popden_2010_gpw4
Contact person:	

FIGURE A-1.2.2: POPULATION GROWTH, 2000-2010

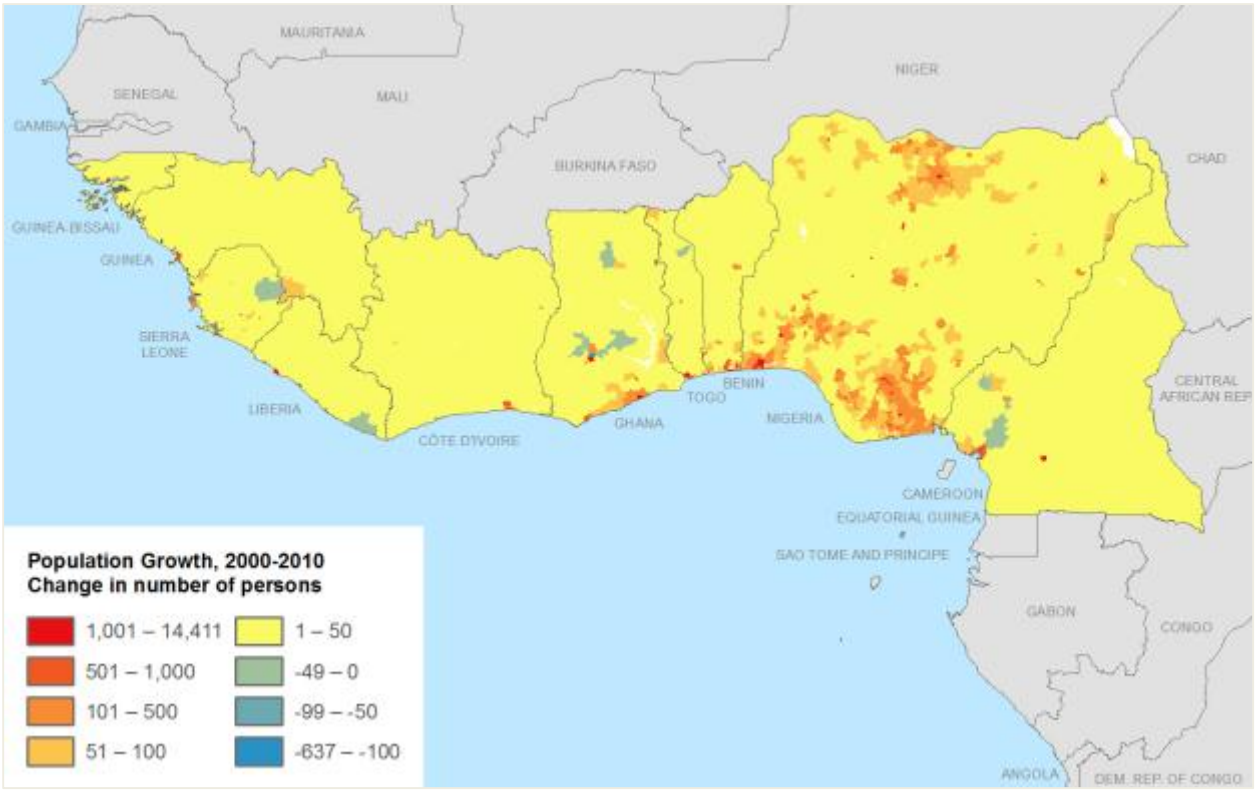

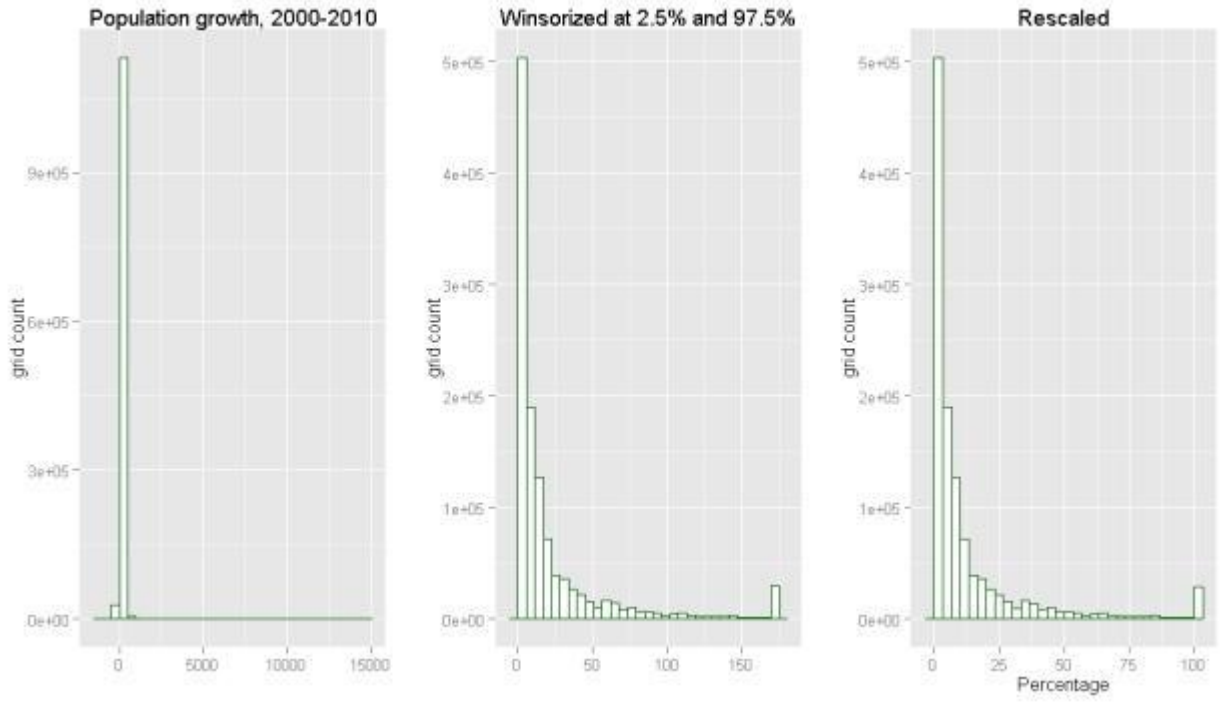

TABLE A-1.2.2: POPULATION GROWTH, 2000-2010

Title:	Population Growth, 2000–2010
Indicator Code:	POPG
Component:	Adaptive Capacity
Rationale:	Population growth in the coastal zone is mostly a function of migration related to coastal urbanization, so this indicator provides insights into highly exposed coastal areas that are seeing high population growth and migration.
URL:	The 2010 Gridded Population of the World, Version 4, is in development. Information on Version 3 is available at: http://sedac.ciesin.columbia.edu/data/collection/gpw-v3
Data Set:	Gridded Population of the World (GPW), Version 4 (in production). GPW depicts the distribution of human population across the globe. It provides globally consistent and spatially explicit human population information and data for use in research, policy making, and communications. This is a gridded, or raster, data product that renders global population data at the scale and extent needed to demonstrate the spatial relationship of human populations and the environment globally. The purpose of GPW is to provide a spatially disaggregated population layer that is compatible with data sets from social, economic, and Earth science fields. The gridded data set is constructed from national or subnational input units (usually administrative units) of varying resolutions. The native grid cell resolution of GPWv4 is 30 arc-seconds, or ~1km at equator.
Units:	Change in number of persons per grid cell
Limitations:	
Spatial Extent:	Global
Spatial Resolution:	30 arc seconds (~1km)
Year of Publication:	Expected 2014
Time Period:	2000 and 2010
Additional Notes:	The population growth raster is derived by subtracting GPWv4 2000 population raster from the GPWv4 2010 population raster.
Date:	May 12, 2014
Format:	Raster
File Name:	coastal_wa_gpw4_popdif_2010_2000
Contact person:	

FIGURE A-1.2.3: SUB-NATIONAL POVERTY AND EXTREME POVERTY PREVALENCE

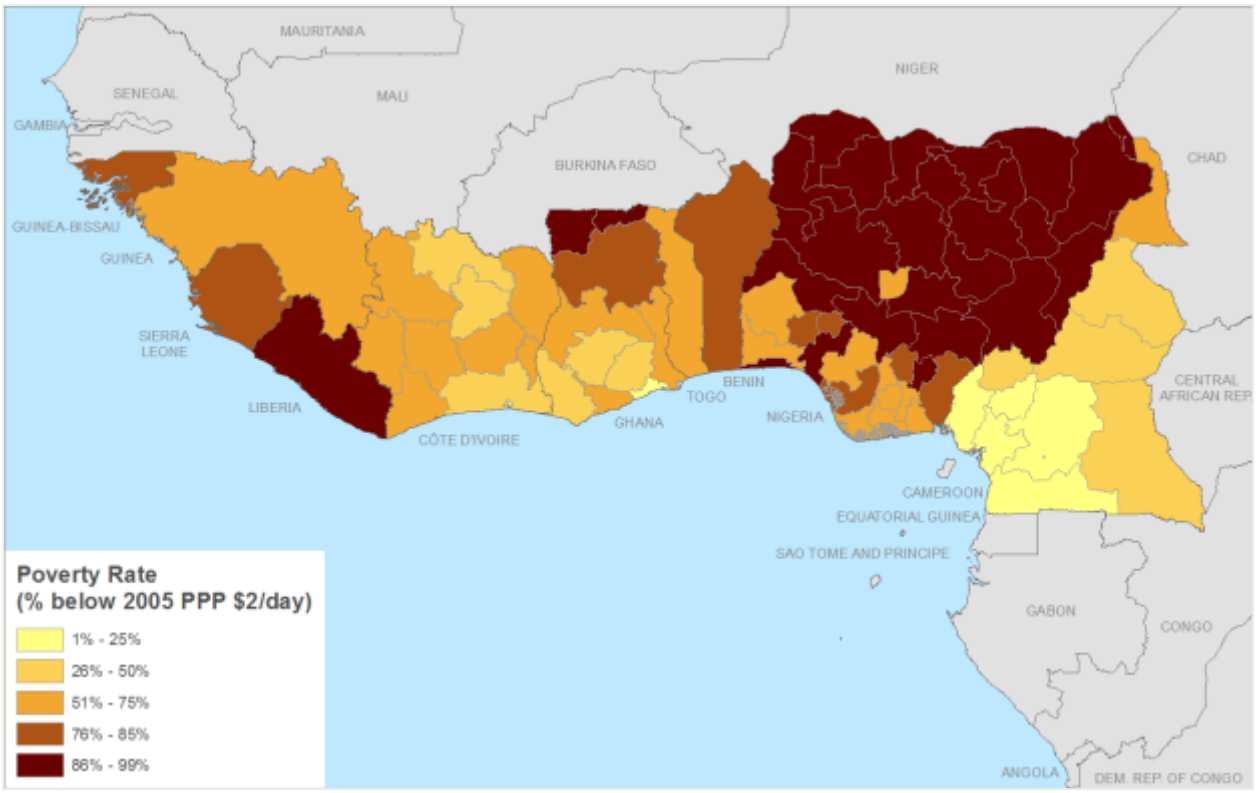

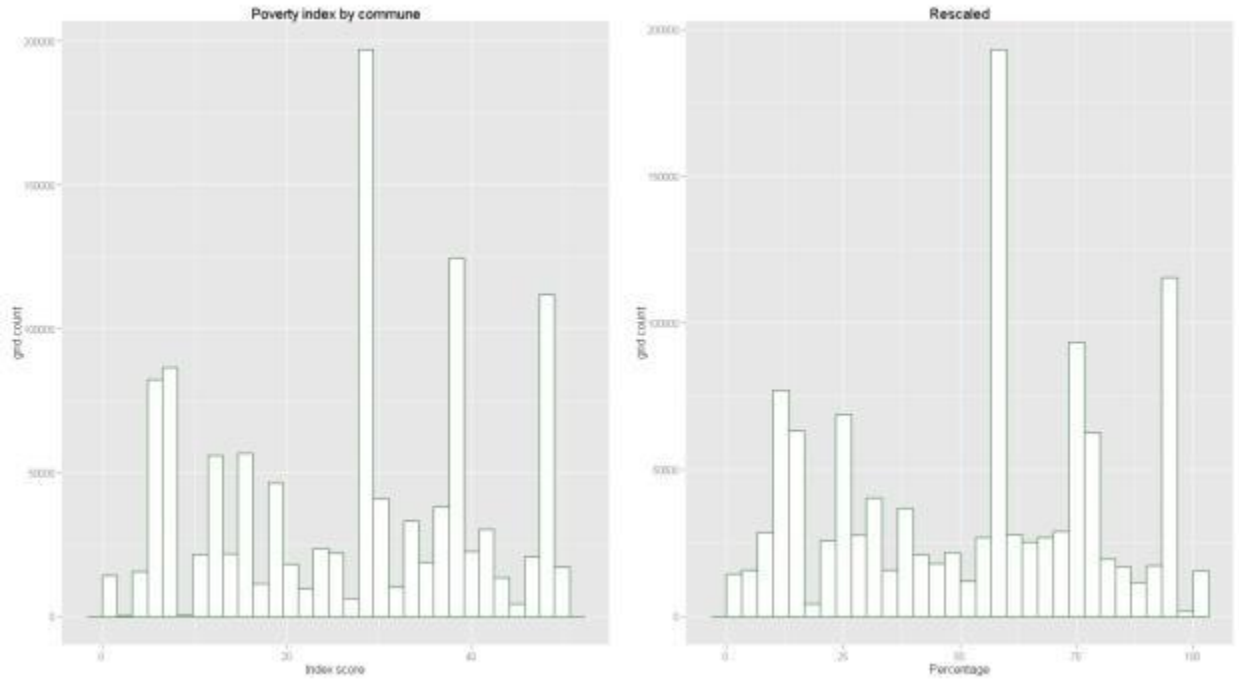

TABLE A-1.2.3: SUB-NATIONAL POVERTY AND EXTREME POVERTY PREVALENCE

Title:	Sub-National Poverty and Extreme Poverty Prevalence
Indicator Code:	POV
Component:	Sensitivity
Rationale:	Poverty levels will affect the "defenselessness" of populations in the low elevation coastal zone.
URL:	http://harvestchoice.org/maps/sub-national-poverty-and-extreme-poverty-prevalence
Data Set:	Estimated poverty measures at 2005 international equivalent purchasing power parity (PPP) dollars $1.25/day and $2/day international poverty lines. Data developed by the Harvest Choice project funded by the Bill and Melinda Gates Foundation.
Units:	Share of total population
Limitations:	
Spatial Extent:	24 countries in sub-Saharan Africa
Spatial Resolution:	Province or district level
Year of Publication:	December 2012
Time Period:	2005
Additional Notes:	Version r12.12
Date:	January 9, 2014
Format:	Shapefile
File Name:	svyMaps_poor_r12.12.shp
Contact person:	N/A
Contact details:	N/A

FIGURE A-1.2.4: MATERNAL EDUCATION LEVELS

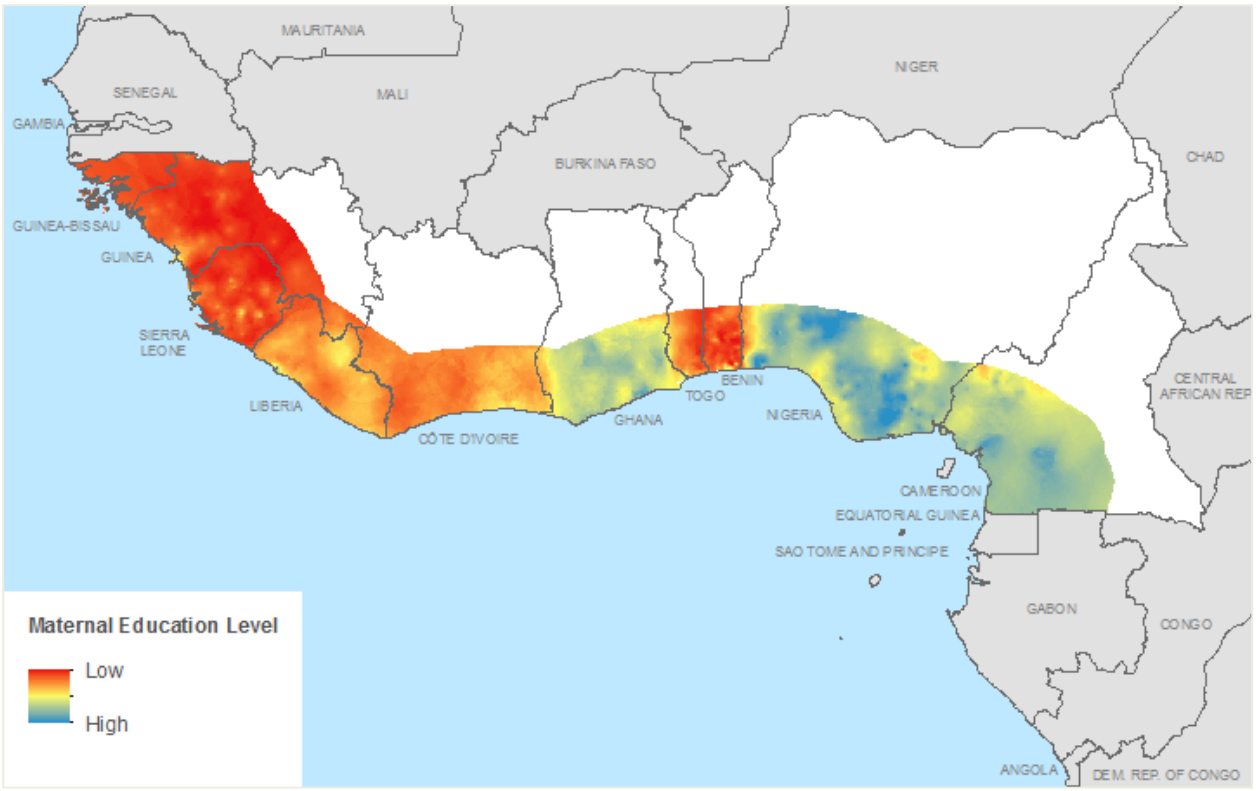

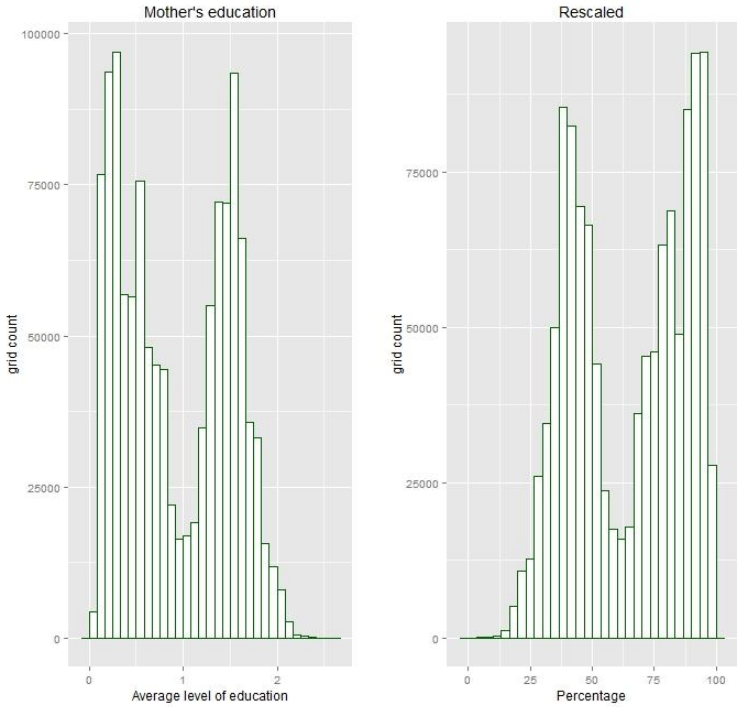

TABLE A-1.2.4: MATERNAL EDUCATION LEVELS

Title:	**Maternal Education Levels**
Indicator Codes:	MEDUC
Component:	Adaptive Capacity
Rationale:	Education can directly influence risk perception, skills and knowledge and indirectly reduce poverty, improve health and promote access to information and resources. When facing natural hazards or climate risks, educated individuals, households and societies are assumed to be more empowered and more adaptive in their response to, preparation for, and recovery from disasters (Muttarak and Lutz, 2014). According to the DHS website, education is a key background indicator in the DHS that helps contextualize a country's health and development situation. There is a strong association between a mother's education and improved health, higher levels of knowledge, and increased levels of empowerment of women.
Source Data Set:	Individual level survey data and cluster points were downloaded from the Measure Demographic and Health Survey (DHS) Spatial Data Repository at http://spatialdata.dhsprogram.com/.
Units:	Years of formal education
Computation:	We processed the individual level data from the DHS surveys to develop average levels of education at the cluster level, which on average represent 100 households. To create a surface from the cluster points, we followed the proceeding steps. We created 30 arc-second (0.00833 degrees; ~1km) *prediction* and *prediction standard error* surfaces from the cluster point data using ArcGIS's Empirical Bayesian Kriging tool. The rasters were subset to the Mali national boundary extent using ArcGIS Extract by Mask tool and a 30 arc-second raster mask generated from a 30 arc-second fishnet. Raster values were extracted using ArcGIS Extract Values to Points tool and the 30 arc-second fishnet centroids. The outputs were exported to .csv tables for re-coding and statistical analysis.
Scoring system:	Raster values were re-scaled to 0-100, with high levels of mother's education equating to low levels of "lack of adaptive capacity"
Limitations:	For limitations, see the DHS Data Quality and Use page, available at: https://www.measuredhs.com/data/Data-Quality-and-Use.cfm.
Spatial Extent:	The 10 coastal West African countries included in this study
Spatial Resolution:	The spatial resolution of the areas represented by each cluster point varies depending on the density of cluster points. The resulting grid was at 30 arc-seconds.
Year of Publication:	The year of the DHS data varied by country. See Time Period field.
Time Period:	Benin (2006), Cameroon (2011), Côte d'Ivoire (2012), Ghana (2008), Guinea (2012), Liberia (2011), Nigeria (2010), Sierra Leone (2008), Togo (1998)
Additional Notes:	
Date:	
Format:	
File Name:	
Contact person:	Valentina Mara, CIESIN

FIGURE A-1.2.5: MARKET ACCESSIBILITY

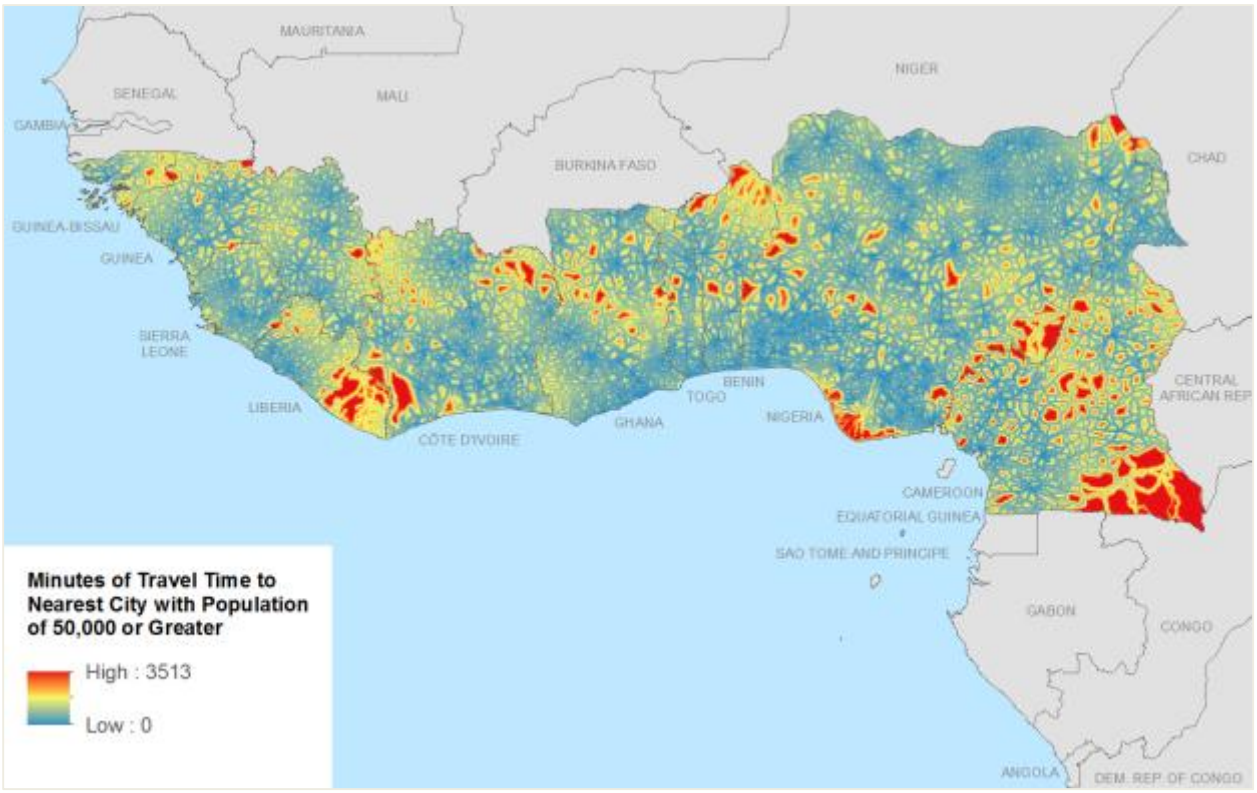

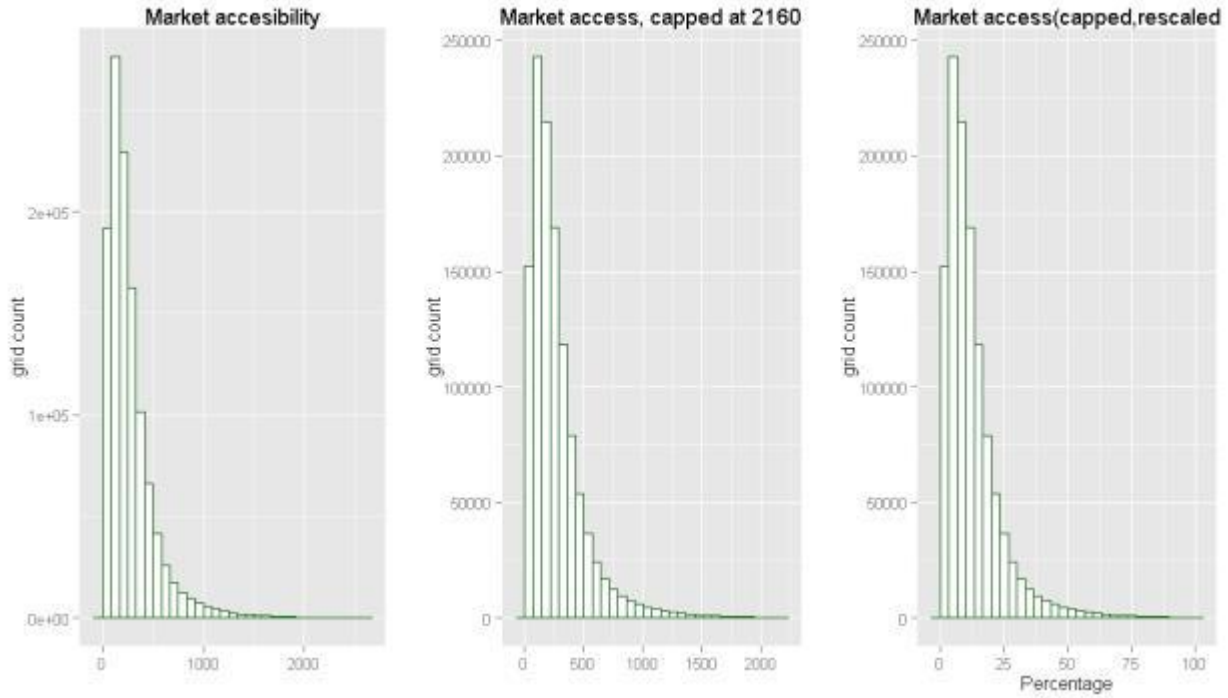

TABLE A-1.2.5: MARKET ACCESSIBILITY

Title:	Market Accessibility
Indicator Code:	MARK
Component:	Adaptive Capacity
Rationale:	An extensive literature shows that road networks and market accessibility plan an important role in development and access to health care and other social services. Greater spatial isolation is assumed to produce higher vulnerability to climate stressors.
URL:	http://bioval.jrc.ec.europa.eu/products/gam/index.htm
Data Set:	Travel Time to Major Cities: A Global Map of Accessibility Accessibility is defined as "the travel time to a location of interest using land (road/off road) or water (navigable river, lake and ocean) based travel." It is computed using a cost-distance algorithm which computes the "cost" (in units of time) of traveling between two locations on a regular raster grid. The raster grid cells contain values which represent the cost required to travel across them, hence this raster grid is often termed a friction-surface. The friction-surface contains information on the transport network and environmental and political factors that affect travel times between locations. Transport networks can include road and rail networks, navigable rivers and shipping lanes. The locations of interest are termed targets, and in the case of this dataset, the targets are cities with population of 50,000 or greater in the year 2000. Citation: Nelson, A. 2008. Travel time to major cities: A global map of accessibility. Global Environment Monitoring Unit–Joint Research Centre of the European Commission, Ispra Italy. Accessed 9/3/2013.
Units:	Pixel values represent minutes of travel time to nearest city with population of 50,000 or greater in the year 2000.
Limitations:	Dates of input data sources range from 1987 (e.g., navigable rivers) to 2008 (e.g., shipping layers), and the road network is based on available public domain data. The data are not to be used for characterizing the general accessibility of an area. It is a measure of access to markets. Website indicates "The assumptions made in the generation of this accessibility map can be found in the description and data sources links on the left," but no description of assumptions were found.
Spatial Extent:	Global
Spatial Resolution:	The data are in geographic projection with a resolution of 30 arc seconds (~1km).
Year of Publication:	2008
Time Period:	Dates of input data sources range from 1987 (e.g., navigable rivers) to 2008 (e.g., shipping layers).
Additional Notes:	Data sources: Target locations: Populated Places Frictions surface components: Road network, railway network, navigable rivers, major waterbodies, shipping lanes, national borders, land cover, urban areas, elevation, and slope.
Date:	Downloaded from: http://bioval.jrc.ec.europa.eu/products/gam/index.htm on 9/3/2013
Format:	Esri Grid (integer)
File Name:	access_50k.gdb
Contact person:	

FIGURE A-1.2.6: CONFLICT (POLITICAL VIOLENCE)

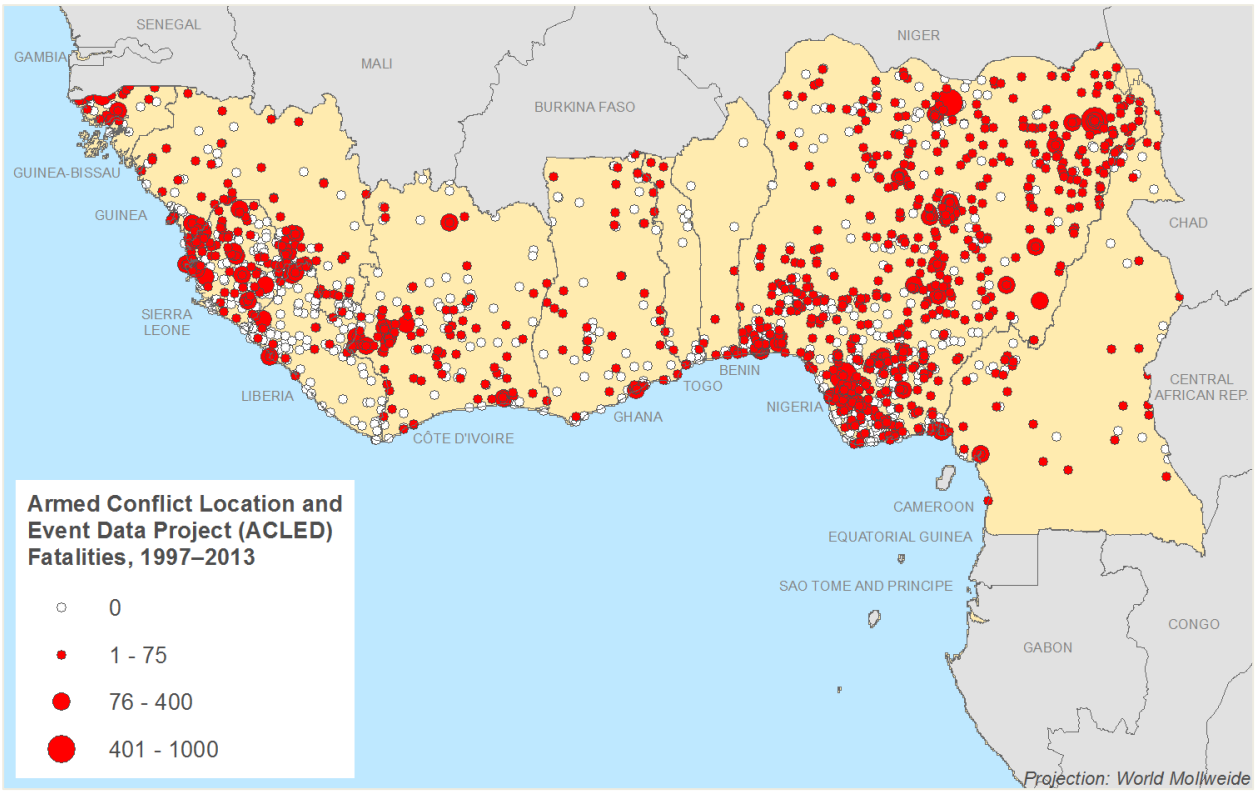

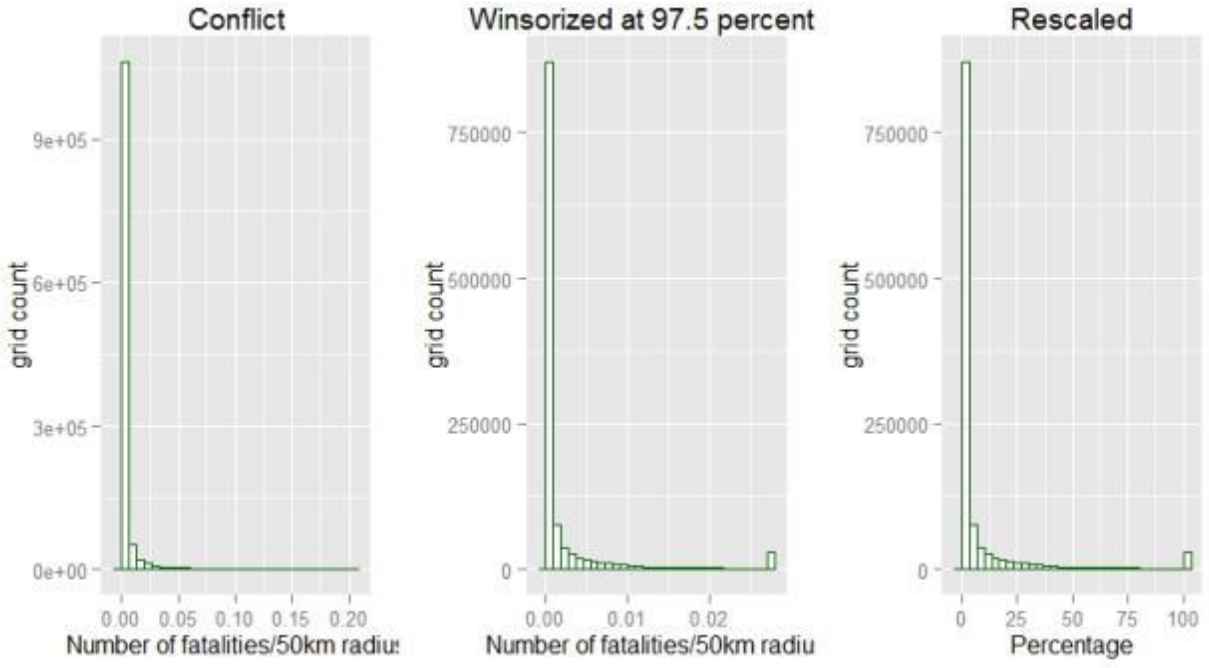

TABLE A-1.2.6: CONFLICT (POLITICAL VIOLENCE)

Title:	Conflict (Political Violence)
Indicator Code:	CONF
Component:	Sensitivity
Rationale:	Armed conflict reduces human security and increases the sensitivity of populations to climate stressors.
URL	http://www.acleddata.com/data/africa/
Data Set:	Armed Conflict Location and Event Dataset (ACLED) codes the dates and locations of all reported political violence events in over 50 developing countries. Political violence includes events that occur within civil wars and periods of instability. Citation: Raleigh, Clionadh, Andrew Linke, Håvard Hegre, and Joakim Karlsen. 2010. Introducing ACLED-Armed Conflict Location and Event Data. Journal of Peace Research 47(5) 1-10.
Units:	A dot density grid was created from the points
Limitations:	Event data are derived from a variety of sources including reports from developing countries and local media, humanitarian agencies, and research publications. Gaps in the record are possible.
Spatial Extent:	Africa
Spatial Resolution:	Points
Year of Publication:	2013
Time Period:	1997 to 2013
Additional Notes:	
Date:	Downloaded on 4 April 2014
Format:	Shapefile
File Name:	Full1997-2013Africa.shp
Contact person:	

A-1.3 ECONOMIC SYSTEM DATA LAYERS

FIGURE A-1.3.1: GROSS DOMESTIC PRODUCT (GDP)

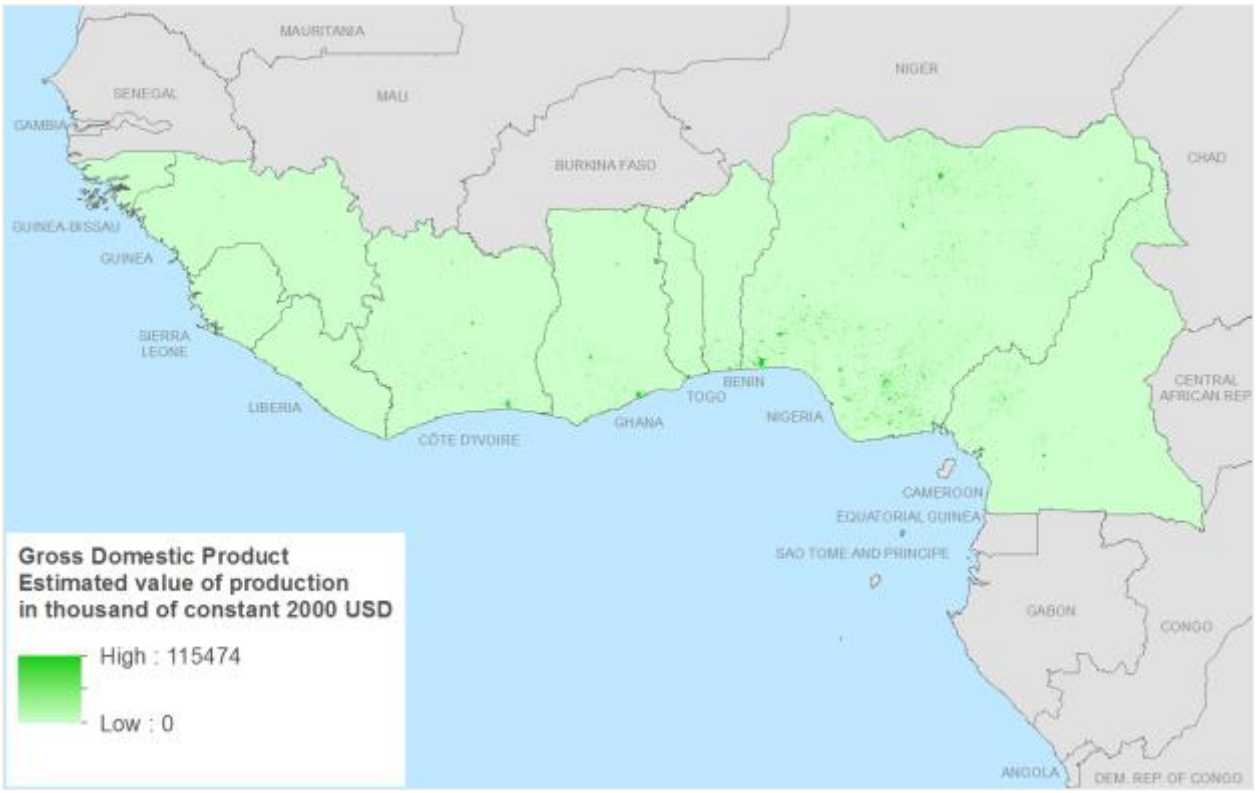

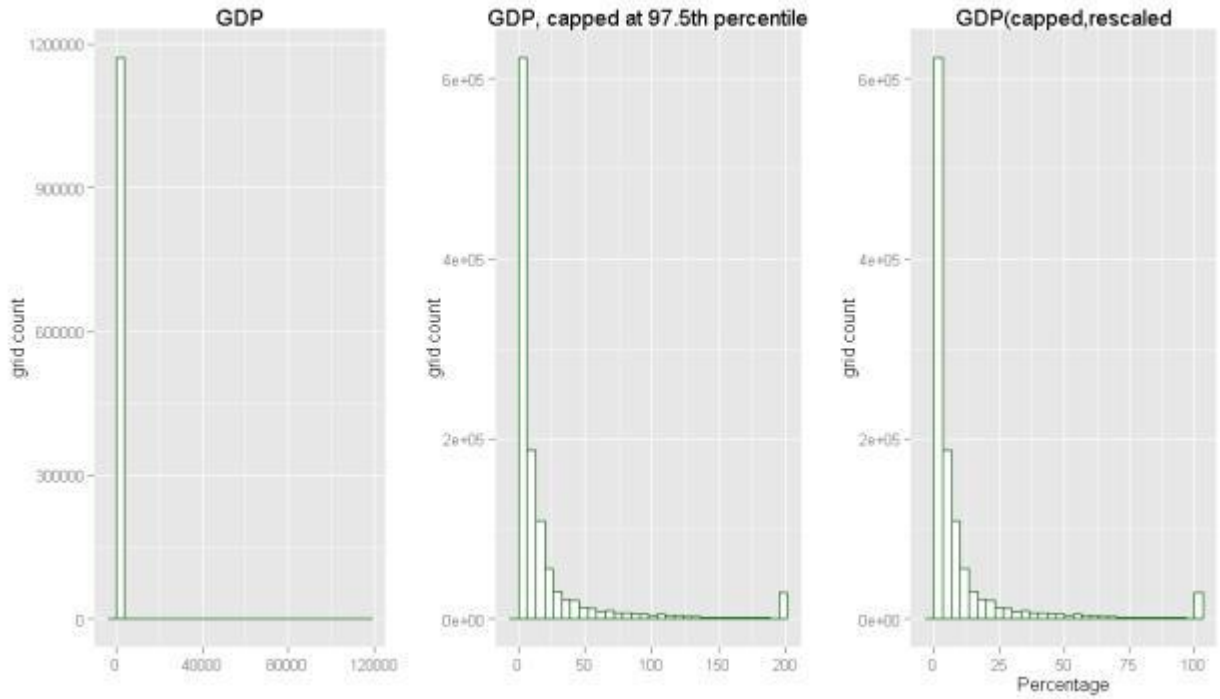

TABLE A-1.3.1: GROSS DOMESTIC PRODUCT (GDP)

Title:	**Gross Domestic Product 2010**
Indicator Code:	GDP
Component:	Economic System
Rationale:	GDP represents the value of exposed economic assets.
URL:	http://preview.grid.unep.ch/index.php?preview=data&events=socec&evcat=1
Data Set:	In the distributed global GDP dataset sub-national GRP and national GDP data are allocated to 30 arc second (approximately 1km) grid cells in proportion to the population residing in that cell. The method also distinguishes between rural and urban population, assuming the latter to have a higher GDP per capita. Input data are from 1) a global time-series dataset of GDP, with subnational gross regional product (GRP) for 74 countries, compiled by the World Bank Development Economics Research Group (DECRG). 2) Gridded population projections for the year 2009, based on a population grid for the year 2005 provided by LandScanTM Global Population Database (Oak Ridge, TN: Oak Ridge National Laboratory). This dataset has been extrapolated to year 2010 by UNEP/GRID-Geneva. Unit is estimated value of production per cell, in thousand of constant 2000 USD. Cell level anomalies may occur due to poor alignment of multiple input data sources, and it is strongly recommended that users attempt to verify information, or consult original sources, in order to determine suitability for a particular application. This product was compiled by DECRG for the Global Assessment Report on Risk Reduction (GAR). It was modelled using global data. Credit: GIS processing World Bank DECRG, Washington, D.C., extrapolation UNEP/GRID-Geneva.
Units:	Unit is estimated value of production per cell, in thousand of constant 2000 USD.
Limitations:	
Spatial Extent:	Global
Spatial Resolution:	30 arc seconds (~1km)
Year of Publication:	2012
Time Period:	2010
Additional Notes:	
Date:	5/7/2014
Format:	Geotiff
File Name:	GDP.tif
Contact person:	
Contact details:	

FIGURE A-1.3.2: CROP HARVESTED AREAS AND YIELDS

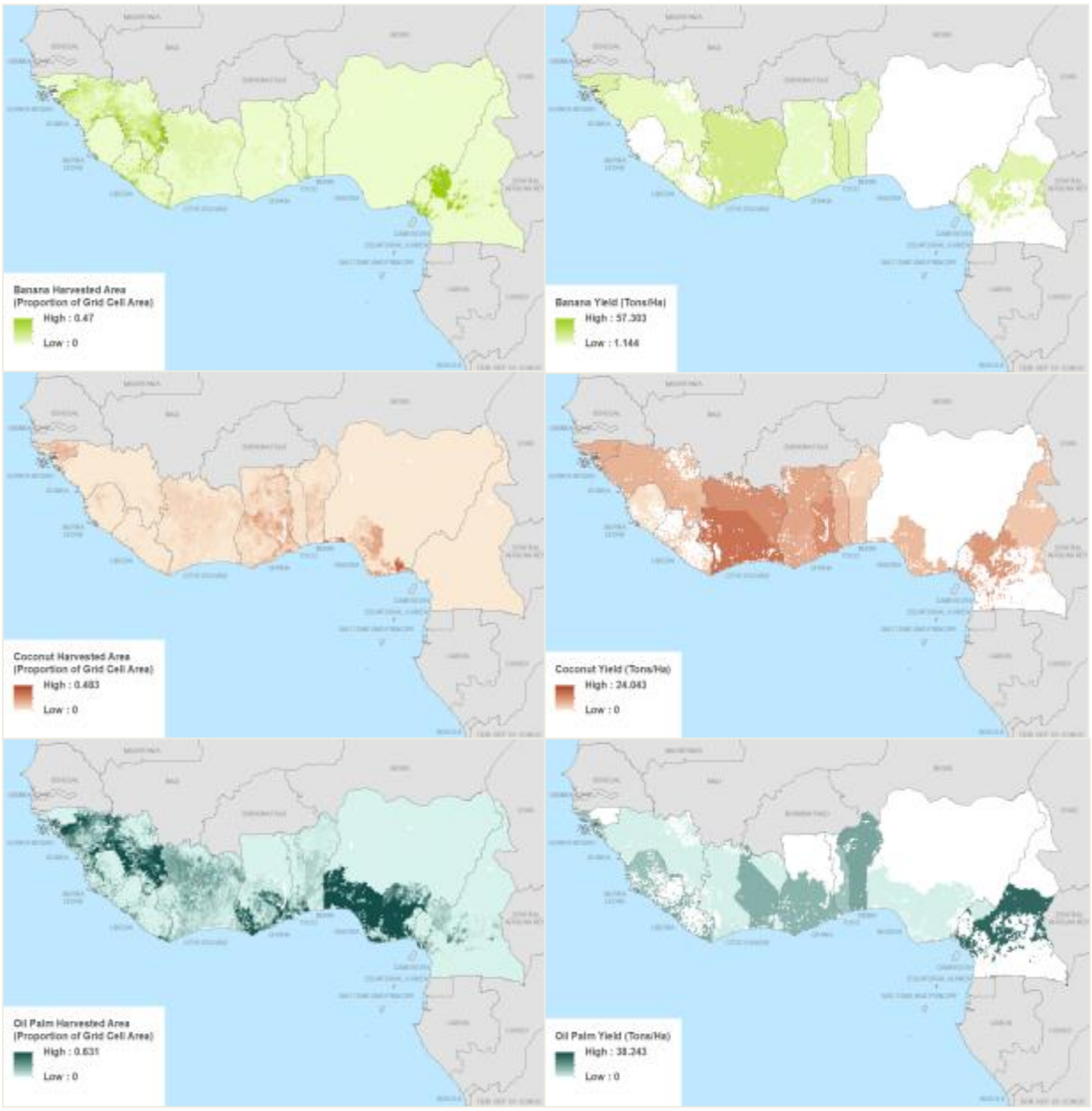

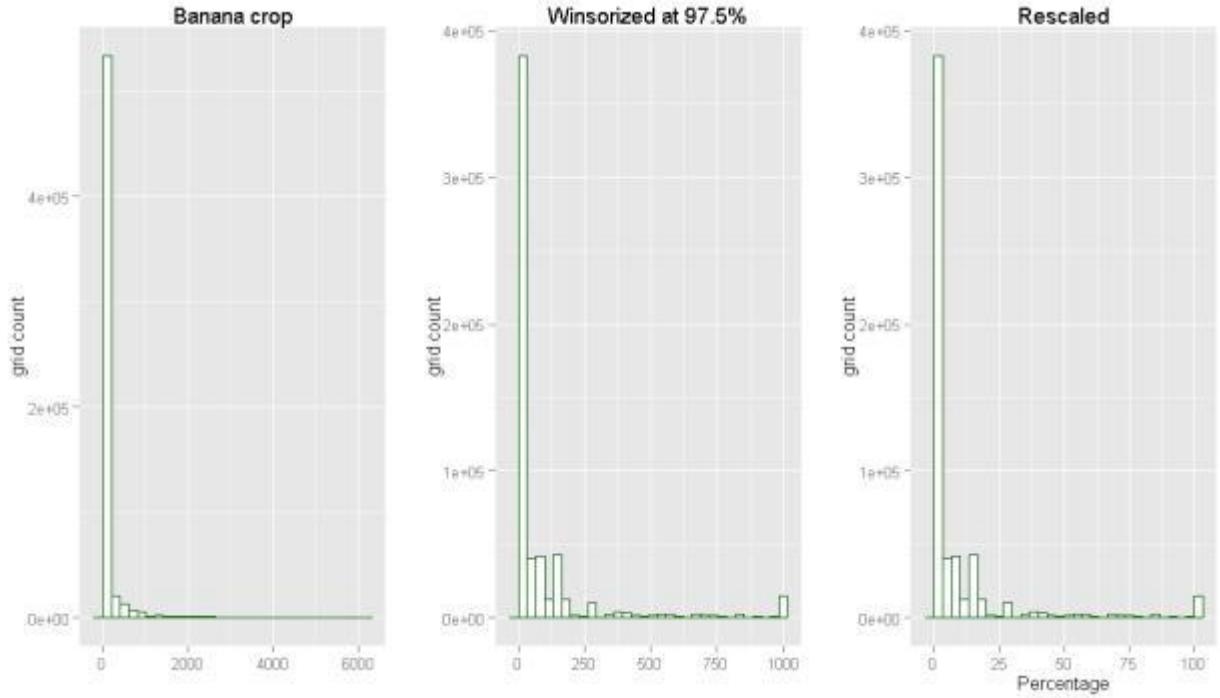
Banana crop
Winsorized at 97.5%
Rescaled
grid count
Percentage

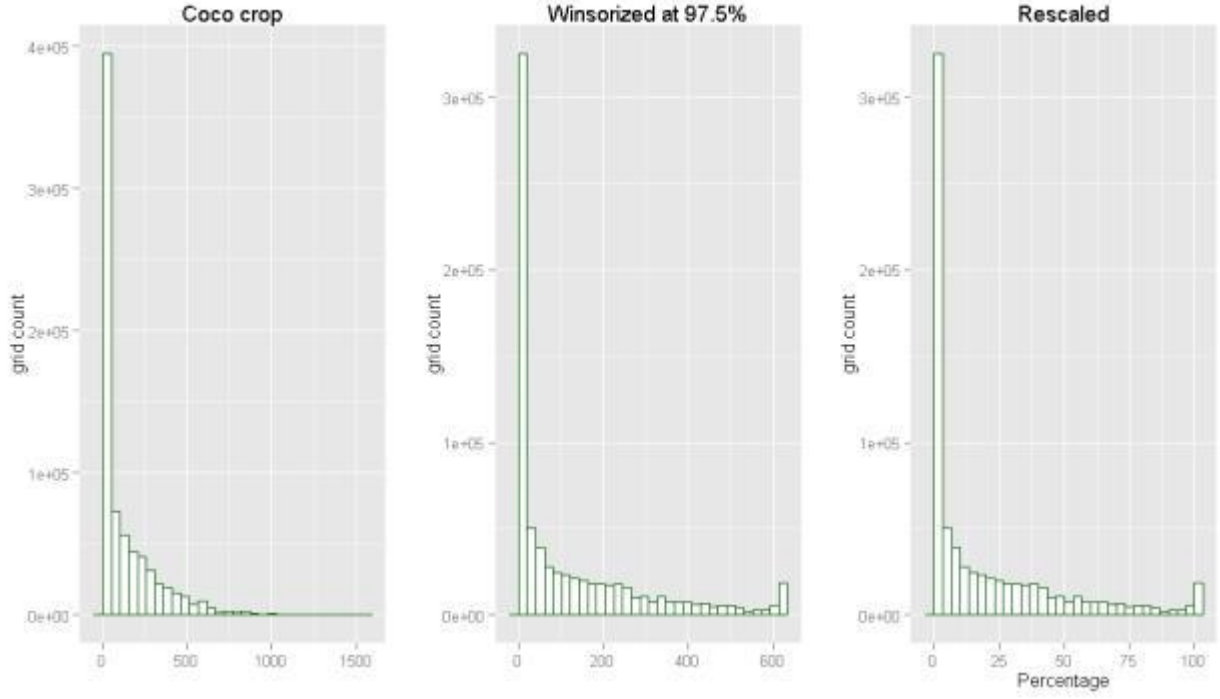
Coco crop
Winsorized at 97.5%
Rescaled
grid count
Percentage

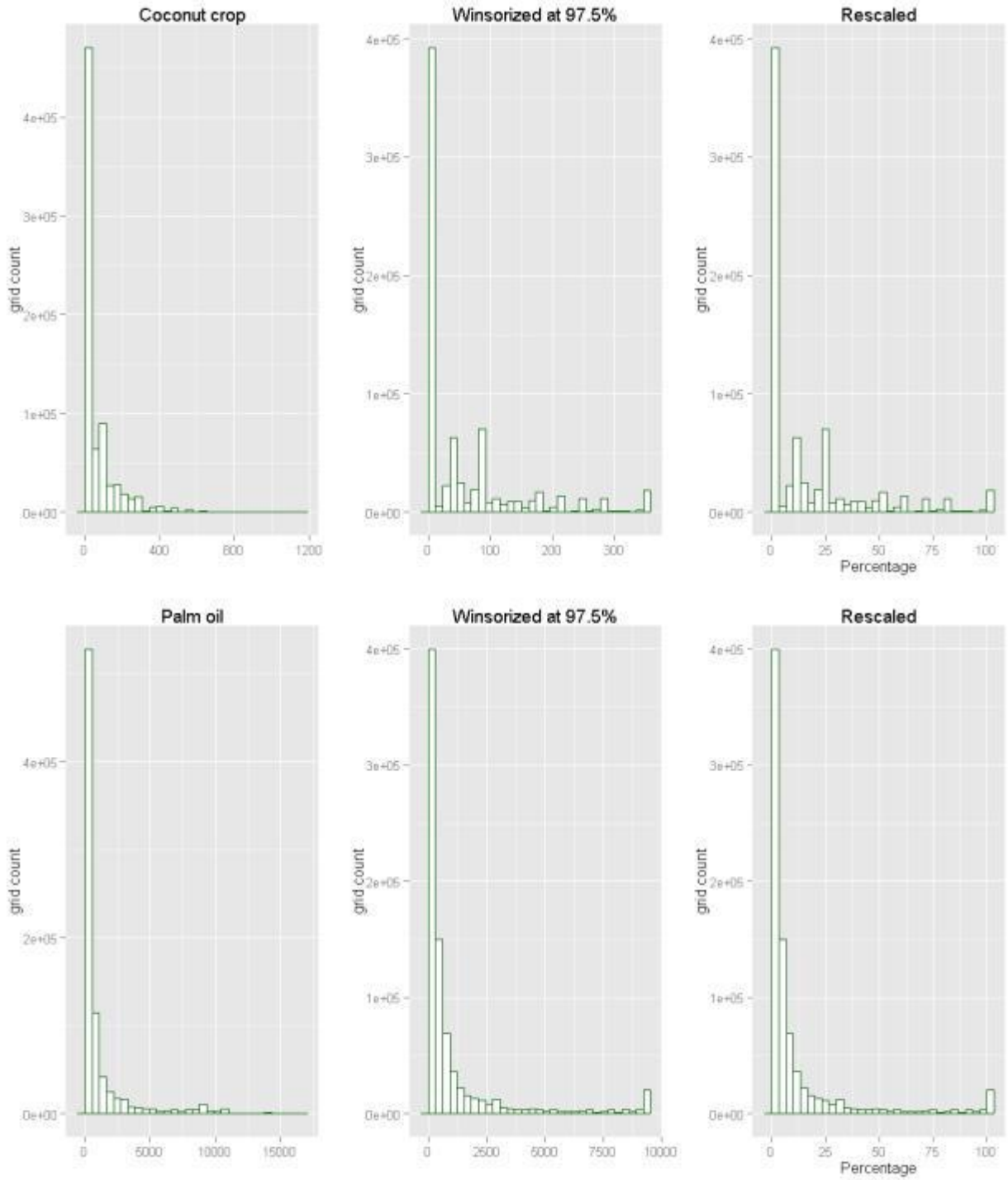
Coconut crop
Winsorized at 97.5%
Rescaled
Palm oil
Winsorized at 97.5%
Rescaled
grid count
Percentage

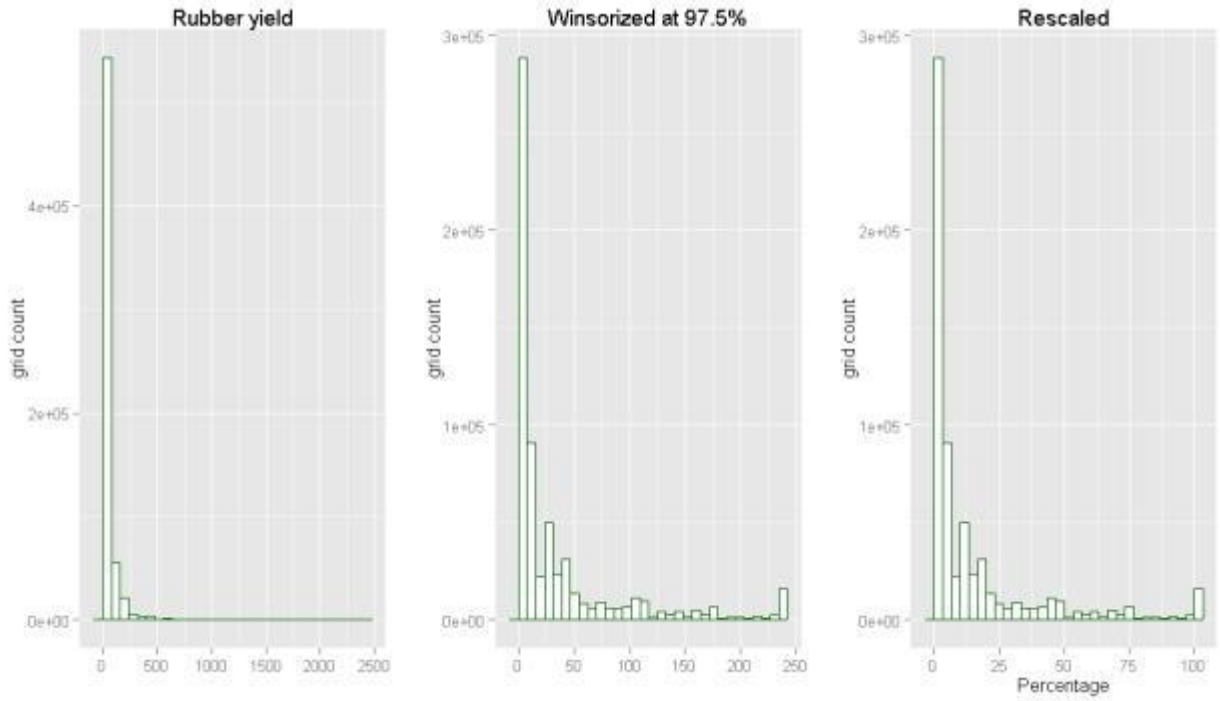
Rubber yield
Winsorized at 97.5%
Rescaled
grid count
Percentage

TABLE A-1.3.2: CROP HARVESTED AREAS AND YIELDS

Title:	**Crop Harvested Area and Yields**
Indicator Code:	CROPS
Component:	
Rationale:	Commercial crops are economically valuable to the countries of West Africa, and some are at high risk of sea-level rise and storm surge impacts.
URL:	http://www.geog.mcgill.ca/~nramankutty/Datasets/Datasets.html Harvested Area and Yields of 175 crops (M3-Crops Data): http://www.geog.mcgill.ca/landuse/pub/Data/175crops2000/
Data Set:	The data collection includes geographic distributions for 175 crops. Mapped crops above include area and yield for cocoa, bananas, coconut, palm oil, and rubber. Monfreda et al. (2008), "Farming the planet: 2. Geographic distribution of crop areas, yields, physiological types, and net primary production in the year 2000", *Global Biogeochemical Cycles,* Vol.22, GB1022, doi:10.1029/2007GB002947.
Units:	Metric tons per grid cell
Processing Steps	M3-Crops data set rasters include: crop_harea = Harvested Area (unit = proportion of grid cell area) crop_yield = Yield (unit = tons per ha) Processing steps to calculate production in metric tons (per grid cell): (1) crop_harea * afareag_5min_ha = crop_harea_ha (where, afareag_5min_ha is a 5min land area grid in units of hectares created from GPWv3 land area grids) (2) crop_harea_ha * crop_yield = crop_yield_tons Regarding crop_harea : Note that values can be greater than 1.0 because of multiple cropping. Acc to Monfreda et al. (2008), "Some crops are harvested multiple times per year, which means that the harvested area exceeds the physical area of the cropland that they are grown on." Also, crop area was initially set to zero when the agricultural inventory data used in the study made no reference to a crop in a particular political unit. Missing data values were interpoloated, but only to a distance of 2 degrees (~220km). Grid cells missing data more than 2 degrees away from cells with data remained null.) Regarding crop yield : Acc to Monfreda et al. (2008), yield was set to null in grid cells with crop area of zero.
Limitations:	
Spatial Extent:	Global
Spatial Resolution:	5 arc minute (10 km)
Year of Publication:	2008
Time Period:	2000
Additional Notes:	
Date:	13 January 2014
Format:	American Standard Code for Information Interchange (ASCII)
File Name:	banana_harea.asc, banana_yield.asc, coconut_harea.asc, coconut_yield.asc, oilpalm_harea.asc, oilpalm_yield.asc, rubber_harea.asc, rubber_yield.asc, cocoa_harea.asc, cocoa_yield.asc
Contact person:	N/A
Contact details:	N/A

FIGURE A-1.3.3: URBAN BUILT-UP AREAS

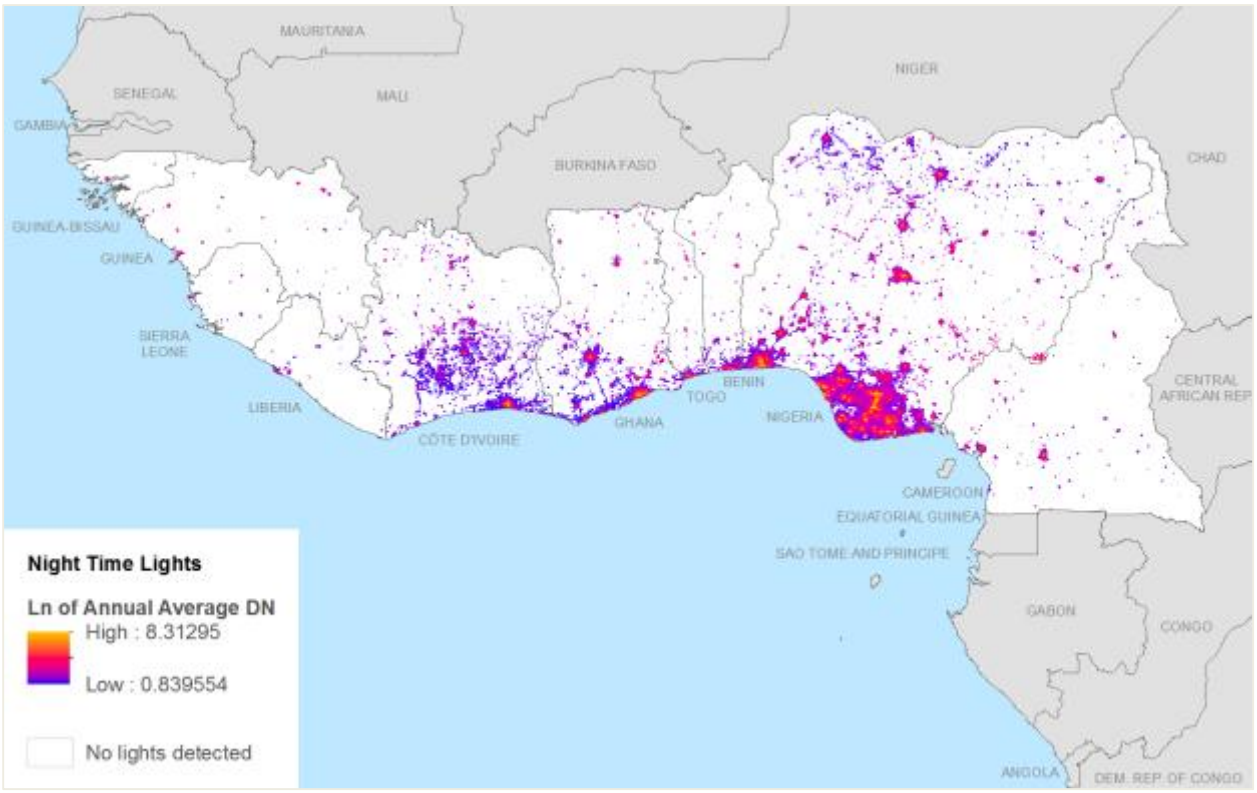

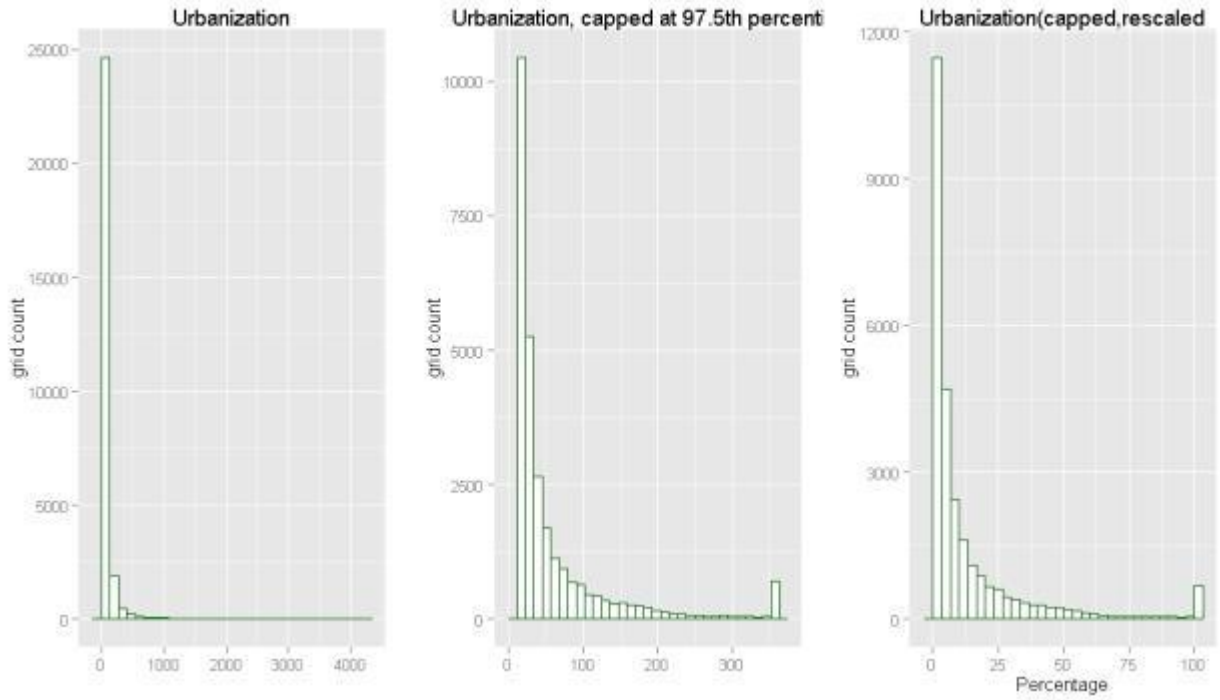

TABLE A-1.3.3: URBAN BUILT-UP AREAS

Title:	Urban Built-Up Areas
Indicator Code:	URBN
Component:	Economic Systems
Rationale:	Night-time lights intensity represents a proxy measure of economic activity.
Data Set:	Version 4 DMSP-OLS Nighttime Lights Time Series 2010 annual global composite of radiance lights inter-calibrated to the digital number (DN) values of gain 55 for satellite F16 (2006) The night time lights data are collected by the Defense Meteorological Satellite Program-Optical Line Scanner (DMSP-OLS) instrument. These data are commonly used for identifying human settlements and economic activity (e.g. Small et al. 2005; Zhang and Seto 2011; Henderson et al. 2012; Small and Elvidge 2012; Pandey et al. 2013). The DNs are on a unitless scale ranging from 0 (no light) to 4000 (greatest light intensity). The resolution of the grids is 30 arc seconds, or approximately 1 sq. km at the equator. Citation: NOAA. NGDC. Version 4 DMSP-OLS Nighttime Lights Time Series. 1999 and 2010 annual global composite of radiance lights inter-calibrated to the DN values of gain 55 for satellite F16-2006. Courtesy of C. Elvidge, Earth Observation Group, NOAA/NGDC. (Image and data processing by NOAA's National Geophysical Data Center. DMSP data collected by U.S. Air Force Weather Agency). http://www.ngdc.noaa.gov/dmsp/index.html
Units:	DN (Digital Number)
Limitations:	Night-time lights are an imperfect measure of economic activity insofar as they do not adequately capture agricultural activities, but as a first approximation they do a far better job of spatially locating economic activity than equivalent gridded GDP products.
Spatial Extent:	Global
Spatial Resolution:	30 arc-seconds (~1km).
Year of Publication:	2010
Time Period:	2010 annual global composite
Additional Notes:	
Date:	Received from Christopher Elvidge and Kimberly Baugh of the Earth Observation Group, NOAA National Geophysical Data Center.
Format:	raster
File Name:	F16_20100111_20101209
Contact person:	

FIGURE A-1.3.4: ROAD NETWORK

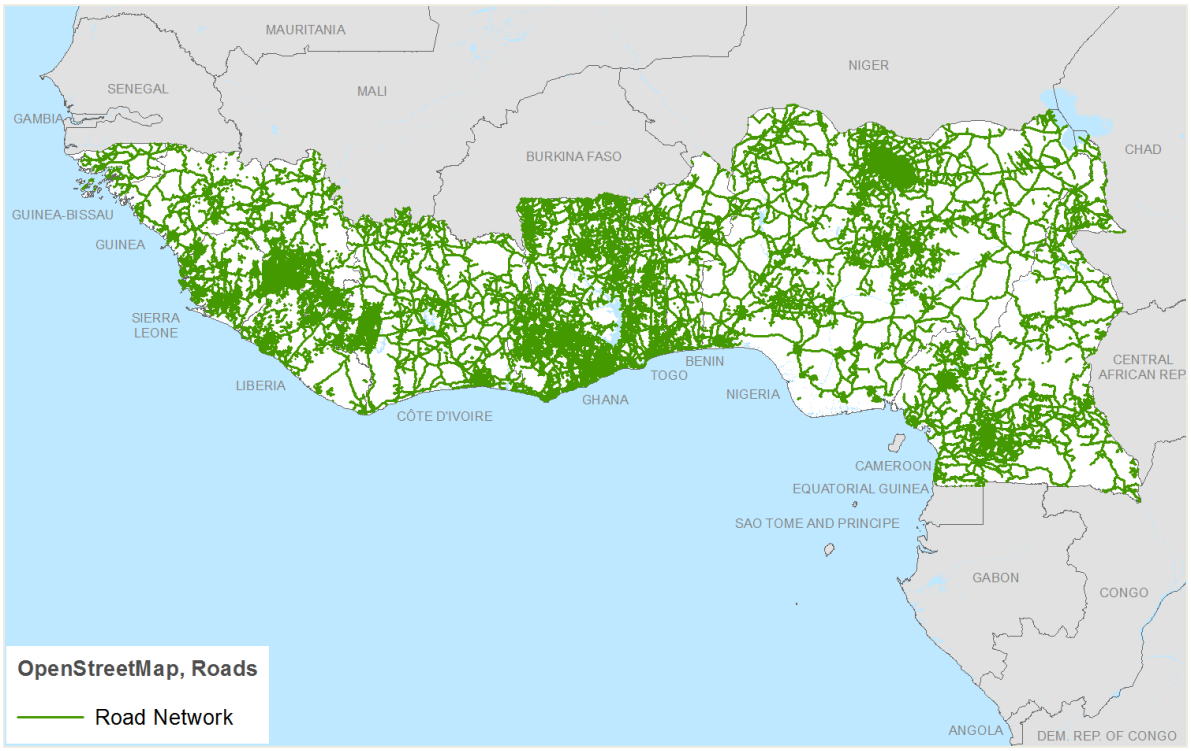

TABLE A-1.3.4: ROAD NETWORK

Title:	**Road Network**
Indicator Code:	ROAD
Component:	Economic System
Rationale:	Roads link rural production to urban markets, and represent an important exposed infrastructure asset for all countries.
URL:	http://export.hotosm.org/en/wizard_area
Data Set:	OpenStreetMap (OSM), http://www.openstreetmap.org/. Data downloaded in March 2014.
Units:	There are multiple road classes
Limitations:	OSM data are crowd sourced and are of uncertain accuracy, but
Spatial Extent:	Global
Spatial Resolution:	
Year of Publication:	2013
Time Period:	
Additional Notes:	We communicated with Mikel Maron of OSM and were told to go to http://export.hotosm.org/en/wizard_area, draw a box and name the area, and "Create Job". On the next page, select "Highways" from the "Select Preset File" drop down. Uncheck "Add Default Tags?". Then click "Save". The following page will show the job status as it runs, and when finished, will have download links. Due to the size limitation of the bounding box, six different boxes for our region of interest were drawn. For each box, the data was downloaded and merged in ArcGIS.
Date:	5/12/2014
Format:	Shape file
File Name:	planet_osm_line.shp
Contact person:	Mikel Maron, OSM

A-1.4 NATURAL SYSTEM DATA LAYERS

FIGURE A-1.4.1: MANGROVE FORESTS DISTRIBUTIONS

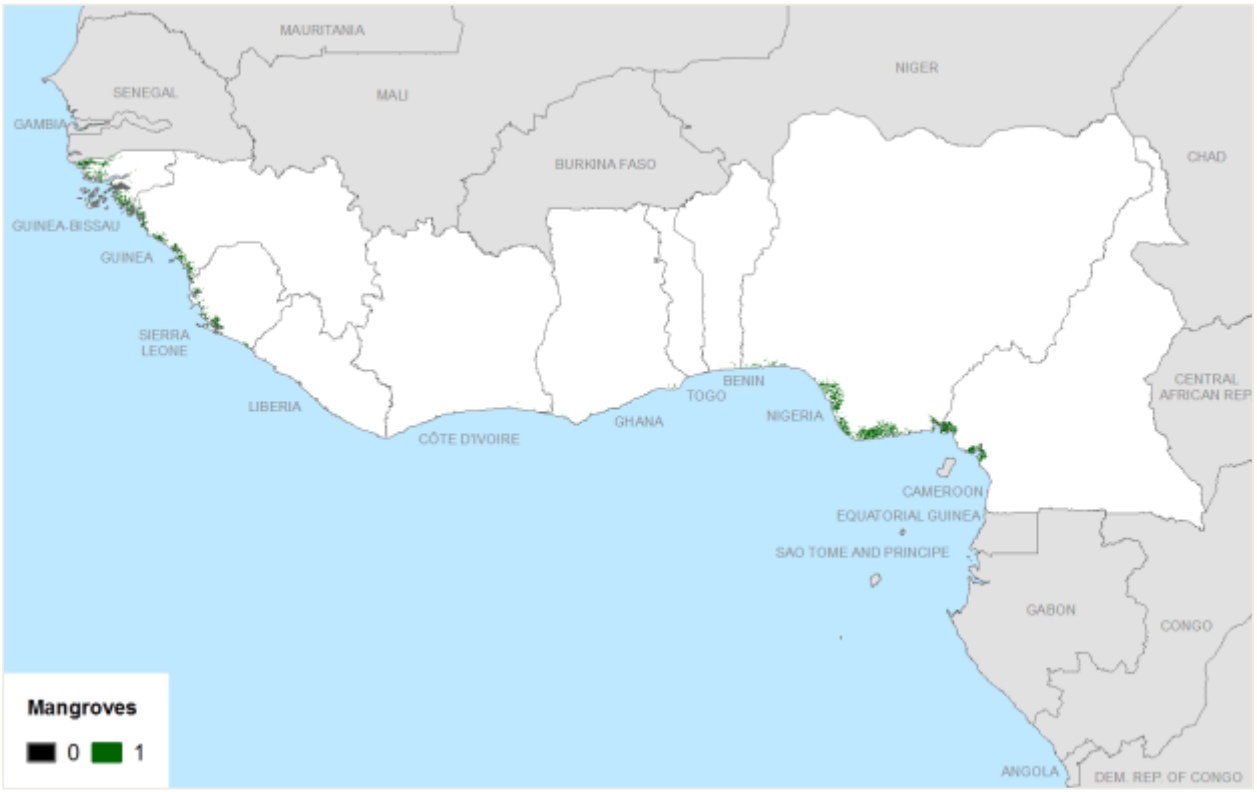

TABLE A-1.4.1: MANGROVE FORESTS DISTRIBUTIONS

Title:	**Mangrove Forests Distributions, 2000**
Indicator Code:	MANG
Component:	Exposed Systems
Rationale:	Mangroves are vulnerable to SLR and storm surge.
URL:	To be released soon via http://beta.sedac.ciesin.columbia.edu/data/set/lulc-global-mangrove-forests-distribution-2000
Data Set:	The Global Mangrove Forests Distribution, 2000 data set is a compilation of the extent of mangrove forests from the Global Land Survey and the Landsat archive with hybrid supervised and unsupervised digital image classification techniques. The data are available at a 30-meter spatial resolution. The total area of mangroves in the year 2000 was estimated at 137,760 km^2 in 118 countries and territories in the tropical and subtropical regions of the world. This figure is more than 12 percent less than previous estimates; and if the current rate of loss continues, predictions suggest that 100 percent of these forests will be lost in the next century. Data citation: Giri, C., E. Ochieng, L.L.Tieszen, Z. Zhu, A. Singh, T. Loveland, J. Masek, and N. Duke. (2013). Global Mangrove Forests Distribution, 2000. Palisades, NY: NASA Socioeconomic Data and Applications Center (SEDAC). The original citation for this data set is: Giri, C., Ochieng, E., Tieszen, L.L., Zhu, Z., Singh, A., Loveland, T., Masek, J., and Duke, N.. 2010. Status and Distribution of Mangrove Forests of the World Using Earth Observation Satellite Data. *Global Ecology and Biogeography: A Journal of Macroecology* 20(1):154-159. Retrieved from 10.1029/2006JD007377.
Units:	
Limitations:	
Spatial Extent:	Global
Spatial Resolution:	30-meter
Year of Publication:	2010
Time Period:	2000
Additional Notes:	
Date:	15 January 2014
Format:	img
File Name:	globalgeo_new.img
Contact person:	Malanding Jaiteh

FIGURE A-1.4.2: FOREST COVER CHANGE, 2000–2012

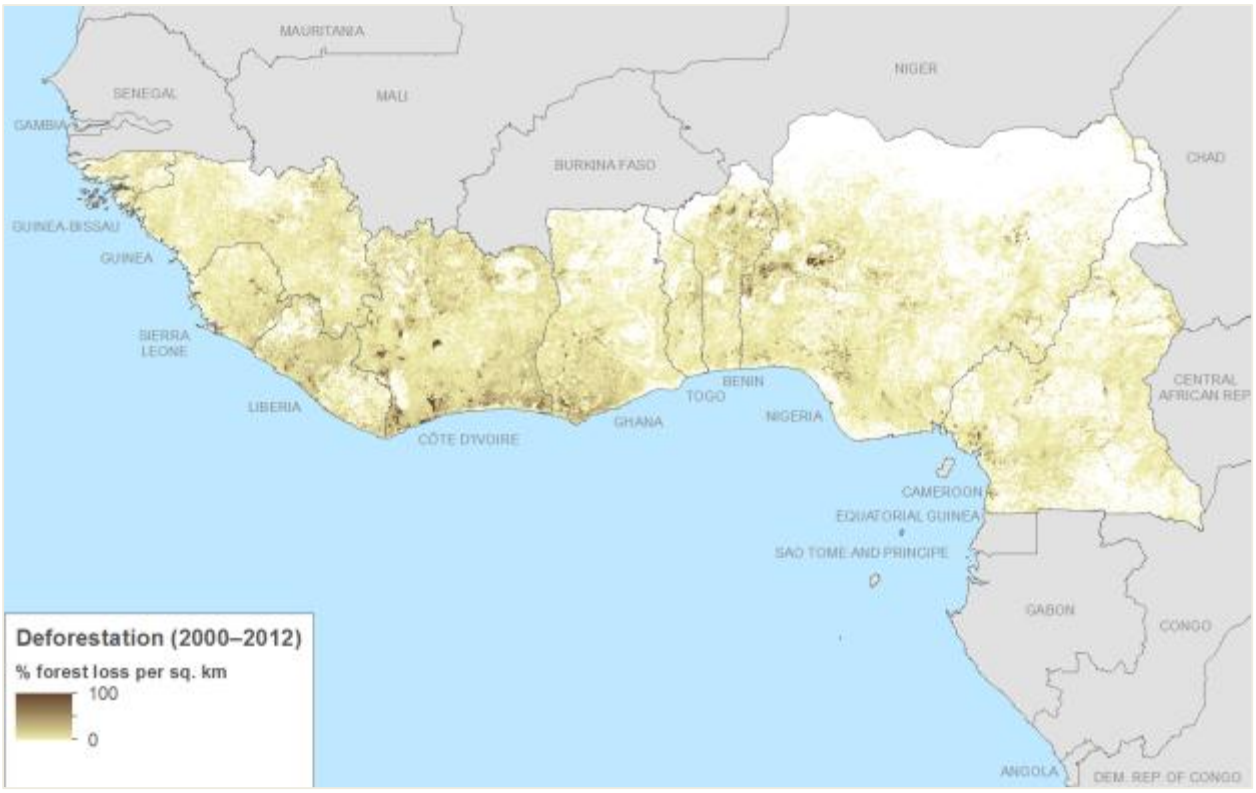

TABLE A-1.4.2: FOREST COVER CHANGE, 2000–2012

Title:	**Forest Cover Change, 2000–2012**
Indicator Code:	FOREST
Component:	Exposed Systems
Rationale:	Data on forest loss from 2000–2012 could be combined with the mangrove cover for the year 2000 to come up with a contemporary mangrove map.
URL:	http://earthenginepartners.appspot.com/science-2013-global-forest
Data Set:	Global Forest Change Results from time-series analysis of 654,178 Landsat images in characterizing forest extent and change, 2000–2012. Trees are defined as all vegetation taller than 5m in height and are expressed as a percentage per output grid cell as '2000 Percent Tree Cover'. 'Forest Loss' is defined as a stand-replacement disturbance, or a change from a forest to non-forest state. 'Forest Gain' is defined as the inverse of loss, or a non-forest to forest change entirely within the study period. 'Forest Loss Year' is a disaggregation of total 'Forest Loss' to annual time scales. Reference 2000 and 2012 imagery are median observations from a set of quality assessment-passed growing season observations The original citation for this data set is: Hansen, M. C. et al. (2013). High-Resolution Global Maps of 21st-Century Forest Cover Change. *Science*.342(6160), 850-853. doi:10.1126/science.1244693.
Units:	Percent of 1 km pixel deforested between 2000-2012
Limitations:	We chose to use forest loss rather than the balance of forest loss and forest gain on the assumption that forest gain is more likely to be human managed or plantation forests, while forest loss is more likely to reflect losses in natural tree cover.
Spatial Extent:	Global
Spatial Resolution:	30m
Year of Publication:	2013
Time Period:	2000-2012
Additional Notes:	Global tree cover extent, loss, and gain mapped for the period from 2000 to 2012 at a spatial resolution of 30m, with loss allocated annually. Global analysis based on Landsat data. CIESIN aggregated the loss data to a 1 kilometer resolution, with results represented in the percentage of the grid cell area that experienced forest cover loss from 2000 to 2012.
Date:	
Format:	
File Name:	
Contact person:	

FIGURE A-1.4.3: GLOBAL LAKES AND WETLANDS

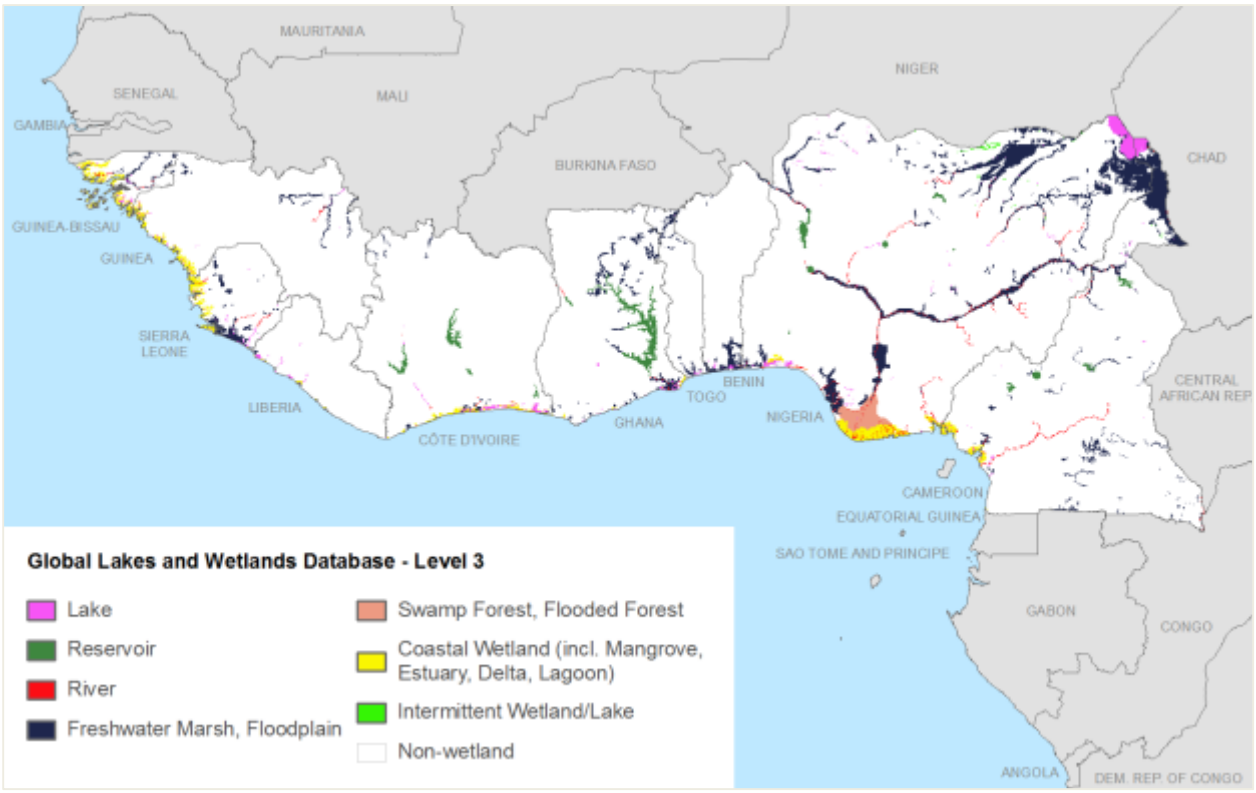

TABLE A-1.4.3: GLOBAL LAKES AND WETLANDS

Title:	**Global Lakes and Wetlands**
Indicator Code:	GLWD-3
Component:	Exposed Systems
Rationale:	Wetland areas could be submerged by SLR and lakes are vulnerable to drought.
URL:	http://worldwildlife.org/publications/global-lakes-and-wetlands-database-lakes-and-wetlands-grid-level-3
Data Set:	The Global Lakes and Wetlands Database (Level 3) was developed through a partnership between WWF, the Center for Environmental Systems Research, and the University of Kassel, Germany. It draws upon the best available maps, data, and information to display lakes and wetlands on a global scale (1:1 to 1:3 million resolution). The application of GIS functionality enables the generation of a database that focuses on: (1) large lakes and reservoirs, (2) smaller water bodies, and (3) wetlands. Level 3 (GLWD-3) comprises lakes, reservoirs, rivers, and different wetland types in the form of a global raster map at 30-second resolution. For GLWD-3, the polygons of GLWD-1 and GLWD-2 were combined with additional information on the maximum extents and types of wetlands. Class 'lake' in both GLWD-2 and GLWD-3 also includes man-made reservoirs, as only the largest reservoirs have been distinguished from natural lakes.
Units:	The original data include the following classes: 1 Lake 2 Reservoir 3 River 4 Freshwater Marsh, Floodplain 5 Swamp Forest, Flooded Forest 6 Coastal Wetland (incl. Mangrove, Estuary, Delta, Lagoon) 7 Pan, Brackish/Saline Wetland 8 Bog, Fen, Mire (Peatland) 9 Intermittent Wetland/Lake 10 50-100% Wetland 11 25-50% Wetland 12 Wetland Complex (0-25% Wetland) For this mapping exercise we only included classes 4-7 as being more likely to be found in the coastal zone.
Limitations:	
Spatial Extent:	Global
Spatial Resolution:	30 arc seconds (~1km)
Year of Publication:	2004
Time Period:	
Additional Notes:	For this exercise we selected wetland types 4, 5, 6, and 7.
Date:	1/15/14
Format:	Shape file
File Name:	glwd_3
Contact person:	
Contact details:	

FIGURE A-1.4.4: THREATENED SPECIES RICHNESS

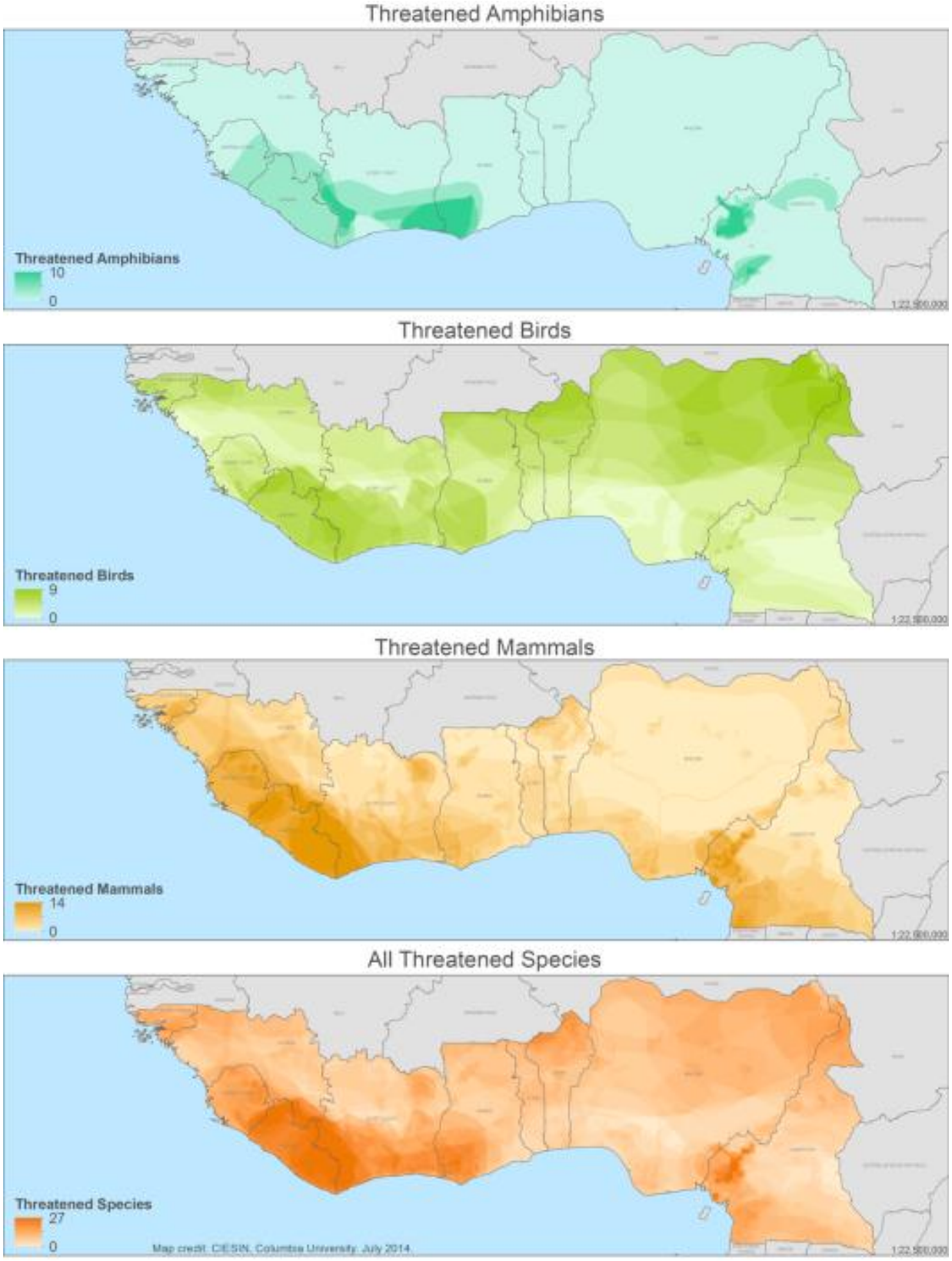

TABLE A-1.4.4: THREATENED SPECIES RICHNESS

Title:	Threatened Species Richness
Indicator Code:	THREAT
Component:	Exposed Systems
Rationale:	Areas with higher species richness are at greater risk to climate stressors.
URL:	This data set is available from CIESIN but is not yet being distributed.
Data Set:	CIESIN has gridded the entire collection of IUCN Red List species distribution maps for amphibians, birds, and mammals. The data are available from: http://www.iucnredlist.org/technical-documents/spatial-data. All threatened species by threat status (vulnerable, endangered, and critically endangered) and by class were added to create a threatened species density map.
Units:	Number of threatened species per 1km grid cell
Limitations:	Data limitations are documented on the Red List web site.
Spatial Extent:	Global
Spatial Resolution:	1 km
Year of Publication:	2012
Time Period:	2012 (updated regularly)
Additional Notes:	
Date:	16 January 2014
Format:	
File Name:	
Contact person:	Malanding Jaiteh

FIGURE A-1.4.5: PROTECTED AREAS

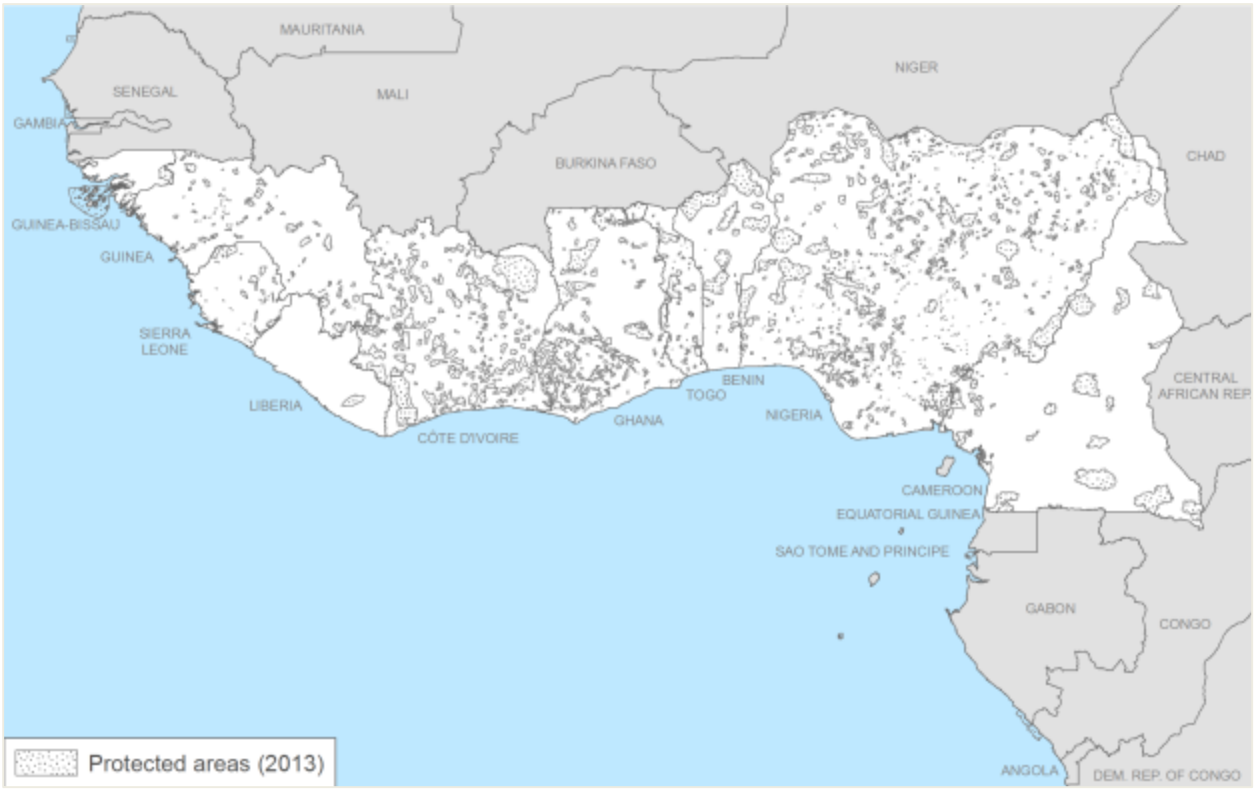

TABLE A-1.4.5: PROTECTED AREAS

Title:	Protected Areas
Indicator Code:	PA
Component:	Exposed System
Rationale:	Protected areas, and particularly marine protected areas, can assist in the protection of mangroves and other ecosystems that have important buffering capabilities in the coastal zone.
URL:	http://www.unep-wcmc.org/
Data Set:	IUCN and UNEP-WCMC. (2013). The World Database on Protected Areas (WDPA): January 2013. Cambridge, UK: UNEP-WCMC.
Units:	N/A
Limitations:	Data shows extent of nationally designated protected areas (PAs). PAs with area information but no boundary information are represented by a circular buffer of equivalent area.
Spatial Extent:	Global
Spatial Resolution:	Vector data.
Year of Publication:	2013
Time Period:	2012
Additional Notes:	
Date:	14 January 2014
Format:	Feature class
File Name:	
Contact person:	Malanding Jaiteh

U.S. Agency for International Development
1300 Pennsylvania Avenue, NW
Washington, DC 20523
Tel: (202) 712-0000
Fax: (202) 216-3524
www.usaid.gov